

# Texture of One Equality in Neutrino Mass Matrix

A. Ismael<sup>1,2\*</sup>, E. I. Lashin<sup>1,2,3†</sup>, M. AlKhateeb<sup>4,5‡</sup> and N. Chamoun<sup>6§</sup>

<sup>1</sup> Department of Physics, Faculty of Science, Ain Shams University, Cairo 11566, Egypt.

<sup>2</sup> Centre for Fundamental Physics, Zewail City of Science and Technology, 6 October City, Giza 12578, Egypt.

<sup>3</sup> The Abdus Salam, ICTP, P. O. Box 586, 34100 Trieste, Italy.

<sup>4</sup> Department of Physics, Faculty of Science, Damascus University, Syria.

<sup>5</sup> Département de Physique, Université de Cergy-Pontoise, F-95302 Cergy-Pontoise, France.

<sup>6</sup> Physics Department, HIAST, P.O.Box 31983, Damascus, Syria.

March 1, 2025

## Abstract

We carry out a phenomenological and analytical study of the texture structures for the Majorana neutrino mass matrix characterized by single equality between two independent matrix elements, with vanishing non-physical phases whose role in the definition we clarify. We find that all textures are viable in both types of hierarchy, except for one inverted hierarchy texture. We also present symmetry realizations for some patterns by using Abelian flavor symmetries within type-I, type-II and mixed type-(I+II) seesaw scenarios.

**Keywords:** Neutrino Physics; Flavor Symmetry;

**PACS numbers:** 14.60.Pq; 11.30.Hv;

## 1 Introduction

The neutrino oscillation observations present conclusive evidence that neutrinos are massive and that their flavor states do oscillate. Moreover, they open the door for physics beyond the standard model [1–5]. If we work in the flavor basis, where charged lepton mass matrix  $M_l$  is diagonal and assume the neutrinos are of Majorana-type, then the neutrino mass matrix  $M_\nu$  becomes symmetric with 12 free parameters. However, one can fix 3 “unphysical phases” without changing the physics leaving thus 9 physical free parameters in  $M_\nu$ . This number is still greater than the number of parameters which can be measured by the experiments. There are experimental bounds only on the values of the mass-squared differences, the three mixing angles ( $\theta_{12}$ ,  $\theta_{23}$ ,  $\theta_{13}$ ), and the Dirac phase  $\delta$ . However, no experimental constraints on the two Majorana-phases ( $\rho$  and  $\sigma$ ) up till now. In order to reduce the number of free parameters, some phenomenological models have been studied such as textures characterized by zero elements [6–9], zero minors [10–12], two vanishing subtraces [13] and partial  $\mu$ - $\tau$  symmetry [14].

---

\*ahmedEhusien@sci.asu.edu.eg

†slashin@zewailcity.edu.eg, elashin@ictp.it

‡mohkha88@gmail.com

§nidal.chamoun@hiast.edu.sy

In light of the recent experimental data in [15], we carry out in this paper a complete numerical investigation of all possible textures characterized by one equality between two independent matrix elements in  $M_\nu$  at all  $\sigma$ -levels. This work is particularly motivated by existing studies in the literature involving equalities between the entries or cofactors [16] in  $M_\nu$ , or involving hybrid textures [17, 18] where one imposes an equality constraint and another one-zero constraint. The work of [19] concerning textures where two independent entries are opposite each other is related to our current work, however they are not equivalent since both works adopt vanishing unphysical phases where one has no longer phase freedom allowing to relate one form to the other.

One important point that is usually mentioned only in passing concerns the role of the unphysical phases in the definition of the texture, in that some studies, e.g. [16], define the texture as the form of  $M_\nu$  which satisfies the specific defining constraint for at least one choice of the unphysical phases, whereas in other studies, e.g. [17, 18], the texture is defined after fixing the unphysical phases. The two definitions are not equivalent, and there are advantages/disadvantages in adopting one or the other of the two definitions. In this paper, we shall underline the difference between these two approaches for defining any given texture, contrasting their good and bad points, but for the phenomenology and the analysis, we shall stick to the second definition, putting all the unphysical phases to zero, because it corresponds to a tighter allowable parameter space, which would increase the predictability power of the texture. Moreover, the specific definition fixing the unphysical phases to zero makes the computations simpler and especially, since the corresponding constraint involves analytic functions of the matrix entries, makes it a relatively simple task to find realization paradigms.

The texture with the constraint of one complex equality (2 real conditions) corresponds to a reduction by 2 degrees of freedom of the 9 physical parameters of  $M_\nu$ , so by varying all the seven free parameters ( $\theta_{12}, \theta_{23}, \theta_{13}, \delta, \rho, \sigma, \delta m^2$ ) randomly over their allowed experimental ranges, we can reconstruct  $M_\nu$  and see whether it meets the remaining experimental bounds getting, thus, allowed regions in the parameter space. We find that out of the 15 possible patterns, all of them can accommodate the experimental data in the case of normal hierarchy ( $m_1 < m_2 < m_3$ ), while 14 of them can survive in the case of inverted hierarchy ( $m_3 < m_1 < m_2$ ).

In this study, we introduce the numerical discussion and correlation plots for nine possible textures, noting that the remaining six patterns are related to six of the studied nine patterns by a  $\mu - \tau$  interchange symmetry\*. Although the current experimental data do not respect the  $\mu - \tau$  interchange symmetry (e.g.  $\theta_y$  data is not symmetric around  $45^\circ$ ), and so in principle one can not relate automatically the allowed regions of two  $\mu - \tau$ -symmetry-related patterns, however we found that the corresponding correlation plots deviate very slightly from each other, and thus we opted to limit the presentation to nine patterns.

We then introduce symmetry realizations for some viable patterns by using  $Z_2 \times Z_6$  abelian flavor symmetry within the type-I seesaw scenario and  $Z_2 \times Z'_2$  symmetry within the type-II seesaw scenario. The realization within mixed type-(I+II) scenarios by using  $Z_2 \times Z'_2 \times U(1)^3$  symmetry are also presented where  $U(1)^3$  represents a separate lepton number symmetry, which is softly broken by the 3-dim operators, like the right-handed neutrino mass terms, to avoid the

---

\*Actually, for the unviable texture of inverted type, ( $C_1$ ), we could find acceptable points but only at the  $3\sigma$  level and just barely (out of  $10^{10}$  points thrown randomly and uniformly in their respective ranges, only 8 points were acceptable), so that the corresponding acceptable region of the parameter space was scarce and restricted enough not to be of statistical significance, in contrast to the related  $\mu$ - $\tau$ -symmetry texture  $C_2$  which is viable for both types of hierarchies. However, for all the other textures, the phenomenology does not change much under  $\mu$ - $\tau$ -symmetry.

existence of the Goldstone bosons.

The plan of the paper is as follows: In section 2, we state explicitly the role of the unphysical phases in the texture definition, whereas in the following section 3 we introduce our notations, adopted conventions, and the experimental bounds of the oscillation and non-oscillation parameters. In section 4, we present the formulae that define the mass ratios ( $\frac{m_1}{m_3}, \frac{m_2}{m_3}$ ) and the neutrino masses ( $m_1, m_2, m_3$ ) besides one table classifying all possible texture structures. In section 5, we discuss the numerical analysis for each independent texture together with two tables summarizing the different predictions at all  $\sigma$ -levels. In section 6, we present symmetry realizations for some viable texture structures in different seesaw schemes. We end up with a summary and conclusion in section 7. In one appendix, we write down the  $Z_2 \times Z_2'$  invariant terms for the type-II scalar potential in one specific case.

## 2 Unphysical phases and the texture definition

We contrast in this section two ways used to define a texture given by a certain constraint relating the different entries of  $M_\nu$ . We assume we are in the flavor basis of the charged leptons which is defined up to a 3-dim phase matrix  $P$ , the unphysical charged lepton phases. One can absorb  $P$  by redefining equally the “gauge” neutrino fields, upon which  $M_\nu$  is “phased” as<sup>†</sup>:

$$(\nu \rightarrow P\nu) \Rightarrow (M_\nu \rightarrow M'_\nu = P^* M_\nu P^*) \quad (1)$$

Let’s call a change of  $P$  a change of basis (or “gauge”). For a fixed parametrization of the  $V_{\text{PMNS}}$  (e.g. the familiar PDG [20], or the parametrization that we shall adopt where the third column is real), any  $M_\nu$  can be decomposed uniquely as:

$$M_\nu = (PV_{\text{PMNS}})M^d(PV_{\text{PMNS}})^T, \quad (2)$$

where  $M^d$  is diagonal with positive masses, so we write

$$P^* M_\nu P^* = M_\nu^{\text{phys}} = V_{\text{PMNS}} M^d (V_{\text{PMNS}})^T \quad (3)$$

The two matrices  $M_\nu$  and  $M_\nu^{\text{phys}}$  differ only in the unphysical phases but have the same physics and no way to distinguish one from the other by physical measurements.

The role of the unphysical phases in the definition of the texture differs in the two approaches. In the first approach, call it the “generalized” definition, the texture is defined by satisfying a given constraint in at least one basis  $P$ , whereas in the second approach, call it the “specific” definition, the given constraint is met in one specific basis, say  $P = 0$ , i.e. it is defined as a constraint on the elements of  $M_\nu^{\text{phys}}$  rather than those of  $M_\nu$ . The generalized definition provides a less stringent constraint leading to an increase of the acceptable points in the correlation plots, which is a disadvantage regarding the predictability of the model. However, this generalized approach optimally leads to a definition which is independent of  $P$ , acquiring thus the advantage of a basis (or “gauge”)-independent definition. The systematic way in the generalized approach to reach a  $P$ -invariant definition of the texture is subtle, in that we start from an explicit definition of the texture in one basis -say where  $P = 0$ -, then we replace the entries of  $M_\nu$  by the entries of the “phased” neutrino mass matrix  $M'_\nu = P^* M_\nu P^*$  by introducing the arbitrary phase

---

<sup>†</sup>We stress here that the Majorana neutrino mass states are not phased, as the corresponding mass term is not phase invariant, but rather we are redefining both the “gauge” neutrino fields and the corresponding mass matrix so that its diagonalizing matrix transforms from, say,  $V_{\text{PMNS}}$  to  $PV_{\text{PMNS}}$ .

$P$ , and then subtly try to eliminate  $P$  in order to find, if possible, the  $P$ -invariant definition of the texture. In contrast, by choosing the basis  $P = 0$  in the specific approach, one fixes the “gauge”, thus the definition is “gauge”-dependent. Let us clarify this point by four examples, where the two definitions coincide in the first two examples whereas they differ in the last two.

- The first example treats the “zero” texture, and to fix the ideas let us assume that the texture corresponds to one vanishing entry, say  $(1, 1)$  in the neutrino mass matrix. The specific definition corresponds to a constraint on  $M^{\text{phys}}$  entries, so

$$M_\nu(1, 1) = 0, \text{ “Specific” Zero texture definition at } P = 0. \quad (4)$$

For the generalized definition, we define our texture by

$$M'_\nu(1, 1) = 0 \Rightarrow e^{-2i(\phi_1)} M_\nu(1, 1) = 0. \quad (5)$$

We see now that the two definitions are equivalent and we have

$$M_\nu(1, 1) = 0, \text{ “Generalized” Zero texture definition.} \quad (6)$$

Note that the zero-texture definition is  $P$ -invariant and is identical in both the specific and the generalized definition cases.

- The vanishing minor texture, and to fix the ideas assume it corresponding to one vanishing minor obtained by deleting the entry  $(1, 1)$  in  $M_\nu$ . We thus have

$$M_\nu(2, 2)M_\nu(3, 3) - M_\nu(3, 2)M_\nu(2, 3) = 0, \text{ “Specific” Vanishing minor texture definition at } P = 0. \quad (7)$$

The generalized definition would apply to any  $M_\nu$  where one of the  $M'_\nu = P^* M_\nu P^*$  has the corresponding minor equal to zero. So we put

$$M'_\nu(2, 2)M'_\nu(3, 3) - M'_\nu(3, 2)M'_\nu(2, 3) = 0 \Rightarrow e^{-2i(\phi_2 + \phi_3)} [M_\nu(2, 2)M_\nu(3, 3) - M_\nu(3, 2)M_\nu(2, 3)] = 0 \quad (8)$$

which would give again the same definition

$$M_\nu(2, 2)M_\nu(3, 3) - M_\nu(3, 2)M_\nu(2, 3) = 0, \text{ “Generalized” Vanishing minor texture definition.} \quad (9)$$

The two definitions coincide and the corresponding constraint equation is  $P$ -invariant.

- The third example concerns our Equality texture, and to fix the ideas let us assume it corresponds to an equality of the entries  $(1, 1)$  and  $(2, 2)$  in the neutrino mass matrix. Thus, we start by the specific definition given in the  $P = 0$  slice of vanishing unphysical phases, so we have

$$M_\nu(1, 1) = M_\nu(2, 2), \text{ “Specific” Equality texture definition at } P = 0. \quad (10)$$

Then, for the generalized definition, we define our texture by

$$M'_\nu(1, 1) = M'_\nu(2, 2) \Rightarrow e^{2i(\phi_2 - \phi_1)} M_\nu(1, 1) = M_\nu(2, 2). \quad (11)$$

We try now to eliminate the arbitrary phases and find that the generalized definition of the equality texture would amount to

$$|M_\nu(1, 1)| = |M_\nu(2, 2)|, \text{ “Generalized” Equality texture definition.} \quad (12)$$

Note that this generalized definition is again independent of the unphysical phases and so applies irrespective of which  $P$  we choose. However, we see that the generalized definition represents just one “real” constraint in contrast to the “complex” constraint in the specific definition.



- The specific definition of the  $\mu$ - $\tau$ -symmetry is given simply as

$$M_\nu(1,2) = M_\nu(1,3) \quad , \quad M_\nu(2,2) = M_\nu(3,3), \quad \text{“Specific” } \mu\text{-}\tau\text{-symmetry at } P=0, \quad (13)$$

and so the generalized  $\mu$ - $\tau$ -symmetry would be given by any neutrino mass matrix  $M_\nu$  satisfying

$$M'_\nu(1,2) = M'_\nu(1,3) \quad , \quad M'_\nu(2,2) = M'_\nu(3,3), \quad (14)$$

for one of the many  $M'_\nu$ s related to  $M_\nu$  by an arbitrary phase  $P$ . This leads to

$$e^{-i(\phi_1+\phi_2)}M_\nu(1,2) = e^{-i(\phi_1+\phi_3)}M_\nu(1,3) \quad , \quad e^{-2i\phi_2}M_\nu(2,2) = e^{-2i\phi_3}M_\nu(3,3) \quad (15)$$

. Eliminating the arbitrary phases in a clever way in order to reach a definition not showing the unphysical phases leads to the generalized definition [21]

$$\begin{aligned} |M_\nu(1,2)| &= |M_\nu(1,3)|, |M_\nu(2,2)| = |M_\nu(3,3)| \quad , \quad \text{“Generalized” } \mu\text{-}\tau\text{-symmetry} \\ \arg(22) - \arg(33) + 2\arg(13) - 2\arg(12) &= 0 \quad : \quad \arg(ij) \equiv \arg(M_\nu(ij)) \end{aligned} \quad (16)$$

Note again that the generalized definition is formulated such that the effect of any unphysical parameter cancels out. Put it differently, in order to check whether a given matrix meets the texture definition, it suffices to restrict to the case  $P=0$ .

Even though the specific definition is a basis(gauge)-dependent definition, however nothing wrong with it in the sense that any mass matrix can be, in a unique way by phasing, put into the slice of vanishing unphysical phases  $P=0$ , where the definition is given, and so can be tested whether or not it meets the texture criteria. This specific approach is adopted by all studies (e.g. [9,14]) which pick the slice  $P=0$  for simplicity, but surely the phenomenology will be different from that of the generalized definition.

Note also that it is not always possible to put the generalized definition in a form independent of the unphysical phases like what we did in Eqs. (12,16), so for a vanishing-trace texture [22] defined by ( $\text{Tr}(M_\nu)=0$ ) one can not get rid of the  $P$  in the generalized definition ( $\exists \alpha, \beta \in \mathbb{R} : M_\nu(1,1) + e^{i\alpha}M_\nu(2,2) + e^{i\beta}M_\nu(3,3) = 0$ ). Numerically, the generalized definition corresponds to scanning the parameter space of  $P$  with arbitrary values, whereas in the specific definition,  $P$  is fixed (namely to zero) and we do not scan it.

Mathematically, we define an equivalence relation on the 12-dim space  $\mathcal{M}$  of complex symmetric  $3 \times 3$  matrices  $A$  by:

$$A \sim A' \Leftrightarrow \exists \text{phase matrix } P : A' = P.A.P \quad (17)$$

and the texture is defined actually on the set of equivalence classes  $\mathcal{M}/\sim \equiv \{[M]\}$ . Pictorially, we can represent  $\mathcal{M}$  by the plane with polar coordinates, and any 3-dim equivalence class of  $A$  is represented by the half-line  $D$  from the origin towards  $A$  corresponding to a fixed polar angle, whereas the 9-dim slice of  $P=0$  is represented by the unit-circle  $S$ . Thus, changing  $M^{\text{phys}}$  would mean changing the polar angle, whereas changing the unphysical phases corresponds to changing the polar radius. We see in Fig. 1, that any  $D$  intersects  $S$  once and only once at a point  $f(A)$ , which we call the ‘projection’ of  $A$  onto  $S$ . The two ways to define the texture satisfying a certain constraint  $C$  given by  $g(M)=0$ , where  $g$  is a vector function of 12-real variables, is as follows.

$$\text{“Generalized” definition: } A \in \text{texture} \Leftrightarrow \exists A' \in D : A' \text{ satisfies } C : g(A') = 0 \quad (18)$$

$$\text{“Specific” definition: } A \in \text{texture} \Leftrightarrow f(A) \text{ satisfies } C : g(f(A)) = 0 \quad (19)$$



have the phase freedom that they do have in the low scale effective theory. So, it is easier to fix the phase, say to  $P = 0$ , for the realization models, and consider the defining symmetry, which leads to the texture form, valid at this particular choice of phase. Actually, the nonphysical phases may in principle be determinable in a hitherto unknown fundamental theory, and that when integrating out high scale fields a limited effective Lagrangian survives where these phases are unobservable.

However, once we adopt the specific definition we no longer have freedom of phasing the neutrino mass matrix. In this regard, one can see that the work of [19] and our current work are not equivalent, in that both adopt the specific definition, so two matrices  $(M_{+\nu}, M_{-\nu})$  satisfying say  $(M_{+\nu}^{\text{phys}}(1,1) = +M_{+\nu}^{\text{phys}}(2,2), M_{-\nu}^{\text{phys}}(1,1) = -M_{-\nu}^{\text{phys}}(2,2))$  are not related and have different physics. Had the generalized definition been adopted then both textures of two-equal-elements or two-opposite-elements would have been equivalent because

$$M_\nu(a,b) = M_\nu(c,d), P = \text{diag}(e^{if_1}, e^{if_2}, e^{if_3}) : f_a + f_b - f_c - f_d = \pi \Rightarrow M'_\nu(a,b) = -M'_\nu(c,d) \quad (21)$$

### 3 Notations

As said above, we restrict the study to vanishing unphysical phases. In the flavor basis, the Majorana neutrino mass matrix  $M_\nu$  can be diagonalized by a unitary transformation,

$$V^\dagger M_\nu V^* = \begin{pmatrix} m_1 & 0 & 0 \\ 0 & m_2 & 0 \\ 0 & 0 & m_3 \end{pmatrix}, \quad (22)$$

with  $m_i$  (for  $i = 1, 2, 3$ ) are real and positive neutrino masses. We adopt the parameterization where the third column of  $V$  is real. The three mixing angles  $(\theta_{12}, \theta_{23}, \theta_{13})$  and three phases  $(\rho, \sigma, \delta)$  are introduced as:

$$P = \text{diag}(e^{i\rho}, e^{i\sigma}, 1), U = R_{23}(\theta_{23}) R_{13}(\theta_{13}) \text{diag}(1, e^{-i\delta}, 1) R_{12}(\theta_{12}),$$

$$V = UP = \begin{pmatrix} c_{12}c_{13}e^{i\rho} & s_{12}c_{13}e^{i\sigma} & s_{13} \\ (-c_{12}s_{23}s_{13} - s_{12}c_{23}e^{-i\delta})e^{i\rho} & (-s_{12}s_{23}s_{13} + c_{12}c_{23}e^{-i\delta})e^{i\sigma} & s_{23}c_{13} \\ (-c_{12}c_{23}s_{13} + s_{12}s_{23}e^{-i\delta})e^{i\rho} & (-s_{12}c_{23}s_{13} - c_{12}s_{23}e^{-i\delta})e^{i\sigma} & c_{23}c_{13} \end{pmatrix}, \quad (23)$$

where  $R_{ij}(\theta_{ij})$  is the rotation matrix in the  $(i, j)$ -plane by angle  $\theta_{ij}$  and  $c_{12} \equiv \cos \theta_{12} \dots$ . We note that the  $\mu$ - $\tau$  permutation transformation:

$$T : \theta_{23} \rightarrow \frac{\pi}{2} - \theta_{23} \text{ and } \delta \rightarrow \delta \pm \pi, \quad (24)$$

interchanges the indices 2 and 3 of  $M_\nu$  and keeps the index 1 intact:

$$\begin{aligned} M_{\nu 11} &\leftrightarrow M_{\nu 11} & M_{\nu 12} &\leftrightarrow M_{\nu 13} \\ M_{\nu 22} &\leftrightarrow M_{\nu 33} & M_{\nu 23} &\leftrightarrow M_{\nu 23}. \end{aligned} \quad (25)$$

The solar and atmospheric neutrino mass-squared differences are defined as:

$$\delta m^2 \equiv m_2^2 - m_1^2, \quad \Delta m^2 \equiv \left| m_3^2 - \frac{1}{2}(m_1^2 + m_2^2) \right|, \quad (26)$$

and data indicate that their ratio, denoted by  $R_\nu$ , is quite small:

$$R_\nu \equiv \frac{\delta m^2}{\Delta m^2} \ll 1. \quad (27)$$

By studying neutrinoless double-beta decay and beta-decay kinematics, we obtain two non-oscillation parameters which put constraints on the neutrino mass scales: the effective Majorana mass term:

$$m_{ee} = |m_1 V_{e1}^2 + m_2 V_{e2}^2 + m_3 V_{e3}^2| = |M_{\nu 11}|, \quad (28)$$

and the effective electron-neutrino mass:

$$m_e = \sqrt{\sum_{i=1}^3 (|V_{ei}|^2 m_i^2)}. \quad (29)$$

The ‘sum’parameter  $\Sigma$  is bounded via cosmological observations by:

$$\Sigma = \sum_{i=1}^3 m_i. \quad (30)$$

The last measurable quantity is Jarlskog rephasing invariant quantity [23], which measures CP violation in neutrino oscillation and is given by:

$$J = s_{12} c_{12} s_{23} c_{23} s_{13} c_{13}^2 \sin \delta. \quad (31)$$

The experimental bounds for the oscillation parameters ( $\theta_{12}$ ,  $\theta_{23}$ ,  $\theta_{13}$ ,  $\delta$ ,  $\delta m^2$ ,  $\Delta m^2$  and  $R_\nu$ ) are summarized in Table (1)

Parameter	Hierarchy	Best fit	$1\sigma$	$2\sigma$	$3\sigma$
$\delta m^2$ ( $10^{-5}\text{eV}^2$ )	NH, IH	7.37	[7.21,7.54]	[7.07,7.73]	[6.93,7.96]
$\Delta m^2$ ( $10^{-3}\text{eV}^2$ )	NH	2.53	[2.50,2.57]	[2.45,2.61]	[2.41,2.65]
	IH	2.51	[2.47,2.54]	[2.43,2.58]	[2.39,2.62]
$\theta_{12}$ ( $^\circ$ )	NH, IH	33.02	[32.02,34.09]	[30.98,35.30]	[30.00,36.51]
$\theta_{13}$ ( $^\circ$ )	NH	8.43	[8.30,8.55]	[8.11,8.74]	[7.92,8.90]]
	IH	8.45	[8.27,8.59]	[8.08,8.78]	[7.92,8.94]]
$\theta_{23}$ ( $^\circ$ )	NH	40.69	[39.82,41.89]	[38.93,43.29]	[38.10,51.66]]
	IH	42.42	[40.23, 42.02] $\cup$ [48.86, 51.06]	[39.18, 44.02] $\cup$ [46.89, 52.01]	[38.29, 52.90]
$\delta$ ( $^\circ$ )	NH	248.40	[212.40, 289.80]	[180.00, 342.00]	[0.00, 30.60] $\cup$ [136.80, 360]
	IH	235.80	[201.60, 291.60]	[165.60, 338.40]	[0, 27.00] $\cup$ [124.20, 360]

Table 1: The experimental bounds for the oscillation parameters at 1-2-3 $\sigma$ -levels, taken from the global fit to neutrino oscillation data [15]. Normal and Inverted Hierarchies are respectively denoted by NH and IH

For the non-oscillation parameters  $\Sigma$  and  $m_{ee}$ , we adopt the ranges mentioned in the recent reference [24], while for  $m_e$  we adopt values found earlier [25]:

$$\begin{aligned} \Sigma &< 0.7 \text{ eV}, \\ m_{ee} &< 0.3 \text{ eV}, \\ m_e &< 1.8 \text{ eV}. \end{aligned} \quad (32)$$

## 4 Texture of an equality between two matrix elements

Because  $M_\nu$  is a symmetric matrix and has 6 independent elements, we have 15 possibilities ( $C_6^2 = 15$ ) for equality between two independent matrix elements. The texture structures can be classified into 7 categories, each -except the last- has 2 elements:

$$\begin{aligned}
A_1 : & \begin{pmatrix} a & a & c \\ a & b & d \\ c & d & e \end{pmatrix}, \quad A_2 : \begin{pmatrix} a & b & a \\ b & c & d \\ a & d & e \end{pmatrix}; \\
B_1 : & \begin{pmatrix} a & b & c \\ b & b & d \\ c & d & e \end{pmatrix}, \quad B_2 : \begin{pmatrix} a & b & c \\ b & d & e \\ c & e & c \end{pmatrix}; \\
C_1 : & \begin{pmatrix} a & b & c \\ b & d & e \\ c & e & e \end{pmatrix}, \quad C_2 : \begin{pmatrix} a & b & c \\ b & d & d \\ c & d & e \end{pmatrix}; \\
D_1 : & \begin{pmatrix} a & b & c \\ b & c & d \\ c & d & e \end{pmatrix}, \quad D_2 : \begin{pmatrix} a & b & c \\ b & d & e \\ c & e & b \end{pmatrix}; \\
E_1 : & \begin{pmatrix} a & b & c \\ b & a & d \\ c & d & e \end{pmatrix}, \quad E_2 : \begin{pmatrix} a & b & c \\ b & d & e \\ c & e & a \end{pmatrix}; \\
F_1 : & \begin{pmatrix} a & b & c \\ b & d & b \\ c & b & e \end{pmatrix}, \quad F_2 : \begin{pmatrix} a & b & c \\ b & d & c \\ c & c & e \end{pmatrix}; \\
G_1 : & \begin{pmatrix} a & b & c \\ b & d & a \\ c & a & e \end{pmatrix}, \quad G_2 : \begin{pmatrix} a & b & c \\ b & d & e \\ c & e & d \end{pmatrix}, \quad G_3 : \begin{pmatrix} a & b & b \\ b & c & d \\ b & d & e \end{pmatrix}.
\end{aligned} \tag{33}$$

We see that, apart from the G-category, the two elements in each category are transformed into each other upon carrying out a  $\mu$ - $\tau$  interchange symmetry. Each of the three elements in the G-category is invariant under  $\mu$ - $\tau$  transformation. Therefore, there are 9 independent patterns out of the 15 possible ones. Apart from the G-category, we shall limit our presentation to the first element in each remaining category and denote it by the category letter, i.e. dropping  $A_2$  we take  $A \equiv A_1$  (idem for other categories).

The equality condition is written as:

$$M_{\nu \ ab} - M_{\nu \ cd} = 0, \tag{34}$$

then we get

$$\sum_{k=1}^3 (U_{ak}U_{bk} - U_{ck}U_{dk})\lambda_k = 0, \tag{35}$$

where  $\lambda_1 = m_1 e^{2i\rho}$ ,  $\lambda_2 = m_2 e^{2i\sigma}$  and  $\lambda_3 = m_3$ . By solving Eq. (35), we get the mass ratios as functions of the mixing and phase angles:

$$\frac{m_1}{m_2} = \frac{\Re(A_3)\Im(A_2 e^{2i\sigma}) - \Re(A_2 e^{2i\sigma})\Im(A_3)}{\Re(A_2 e^{2i\sigma})\Im(A_1 e^{2i\rho}) - \Re(A_1 e^{2i\rho})\Im(A_2 e^{2i\sigma})}, \tag{36}$$

$$\frac{m_2}{m_3} = \frac{\Re(A_1 e^{2i\rho})\Im(A_3) - \Re(A_3)\Im(A_1 e^{2i\rho})}{\Re(A_2 e^{2i\sigma})\Im(A_1 e^{2i\rho}) - \Re(A_1 e^{2i\rho})\Im(A_2 e^{2i\sigma})}, \tag{37}$$

where the coefficients  $A_k$  is defined as,

$$A_k = U_{ak}U_{bk} - U_{ck}U_{dk}, \quad k = 1, 2, 3. \quad (38)$$

The neutrino masses are written as,

$$m_3 = \sqrt{\frac{\delta m^2}{(\frac{m_2}{m_3})^2 - (\frac{m_1}{m_3})^2}}, \quad m_1 = m_3 \times \frac{m_1}{m_3}, \quad m_2 = m_3 \times \frac{m_2}{m_3}. \quad (39)$$

As we see, there are seven input parameters ( $\theta_{12}, \theta_{23}, \theta_{13}, \delta, \rho, \sigma, \delta m^2$ ) which together with the two real conditions in Eq. (35) permit us to determine the nine degrees of freedom of  $M_\nu$ . The strategy we follow consists of spanning ( $\theta_{12}, \theta_{23}, \theta_{13}, \delta, \delta m^2$ ) over their experimental ranges at the 1-2-3 $\sigma$ -levels, while two Majorana-phases ( $\rho$  and  $\sigma$ ) are covered over their full ranges. Thus, we can determine the allowed regions in the 7-dim space at the 1-2-3 $\sigma$ -levels satisfying the other experimental constraints of  $\Delta m^2$  together with those of Eq. (32). Moreover, the correlations between any two of the neutrino physical parameters ( $\theta_{12}, \theta_{23}, \theta_{13}, \delta, \rho, \sigma, m_1, m_2, m_3, m_{ee}, m_e, J$ ) can be studied graphically.

## 5 Numerical discussion

In this section, we state the results of our numerical analysis for the nine possible independent textures<sup>§</sup>. For each pattern, we introduce the coefficients  $A$ 's of Eq. (38), and evaluate the analytical expressions for the mass ratios and other neutrino physical parameters, which, however, are found to be too cumbersome to be presented even in their approximate form. The allowed ranges of the neutrino physical parameters ( $\theta_{12}, \theta_{23}, \theta_{13}, \delta, \rho, \sigma, m_1, m_2, m_3, m_{ee}, m_e$  and  $J$ ) at all statistical levels for each type of hierarchy are listed in Tables (2,3). We present 21 correlation plots for each independent pattern for both normal and inverted ordering generated from the accepted points of the neutrino physical parameters at the 2- $\sigma$ -level. Moreover, we state the neutrino mass matrix  $M_\nu$  for each independent texture with either hierarchy type at one representative acceptable point in the parameter space at the 3- $\sigma$ -level. We chose this representative point to be as close as possible to the best fit values for mixing and Dirac phase angles.

For each point, out of  $N$  of order ( $10^6$ - $10^{10}$ ) thrown randomly in the 7-dim space of the parameters ( $\theta_{12}, \theta_{23}, \theta_{13}, \delta, \rho, \sigma, \delta m^2$ ), we test the other experimental constraints of  $\Delta m^2$  together with those of Eq. (32) in order to determine the acceptable regions in the parameter space. We find that among the presented patterns, only the texture  $C$  with inverted hierarchy is ruled out experimentally.

From Tables (2,3), we see that the first neutrino mass  $m_1$  can reach a vanishing value, in normal ordering, for  $A$  and  $C$  patterns at all statistical levels as well as  $G_2$  pattern at the 3- $\sigma$ -level. However, the third neutrino mass  $m_3$  can reach zero value, in inverted ordering, for  $A, B, D, F, G_2, G_3$  patterns at all  $\sigma$ -levels. Thus, out of the nine independent textures, three textures are predicted to allow for singular (non-invertible) neutrino mass matrix for normal ordering, whereas six textures can become singular in the case of inverted ordering. The predictions for the singular textures are consistent with the results found in [18]. The effective Majorana mass ( $m_{ee}$ ) can reach zero value in the case of normal ordering with regard to  $A, C$

---

<sup>§</sup>As said before, we checked that the numerical results of the remaining 6 patterns ( $X_2 : X = A, \dots, F$ ) differ slightly from their  $\mu$ - $\tau$ -symmetry related patterns, although the experimental constraints are not symmetric, so we opted not to present them.

patterns at all  $\sigma$ -levels, and  $G_2$  pattern at the 3- $\sigma$ - level. The allowed values of the  $J$  parameter at the 1-2- $\sigma$ -levels for normal ordering and 1- $\sigma$ - level for inverted ordering are negative in all patterns, which means that  $\delta$  must belong to the third and fourth quarters. For both normal and inverted ordering in all patterns, the correlation between  $(\delta, J)$  is sinusoidal because of tiny variation of the mixing angles compared to the Dirac phase, thus  $J \propto \sin \delta$ . The appearing sinusoidal envelope is not covering a full sine curve, but rather the portion corresponding to the acceptable range of  $\delta$ . We also find a quasi degeneracy characterized by  $m_1 \approx m_2$  for all patterns in inverted type.

In the next subsections, we discuss the numerical results for each independent pattern supplemented by the correlation plots for each hierarchy type. For each pattern apart from  $C$ , there are two large figures where the red (blue) sub-figures represent the correlation plots for normal (inverted) hierarchy. In the first figure, there exist four rows, where the first represents the correlations between the mixing angles while the next three ones depict the correlations between each mixing angle with the CP-violating phases. For the second figure, there are three rows, where the first represents the correlations between the CP-violating phases, the second represents the correlations between the experimentally constrained phase  $\delta$  and each of  $J$ , LNM (the lowest neutrino mass) and  $m_{ee}$ , and the third row shows the degree of hierarchy for each pattern.

Pattern $A \equiv M_{\nu 11} = M_{\nu 12}$												
quantity	$\theta_{12}^\circ$	$\theta_{23}^\circ$	$\theta_{13}^\circ$	$\delta^\circ$	$\rho^\circ$	$\sigma^\circ$	$m_1$ ( $10^{-1}$ eV)	$m_2$ ( $10^{-1}$ eV)	$m_3$ ( $10^{-1}$ eV)	$m_{ee}$ ( $10^{-1}$ eV)	$m_e$ ( $10^{-1}$ eV)	$J$ ( $10^{-1}$ )
						Normal Hierarchy						
$1\sigma$	32.02 – 34.09	39.82 – 41.89	8.30 – 8.55	212.41 – 289.79	0.22 – 179.57	0.03 – 179.98	$5.40 \times 10^{-7} - 0.58$	0.08 – 0.59	0.50 – 0.77	$4.56 \times 10^{-4} - 0.36$	0.08 – 0.59	–0.33 – –0.17
$2\sigma$	30.98 – 35.30	38.93 – 43.28	8.11 – 8.74	181.09 – 341.95	$0.02 - 76.37 \cup 80.60 - 179.84$	0.03 – 127.00 $\cup$ 131.90 – 179.95	$9.99 \times 10^{-5} - 0.60$	0.08 – 0.61	0.49 – 0.78	$3.32 \times 10^{-3} - 0.38$	0.08 – 0.61	–0.34 – –0.00
$3\sigma$	30.00 – 36.51	38.10 – 51.65	7.92 – 8.90	$0.05 - 30.58 \cup 136.80 - 358.31$	0.31 – 179.97	0.02 – 179.97	$1.60 \times 10^{-5} - 0.65$	0.08 – 0.66	0.49 – 0.83	$3.21 \times 10^{-4} - 0.40$	0.08 – 0.66	–0.36 – 0.23
						Inverted Hierarchy						
$1\sigma$	32.02 – 34.09	$40.23 - 42.02 \cup 48.86 - 51.06$	8.27 – 8.59	202.74 – 240.66	0.66 – 179.77	0.30 – 179.92	0.49 – 2.31	0.50 – 2.32	$2.06 \times 10^{-4} - 2.26$	0.24 – 1.37	0.49 – 2.31	–0.29 – –0.12
$2\sigma$	30.98 – 35.30	$39.18 - 44.02 \cup 46.89 - 52.00$	8.08 – 8.78	165.90 – 244.70	0.04 – 179.90	0.05 – 179.93	0.49 – 2.03	0.49 – 2.03	$7.09 \times 10^{-5} - 1.97$	0.23 – 1.03	0.48 – 2.03	–0.31 – 0.07
$3\sigma$	30.00 – 36.50	38.31 – 52.89	7.92 – 8.94	124.30 – 247.39	0.16 – 179.87	0.09 – 179.23	0.48 – 2.05	0.49 – 2.05	$1.03 \times 10^{-4} - 1.99$	0.23 – 1.02	0.48 – 2.05	–0.32 – 0.29
Pattern $B \equiv M_{\nu 12} = M_{\nu 22}$												
quantity	$\theta_{12}^\circ$	$\theta_{23}^\circ$	$\theta_{13}^\circ$	$\delta^\circ$	$\rho^\circ$	$\sigma^\circ$	$m_1$ ( $10^{-1}$ eV)	$m_2$ ( $10^{-1}$ eV)	$m_3$ ( $10^{-1}$ eV)	$m_{ee}$ ( $10^{-1}$ eV)	$m_e$ ( $10^{-1}$ eV)	$J$ ( $10^{-1}$ )
						Normal Hierarchy						
$1\sigma$	32.02 – 34.08	39.82 – 41.89	8.30 – 8.55	212.43 – 289.76	3.13 – 179.97	$0.07 - 25.94 \cup 106.70 - 179.96$	0.14 – 1.21	0.16 – 1.21	0.52 – 1.31	0.05 – 0.96	0.16 – 1.21	–0.33 – –0.17
$2\sigma$	30.98 – 35.29	38.93 – 43.29	8.11 – 8.73	180.01 – 341.92	0.09 – 179.99	0.12 – 179.74	0.12 – 2.01	0.15 – 2.01	0.51 – 2.08	0.04 – 1.65	0.15 – 2.01	–0.34 – 0.00
$3\sigma$	30.00 – 36.50	38.10 – 51.65	7.92 – 8.90	$2.42 - 30.54 \cup 136.80 - 359.73$	0.15 – 179.94	0.15 – 179.94	0.11 – 1.46	0.14 – 1.47	0.51 – 1.55	0.04 – 1.42	0.14 – 1.47	–0.36 – 0.23
						Inverted Hierarchy						
$1\sigma$	32.02 – 34.08	$40.23 - 42.02 \cup 48.86 - 51.05$	8.27 – 8.59	221.48 – 291.57	0.00 – 179.95	0.036 – 179.89	0.49 – 2.33	0.50 – 2.33	$3.49 \times 10^{-5} - 2.28$	0.41 – 2.29	0.49 – 2.33	–0.33 – –0.26 $\cup$ –0.25 – –0.21
$2\sigma$	30.98 – 35.29	$39.18 - 44.02 \cup 46.90 - 51.99$	8.08 – 8.78	213.89 – 334.69	0.03 – 179.99	0.15 – 179.97	0.49 – 2.19	0.49 – 2.20	$1.24 \times 10^{-4} - 2.14$	0.41 – 2.14	0.48 – 2.19	–0.34 – –0.14
$3\sigma$	30.00 – 36.51	38.29 – 52.89	7.92 – 8.94	$124.40 - 138.50 \cup 211.30 - 336.11$	0.05 – 179.84	0.02 – 179.94	0.48 – 2.18	0.49 – 2.18	$6.66 \times 10^{-6} - 2.13$	0.41 – 2.08	0.48 – 2.18	–0.35 – –0.11 $\cup$ 0.21 – 0.26
Pattern $C \equiv M_{\nu 23} = M_{\nu 33}$												
quantity	$\theta_{12}^\circ$	$\theta_{23}^\circ$	$\theta_{13}^\circ$	$\delta$	$\rho$	$\sigma$	$m_1$ ( $10^{-1}$ eV)	$m_2$ ( $10^{-1}$ eV)	$m_3$ ( $10^{-1}$ eV)	$m_{ee}$ ( $10^{-1}$ eV)	$m_e$ ( $10^{-1}$ eV)	$J$ ( $10^{-1}$ )
						Normal Hierarchy						
$1\sigma$	32.02 – 34.09	39.82 – 40.78	8.30 – 8.55	212.40 – 272.16	$0.09 - 109.40 \cup 144.00 - 179.85$	0.12 – 6.39 $\cup$ 114.10 – 179.79	$1.60 \times 10^{-4} - 0.17$	0.08 – 0.19	0.50 – 0.54	$1.21 \times 10^{-3} - 0.07$	0.08 – 0.19	–0.33 – –0.17
$2\sigma$	30.98 – 35.30	38.93 – 41.28	8.11 – 8.74	180.01 – 341.19	0.01 – 179.97	$0.11 - 53.97 \cup 56.28 - 74.37 \cup 78.27 - 179.99$	$2.82 \times 10^{-5} - 0.30$	0.08 – 0.31	0.50 – 0.58	$4.66 \times 10^{-4} - 0.12$	0.08 – 0.31	–0.34 – 0.00
$3\sigma$	30.00 – 36.50	$38.10 - 41.74 \cup 50.17 - 51.63$	7.92 – 8.90	$0.25 - 30.50 \cup 136.90 - 359.84$	0.00 – 179.91	0.05 – 179.97	$2.80 \times 10^{-5} - 0.35$	0.08 – 0.36	0.49 – 0.61	$5.84 \times 10^{-4} - 0.11$	0.08 – 0.36	–0.35 – 0.23
						Inverted Hierarchy						
$1\sigma$	×	×	×	×	×	×	×	×	×	×	×	×
$2\sigma$	×	×	×	×	×	×	×	×	×	×	×	×
$3\sigma$	×	×	×	×	×	×	×	×	×	×	×	×
Pattern $D \equiv M_{\nu 13} = M_{\nu 22}$												
quantity	$\theta_{12}^\circ$	$\theta_{23}^\circ$	$\theta_{13}^\circ$	$\delta^\circ$	$\rho^\circ$	$\sigma^\circ$	$m_1$ ( $10^{-1}$ eV)	$m_2$ ( $10^{-1}$ eV)	$m_3$ ( $10^{-1}$ eV)	$m_{ee}$ ( $10^{-1}$ eV)	$m_e$ ( $10^{-1}$ eV)	$J$ ( $10^{-1}$ )
						Normal Hierarchy						
$1\sigma$	32.02 – 34.09	39.82 – 41.89	8.30 – 8.55	212.42 – 289.79	$0.10 - 45.15 \cup 92.08 - 179.91$	0.02 – 44.11 $\cup$ 95.18 – 179.98	0.22 – 2.12	0.24 – 2.13	0.55 – 2.18	0.10 – 1.47	0.24 – 2.13	–0.33 – –0.17
$2\sigma$	30.98 – 35.29	38.93 – 43.28	8.11 – 8.74	180.01 – 341.94	0.05 – 179.62	0.02 – 179.98	0.20 – 1.93	0.21 – 1.93	0.54 – 2.00	0.09 – 1.36	0.22 – 1.93	–0.34 – 0.00
$3\sigma$	30.00 – 36.51	38.10 – 51.61	7.92 – 8.90	$0.03 - 30.55 \cup 136.80 - 359.97$	0.04 – 179.92	0.15 – 179.76	0.17 – 1.99	0.18 – 2.00	0.52 – 2.06	0.07 – 1.59	0.19 – 2.00	–0.35 – 0.23
						Inverted Hierarchy						
$1\sigma$	32.02 – 34.09	$40.23 - 42.02 \cup 48.86 - 51.0$	8.27 – 8.59	202.03 – 291.53	0.06 – 179.99	0.36 – 179.74	0.49 – 2.27	0.50 – 2.28	$3.13 \times 10^{-4} - 2.22$	0.30 – 2.17	0.49 – 2.27	–0.35 – –0.12
$2\sigma$	30.98 – 35.29	$39.18 - 44.02 \cup 46.89 - 52.01$	8.08 – 8.78	$165.70 - 171.90 \cup 183.30 - 289.80 \cup 292.10 - 320.90$	$0.20 - 51.22 \cup 53.63 - 179.97$	0.02 – 179.94	0.49 – 2.11	0.49 – 2.11	$1.32 \times 10^{-4} - 2.05$	0.30 – 1.81	0.48 – 2.11	–0.34 – 0.01 $\cup$ 0.04 – 0.08
$3\sigma$	30.01 – 36.50	38.29 – 52.89	7.92 – 8.94	$124.20 - 191.10 \cup 195.40 - 317.00 \cup 322.70 - 339.83$	0.20 – 179.99	0.02 – 179.85	0.48 – 2.24	0.49 – 2.25	$1.11 \times 10^{-4} - 2.19$	0.29 – 1.99	0.48 – 2.24	–0.36 – 0.09 $\cup$ –0.04 – –0.01 $\cup$ 0.01 – 0.28

Table 2: The 1-2-3  $\sigma$  predictions for the neutrino physical parameters ( $\theta_{12}$ ,  $\theta_{23}$ ,  $\theta_{13}$ ,  $\delta$ ,  $\rho$ ,  $\sigma$ ,  $m_1$ ,  $m_2$ ,  $m_3$ ,  $m_{ee}$ ,  $m_e$  and  $J$ ) with regard to A, B, C and D categories.



Pattern $E \equiv M_{\nu\ 11} = M_{\nu\ 22}$												
quantity	$\theta_{12}^\circ$	$\theta_{23}^\circ$	$\theta_{13}^\circ$	$\delta^\circ$	$\rho^\circ$	$\sigma^\circ$	$m_1$ (10 <sup>-1</sup> eV)	$m_2$ (10 <sup>-1</sup> eV)	$m_3$ (10 <sup>-1</sup> eV)	$m_{ee}$ (10 <sup>-1</sup> eV)	$m_e$ (10 <sup>-1</sup> eV)	$J$ (10 <sup>-1</sup> )
Normal Hierarchy												
1 $\sigma$	32.02 – 34.09	39.82 – 41.89	8.30 – 8.55	212.41 – 289.79	0.04 – 33.30 $\cup$ 150.90 – 179.92	0.04 – 55.12 $\cup$ 94.34 – 179.95	0.11 – 1.75	0.14 – 1.75	0.51 – 1.82	0.12 – 0.96	0.14 – 1.75	-0.33 – -0.17
2 $\sigma$	30.98 – 35.30	38.93 – 43.28	8.11 – 8.74	180.22 – 341.62	0.00 – 37.61 $\cup$ 149.00 – 179.93	0.04 – 82.22 $\cup$ 86.23 – 179.96	0.10 – 1.57	0.13 – 1.57	0.51 – 1.65	0.11 – 1.22	0.13 – 1.57	-0.34 – 0.00
3 $\sigma$	30.00 – 36.50	38.10 – 51.65	7.92 – 8.90	2.68 – 30.54 $\cup$ 136.80 – 359.86	0.02 – 36.48 $\cup$ 148.90 – 179.89	0.00 – 179.97	0.10 – 1.66	0.13 – 1.66	0.51 – 1.73	0.11 – 1.60	0.13 – 1.66	-0.35 – 0.24
Inverted Hierarchy												
1 $\sigma$	30.02 – 34.09	40.23 – 42.02 $\cup$ 48.86 – 51.06	8.27 – 8.59	202.19 – 291.58	0.08 – 32.95 $\cup$ 152.80 – 179.88	15.01 – 142.37	0.53 – 2.28	0.53 – 2.28	0.18 – 2.22	0.19 – 1.83	0.52 – 2.28	-0.33 – -0.12
2 $\sigma$	30.98 – 35.30	39.18 – 44.02 $\cup$ 46.90 – 52.01	8.08 – 8.78	166.10 – 170.40 $\cup$ 192.70 – 338.38	0.05 – 35.59 $\cup$ 150.60 – 179.98	9.58 – 165.37	0.51 – 2.33	0.52 – 2.33	0.16 – 2.28	0.17 – 2.10	0.51 – 2.33	-0.34 – -0.06 $\cup$ 0.05 – 0.07
3 $\sigma$	30.00 – 36.50	38.29 – 52.89	7.92 – 8.94	0.14 – 26.74 $\cup$ 124.20 – 171.50 $\cup$ 192.70 – 359.40	0.00 – 37.91 $\cup$ 150.40 – 179.99	15.24 – 168.73	0.50 – 2.19	0.51 – 2.19	0.13 – 2.13	0.14 – 1.78	0.50 – 2.18	-0.35 – 0.29
Pattern $F \equiv M_{\nu\ 12} = M_{\nu\ 23}$												
quantity	$\theta_{12}^\circ$	$\theta_{23}^\circ$	$\theta_{13}^\circ$	$\delta$	$\rho$	$\sigma$	$m_1$ (10 <sup>-1</sup> eV)	$m_2$ (10 <sup>-1</sup> eV)	$m_3$ (10 <sup>-1</sup> eV)	$m_{ee}$ (10 <sup>-1</sup> eV)	$m_e$ (10 <sup>-1</sup> eV)	$J$ (10 <sup>-1</sup> )
Normal Hierarchy												
1 $\sigma$	32.02 – 34.09	39.82 – 41.88	8.30 – 8.55	212.47 – 289.78	10.49 – 116.06	36.80 – 147.42	0.21 – 1.61	0.22 – 1.61	0.54 – 1.68	0.08 – 1.49	0.23 – 1.61	-0.33 – -0.17
2 $\sigma$	30.99 – 35.30	38.92 – 43.29	8.11 – 8.74	180.60 – 341.97	2.37 – 178.20	18.94 – 178.30	0.20 – 2.18	0.21 – 2.19	0.54 – 2.24	0.05 – 2.11	0.22 – 2.19	-0.34 – 0.00
3 $\sigma$	30.00 – 36.50	38.10 – 51.63	7.92 – 8.90	0.04 – 30.55 $\cup$ 137.00 – 172.80 $\cup$ 185.50 – 359.98	0.46 – 2.90 $\cup$ 6.75 – 175.70 $\cup$ 178.50 – 179.17	0.03 – 39.51 $\cup$ 44.10 – 179.95	0.19 – 2.16	0.21 – 2.16	0.53 – 2.22	0.04 – 1.92	0.21 – 2.16	-0.36 – 0.23
Inverted Hierarchy												
1 $\sigma$	32.02 – 34.09	40.23 – 42.02 $\cup$ 48.86 – 51.06	8.27 – 8.59	201.63 – 291.58	0.03 – 179.88	0.13 – 179.94	0.49 – 1.93	0.50 – 1.93	$6.86 \times 10^{-5}$ – 1.87	0.30 – 1.71	0.49 – 1.93	-0.33 – -0.11
2 $\sigma$	30.98 – 35.29	39.18 – 44.02 $\cup$ 46.89 – 52.00	8.08 – 8.78	166.14 – 333.51	0.06 – 179.96	0.25 – 179.71	0.49 – 2.06	0.49 – 2.06	$1.53 \times 10^{-5}$ – 2.00	0.29 – 1.97	0.48 – 2.06	-0.34 – 0.08
3 $\sigma$	30.00 – 36.51	38.30 – 52.89	7.92 – 8.94	124.30 – 173.50 $\cup$ 181.00 – 330.87	0.01 – 179.86	0.05 – 179.98	0.48 – 2.00	0.49 – 2.10	$6.13 \times 10^{-5}$ – 2.04	0.28 – 1.98	0.48 – 2.09	-0.36 – 0.06 $\cup$ -0.03 – 0.00 $\cup$ 0.03
Pattern $G_1 \equiv M_{\nu\ 11} = M_{\nu\ 23}$												
quantity	$\theta_{12}^\circ$	$\theta_{23}^\circ$	$\theta_{13}^\circ$	$\delta^\circ$	$\rho^\circ$	$\sigma^\circ$	$m_1$ (10 <sup>-1</sup> eV)	$m_2$ (10 <sup>-1</sup> eV)	$m_3$ (10 <sup>-1</sup> eV)	$m_{ee}$ (10 <sup>-1</sup> eV)	$m_e$ (10 <sup>-1</sup> eV)	$J$ (10 <sup>-1</sup> )
Normal Hierarchy												
1 $\sigma$	32.02 – 34.08	39.82 – 41.89	8.30 – 8.55	212.41 – 289.79	0.00 – 27.79 $\cup$ 163.40 – 179.97	0.06 – 179.98	0.18 – 2.20	0.20 – 2.21	0.54 – 2.26	0.18 – 2.17	0.20 – 2.21	-0.33 – -0.17
2 $\sigma$	30.98 – 35.30	38.93 – 43.28	8.11 – 8.74	180.02 – 260.70 $\cup$ 267.00 – 271.00 $\cup$ 274.40 – 341.98	0.02 – 29.18 $\cup$ 149.60 – 179.99	0.08 – 88.98 $\cup$ 93.51 – 97.62 $\cup$ 101.40 – 179.87	0.15 – 1.92	0.18 – 1.92	0.52 – 1.98	0.17 – 1.02	0.18 – 1.92	-0.34 – 0.00
3 $\sigma$	30.00 – 36.51	38.10 – 51.66	7.92 – 8.90	0.02 – 30.50 $\cup$ 137.10 – 359.94	0.08 – 30.42 $\cup$ 149.70 – 179.99	0.05 – 77.41 $\cup$ 82.15 – 91.70 $\cup$ 104.90 – 179.98	0.15 – 2.18	0.17 – 2.19	0.52 – 2.24	0.17 – 2.03	0.17 – 2.19	-0.33 – 0.24
Inverted Hierarchy												
1 $\sigma$	32.02 – 34.09	40.23 – 42.01 $\cup$ 48.86 – 51.05	8.27 – 8.59	201.60 – 262.90 $\cup$ 280.10 – 291.48	0.02 – 29.58 $\cup$ 158.60 – 179.98	16.67 – 168.14	0.53 – 2.24	0.53 – 2.24	0.18 – 2.18	0.20 – 2.04	0.52 – 2.24	-0.32 – -0.11
2 $\sigma$	30.98 – 35.29	39.18 – 44.02 $\cup$ 46.89 – 52.01	8.08 – 8.78	165.62 – 264.10 $\cup$ 280.20 – 338.37	0.03 – 31.48 $\cup$ 149.80 – 179.90	10.25 – 164.82	0.51 – 2.29	0.51 – 2.29	0.14 – 2.24	0.16 – 1.74	0.50 – 2.29	-0.34 – 0.08
3 $\sigma$	30.00 – 36.50	38.29 – 52.89	7.92 – 8.94	0.06 – 26.94 $\cup$ 124.60 – 261.40 $\cup$ 277.80 – 359.88	0.11 – 32.96 $\cup$ 147.00 – 179.97	15.41 – 166.37	0.50 – 2.29	0.51 – 2.30	0.11 – 2.24	0.14 – 1.70	0.50 – 2.29	-0.35 – 0.28
Pattern $G_2 \equiv M_{\nu\ 22} = M_{\nu\ 33}$												
quantity	$\theta_{12}^\circ$	$\theta_{23}^\circ$	$\theta_{13}^\circ$	$\delta^\circ$	$\rho^\circ$	$\sigma^\circ$	$m_1$ (10 <sup>-1</sup> eV)	$m_2$ (10 <sup>-1</sup> eV)	$m_3$ (10 <sup>-1</sup> eV)	$m_{ee}$ (10 <sup>-1</sup> eV)	$m_e$ (10 <sup>-1</sup> eV)	$J$ (10 <sup>-1</sup> )
Normal Hierarchy												
1 $\sigma$	32.02 – 34.08	39.82 – 41.88	8.30 – 8.55	212.42 – 289.69	45.13 – 165.46	6.73 – 105.31	0.17 – 1.68	0.19 – 1.68	0.53 – 1.75	0.05 – 1.38	0.19 – 1.68	-0.33 – -0.17
2 $\sigma$	30.98 – 35.29	38.95 – 43.29	8.11 – 8.74	180.06 – 341.99	0.13 – 6.23 $\cup$ 22.85 – 42.85 $\cup$ 46.57 – 179.81	0.01 – 149.50 $\cup$ 162.10 – 179.94	0.08 – 2.23	0.12 – 2.23	0.50 – 2.29	0.01 – 2.22	0.12 – 2.23	-0.34 – 0.00
3 $\sigma$	30.00 – 36.50	38.28 – 51.27	7.92 – 8.89	0.05 – 30.54 $\cup$ 136.90 – 359.94	0.00 – 179.96	0.01 – 179.96	$2.10 \times 10^{-5}$ – 1.09	0.08 – 1.10	0.49 – 1.20	$1.99 \times 10^{-3}$ – 1.06	0.08 – 1.10	-0.35 – 0.24
Inverted Hierarchy												
1 $\sigma$	32.02 – 34.08	40.23 – 44.02 $\cup$ 48.86 – 51.06	8.27 – 8.59	201.72 – 291.58	0.06 – 179.98	0.48 – 179.69	0.49 – 2.25	0.50 – 2.25	$8.75 \times 10^{-6}$ – 2.19	0.34 – 2.18	0.49 – 2.25	-0.33 – -0.12
2 $\sigma$	30.98 – 35.29	39.18 – 44.02 $\cup$ 46.90 – 52.01	8.08 – 8.78	169.40 – 175.40 $\cup$ 184.20 – 333.91	0.01 – 179.99	0.20 – 179.87	0.49 – 2.33	0.49 – 2.33	$1.53 \times 10^{-5}$ – 2.27	0.27 – 2.25	0.48 – 2.33	-0.35 – -0.02 $\cup$ 0.02 – 0.06
3 $\sigma$	30.00 – 36.51	38.29 – 52.90	7.92 – 8.94	1.02 – 26.32 $\cup$ 124.30 – 357.56	0.04 – 179.87	0.02 – 179.97	0.48 – 2.18	0.49 – 2.19	$8.61 \times 10^{-5}$ – 2.13	0.24 – 2.11	0.48 – 2.18	-0.36 – 0.28
Pattern $G_3 \equiv M_{\nu\ 12} = M_{\nu\ 13}$												
quantity	$\theta_{12}^\circ$	$\theta_{23}^\circ$	$\theta_{13}^\circ$	$\delta^\circ$	$\rho^\circ$	$\sigma^\circ$	$m_1$ (10 <sup>-1</sup> eV)	$m_2$ (10 <sup>-1</sup> eV)	$m_3$ (10 <sup>-1</sup> eV)	$m_{ee}$ (10 <sup>-1</sup> eV)	$m_e$ (10 <sup>-1</sup> eV)	$J$ (10 <sup>-1</sup> )
Normal Hierarchy												
1 $\sigma$	32.02 – 34.09	39.82 – 41.89	8.30 – 8.55	212.40 – 289.43	40.15 – 178.53	41.26 – 178.50	0.17 – 1.83	0.19 – 1.83	0.53 – 1.90	0.17 – 1.83	0.19 – 1.83	-0.33 – -0.17
2 $\sigma$	30.98 – 35.29	38.93 – 43.28	8.11 – 8.74	180.06 – 338.47	19.08 – 179.72	25.52 – 179.71	0.14 – 2.08	0.17 – 2.08	0.52 – 2.14	0.13 – 2.08	0.17 – 2.08	-0.34 – 0.00
3 $\sigma$	30.00 – 36.51	38.11 – 44.52 $\cup$ 45.57 – 51.65	7.92 – 8.90	0.10 – 30.55 $\cup$ 137.00 – 358.92	0.31 – 179.95	0.03 – -179.40	0.13 – 2.24	0.15 – 2.24	0.51 – 2.30	0.12 – 2.24	0.16 – 2.24	-0.35 – 0.23
Inverted Hierarchy												
1 $\sigma$	32.02 – 34.09	40.23 – 42.02 $\cup$ 48.86 – 51.06	8.27 – 8.59	201.68 – 291.57	0.03 – 179.98	0.04 – 179.99	0.49 – 2.27	0.50 – 2.27	$6.66 \times 10^{-5}$ – 2.22	0.48 – 2.22	0.49 – 2.27	-0.33 – -0.11
2 $\sigma$	30.98 – 35.29	39.18 – 43.97 $\cup$ 46.89 – 52.01	8.08 – 8.78	165.64 – 338.33	0.06 – 179.99	0.01 – 179.97	0.49 – 1.98	0.49 – 1.98	$8.18 \times 10^{-5}$ – 1.92	0.48 – 1.98	0.48 – 1.98	-0.33 – 0.08
3 $\sigma$	30.00 – 36.50	38.29 – 44.51 $\cup$ 45.47 – 52.89	7.92 – 8.94	0.18 – 26.97 $\cup$ 124.20 – 359.89	0.01 – 179.95	0.05 – 179.99	0.48 – 2.25	0.49 – 2.25	$3.78 \times 10^{-4}$ – 2.20	0.47 – 2.25	0.48 – 2.25	-0.35 – 0.28

Table 3: The 1-2-3  $\sigma$  predictions for the neutrino physical parameters ( $\theta_{12}$ ,  $\theta_{23}$ ,  $\theta_{13}$ ,  $\delta$ ,  $\rho$ ,  $\sigma$ ,  $m_1$ ,  $m_2$ ,  $m_3$ ,  $m_{ee}$ ,  $m_e$  and  $J$ ) with regard to E, F and G categories.

### 5.1 Pattern A: $M_{\nu 11} = M_{\nu 12}$

The expressions for  $A_1$ ,  $A_2$  and  $A_3$  coefficients for this pattern are

$$\begin{aligned} A_1 &= c_{12}^2 c_{13}^2 - c_{12} c_{13} (-c_{12} s_{23} s_{13} - s_{12} c_{23} e^{-i\delta}), \\ A_2 &= s_{12}^2 c_{13}^2 - s_{12} c_{13} (-s_{12} s_{23} s_{13} + c_{12} c_{23} e^{-i\delta}), \\ A_3 &= s_{13}^2 - s_{13} s_{23} c_{13}. \end{aligned} \quad (40)$$

For normal ordering, the representative point is taken as:

$$\begin{aligned} (\theta_{12}, \theta_{23}, \theta_{13}) &= (33.2024^\circ, 41.5453^\circ, 8.3851^\circ), \\ (\delta, \rho, \sigma) &= (267.4139^\circ, 118.0098^\circ, 34.0716^\circ), \\ (m_1, m_2, m_3) &= (0.0021\text{eV}, 0.0091\text{eV}, 0.0498\text{eV}), \\ (m_{ee}, m_e) &= (0.0018\text{eV}, 0.0089\text{eV}), \end{aligned} \quad (41)$$

the corresponding neutrino mass matrix (in eV) is

$$M_\nu = \begin{pmatrix} 0.0012 + 0.0013i & 0.0012 + 0.0013i & 0.0085 - 0.0014i \\ 0.0012 + 0.0013i & 0.0213 - 0.0033i & 0.0250 + 0.0027i \\ 0.0085 - 0.0014i & 0.0250 + 0.0027i & 0.0260 - 0.0021i \end{pmatrix}. \quad (42)$$

For inverted ordering, the representative point is taken as:

$$\begin{aligned} (\theta_{12}, \theta_{23}, \theta_{13}) &= (33.3427^\circ, 42.6843^\circ, 8.3368^\circ), \\ (\delta, \rho, \sigma) &= (231.8342^\circ, 17.8908^\circ, 134.1781^\circ), \\ (m_1, m_2, m_3) &= (0.0496\text{eV}, 0.0503\text{eV}, 0.0043\text{eV}), \\ (m_{ee}, m_e) &= (0.0276\text{eV}, 0.0493\text{eV}), \end{aligned} \quad (43)$$

the corresponding neutrino mass matrix (in eV) is

$$M_\nu = \begin{pmatrix} 0.0271 + 0.0049i & 0.0271 + 0.0049i & -0.0296 - 0.0055i \\ 0.0271 + 0.0049i & -0.0189 - 0.0035i & 0.0160 + 0.0023i \\ -0.0296 - 0.0055i & 0.0160 + 0.0023i & -0.0046 - 0.0010i \end{pmatrix}. \quad (44)$$

We see from Table (2) that the mixing angles  $(\theta_{12}, \theta_{23}, \theta_{13})$  extend over their allowed experimental ranges for both normal and inverted hierarchies at all statistical levels. For inverted ordering, we find large forbidden regions for the Dirac phase  $\delta$  such as,  $[240.67^\circ, 291.60^\circ]$  at the 1- $\sigma$ -level,  $[244.71^\circ, 338.40^\circ]$  at the 2- $\sigma$ -level and  $[0^\circ, 27^\circ] \cup [247.40^\circ, 360^\circ]$  at the 3- $\sigma$ -level. There is a gap  $[76.38^\circ, 80.50^\circ]([127.10^\circ, 131.80^\circ])$  for  $\rho(\sigma)$  at the 2- $\sigma$ -level in the case of normal ordering. We see that  $m_1$  can reach a vanishing value in normal type at all  $\sigma$ -levels, whereas  $m_3$  approaches a zero value in inverted type at all  $\sigma$ -levels. Therefore, the singular pattern is predicted in both normal and inverted types at all  $\sigma$ -levels. The allowed values of  $J$  at the 1-2- $\sigma$ -levels for normal ordering and 1- $\sigma$ -level for inverted ordering are negative, so the corresponding  $\delta$  lies in the third or fourth quarters.

For normal ordering plots, there exists a narrow forbidden gap in all correlations including  $\rho$  and  $\sigma$  parameters. We find a moderate mass hierarchy where  $(0.16 \leq \frac{m_2}{m_3} \leq 0.78)$  and a severe mass hierarchy where  $m_2/m_1$  can reach  $10^3$  indicating the possibility of a vanishing  $m_1$ .

For inverted ordering plots, we have a linear correlation between  $(\rho, \sigma)$  represented by two narrow ribbons. We also see from the correlations including  $\delta$  that the number of generated

points tends to increase as the phase  $\delta$  increases. We find a quasi degeneracy characterized by  $m_1 \approx m_2$  as well as a very strong mass hierarchy where  $m_2/m_3$  can reach  $10^4$  indicating the possibility of a vanishing  $m_3$ . Due to a relatively narrow allowed range for  $\delta$ , the appearing portion of the sinusoidal curve corresponding to the correlation between  $(J, \delta)$  is very small.

For both normal and inverted ordering, the correlations between  $(\delta, m_{ee})$  and between  $(\delta, \text{LNM})$  show that when  $m_{ee}$  and LNM increase, the allowed parameter space becomes more restricted.

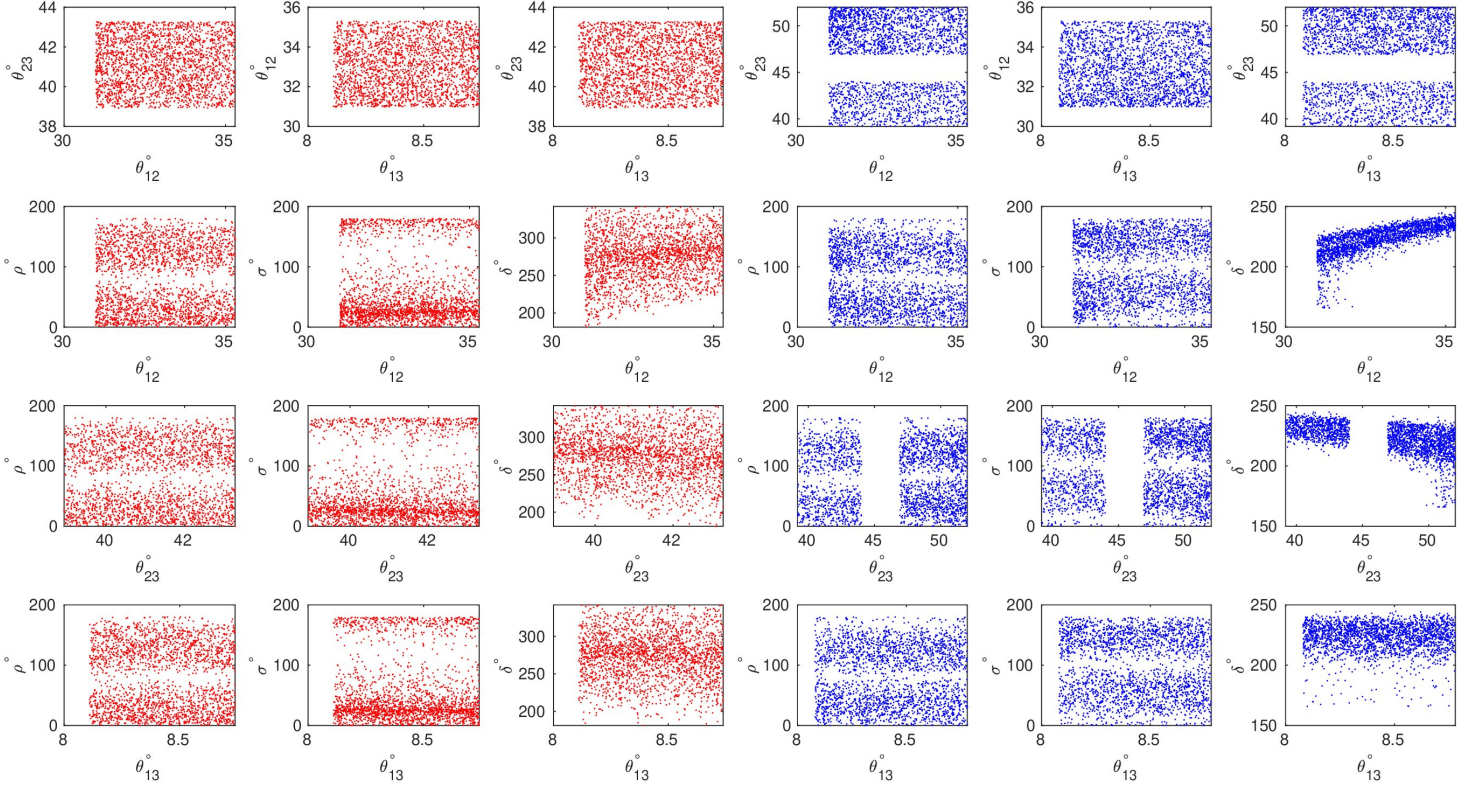


Figure 2: The correlation plots for  $A$  pattern: the red (blue) plots represent the normal (inverted) ordering correlations. The first row represents the correlations between the mixing angles while the next three ones depict the correlations between each mixing angle with the CP-violating phases.

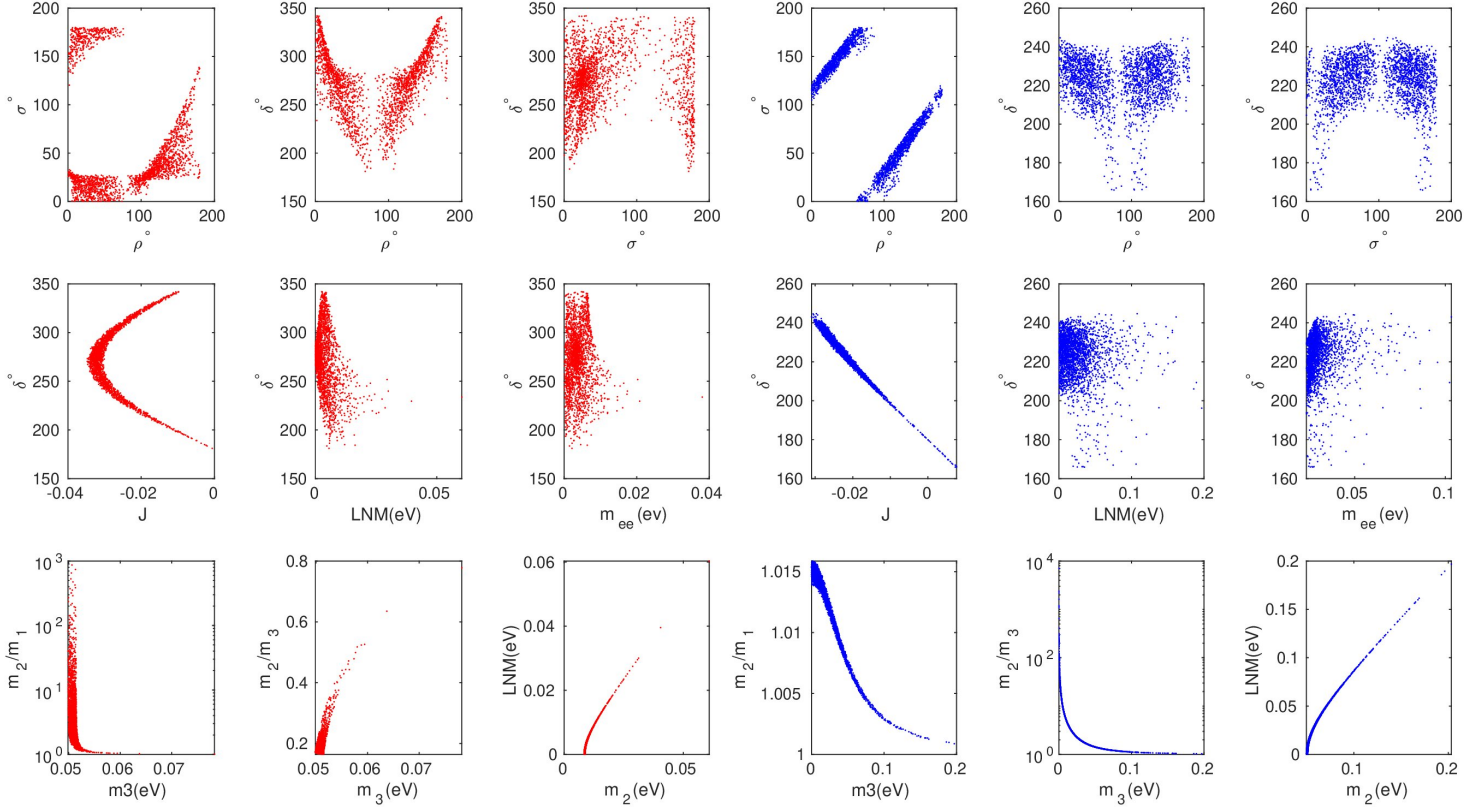


Figure 3: The correlation plots for  $A$  pattern: the red (blue) plots represent the normal (inverted) ordering correlations. The first row represents the correlations between the CP-violating phases, the second one represents the correlations between  $\delta$  and each of  $J$ ,  $LNM$  (the lowest neutrino mass),  $m_{ee}$  parameters. The last one shows the degree of hierarchy.

## 5.2 Pattern B: $M_{\nu 12} = M_{\nu 22}$

The expressions for  $A_1$ ,  $A_2$  and  $A_3$  coefficients for this pattern are

$$\begin{aligned} A_1 &= c_{12}c_{13}(-c_{12}s_{23}s_{13} - s_{12}c_{23}e^{-i\delta}) - (-c_{12}s_{23}s_{13} - s_{12}c_{23}e^{-i\delta})^2, \\ A_2 &= s_{12}c_{13}(-s_{12}s_{23}s_{13} + c_{12}c_{23}e^{-i\delta}) - (s_{12}s_{23}s_{13} + c_{12}c_{23}e^{-i\delta})^2, \\ A_3 &= s_{13}s_{23}c_{13} - s_{23}^2c_{13}^2. \end{aligned} \quad (45)$$

For normal ordering, the representative point is taken as:

$$\begin{aligned} (\theta_{12}, \theta_{23}, \theta_{13}) &= (33.2250^\circ, 40.3964^\circ, 8.4629^\circ), \\ (\delta, \rho, \sigma) &= (258.9409^\circ, 179.8204^\circ, 163.3826^\circ), \\ (m_1, m_2, m_3) &= (0.0244\text{eV}, 0.0259\text{eV}, 0.0560\text{eV}), \\ (m_{ee}, m_e) &= (0.0247\text{eV}, 0.0260\text{eV}), \end{aligned} \quad (46)$$

the corresponding neutrino mass matrix (in eV) is

$$M_\nu = \begin{pmatrix} 0.0243 - 0.0043i & 0.0080 + 0.0004i & -0.0006 + 0.0005i \\ 0.0080 + 0.0004i & 0.0080 + 0.0004i & 0.0393 - 0.0004i \\ -0.0006 + 0.0005i & 0.0393 - 0.0004i & 0.0227 + 0.0003i \end{pmatrix}. \quad (47)$$

For inverted ordering, the representative point is taken as:

$$\begin{aligned} (\theta_{12}, \theta_{23}, \theta_{13}) &= (33.0252^\circ, 42.5959^\circ, 8.3353^\circ), \\ (\delta, \rho, \sigma) &= (283.6350^\circ, 4.5101^\circ, 33.1314^\circ), \\ (m_1, m_2, m_3) &= (0.0488\text{eV}, 0.0496\text{eV}, 0.0017\text{eV}), \\ (m_{ee}, m_e) &= (0.0432\text{eV}, 0.0485\text{eV}), \end{aligned} \quad (48)$$

the corresponding neutrino mass matrix (in eV) is

$$M_\nu = \begin{pmatrix} 0.0390 + 0.0185i & -0.0181 - 0.0080i & 0.0092 + 0.0037i \\ -0.0181 - 0.0080i & -0.0181 - 0.0080i & 0.0219 + 0.0090i \\ 0.0092 + 0.0037i & 0.0219 + 0.0090i & -0.0202 - 0.0090i \end{pmatrix}. \quad (49)$$

We see from Table (2) that the allowed experimental ranges of the mixing angles  $(\theta_{12}, \theta_{23}, \theta_{13})$  can be covered at all  $\sigma$ -levels for both normal and inverted ordering. For normal ordering, at the 3- $\sigma$ -level, there exists a narrow forbidden gap  $[0, 2^\circ]$  for  $\delta$ . We find also, for normal type, a forbidden gap  $[0, 3^\circ]$  ( $[26^\circ, 106^\circ]$ ) for  $\rho$  ( $\sigma$ ) at the 1- $\sigma$ -level. For inverted ordering, there are large disallowed regions for  $\delta$  at all  $\sigma$ -levels:  $[201^\circ, 221^\circ]$  at 1- $\sigma$ -level,  $[166^\circ, 213^\circ]$  at 2- $\sigma$ -level and  $[0^\circ, 27^\circ] \cup [139^\circ, 211^\circ] \cup [337^\circ, 360^\circ]$  at 3- $\sigma$ -level. We note that  $m_1$  does not reach zero at any  $\sigma$ -level in normal type, whereas  $m_3$  can approach a vanishing value at all  $\sigma$ -levels in inverted type. Thus, the singular pattern is predicted in inverted type at all  $\sigma$ -levels. The allowed values of  $J$  at 1-2- $\sigma$ -levels for normal and inverted ordering are negative, so the corresponding  $\delta$  lies in the third or fourth quarters.

For normal ordering plots, there is a quasi linear correlation between  $\sigma$  and  $\delta$ . We see a mild mass hierarchy where  $(0.29 \leq \frac{m_2}{m_3} \leq 0.97)$  as well as a quasi degenerate mass hierarchy where  $(1 \leq \frac{m_2}{m_1} \leq 1.22)$ .

For inverted ordering plots, we find that the correlation between  $\rho$  and  $\sigma$  is linear. We see a quasi degenerate mass spectrum characterized by  $m_1 \approx m_2$  in addition to an acute mass hierarchy where  $\frac{m_2}{m_3}$  can reach  $10^3$  indicating the possibility of a vanishing  $m_3$ .

For both normal and inverted ordering, the correlations between  $(\delta, m_{ee})$  and between  $(\delta, \text{LNM})$  show that when  $m_{ee}$  and LNM increase, the allowed parameter space becomes more limited.

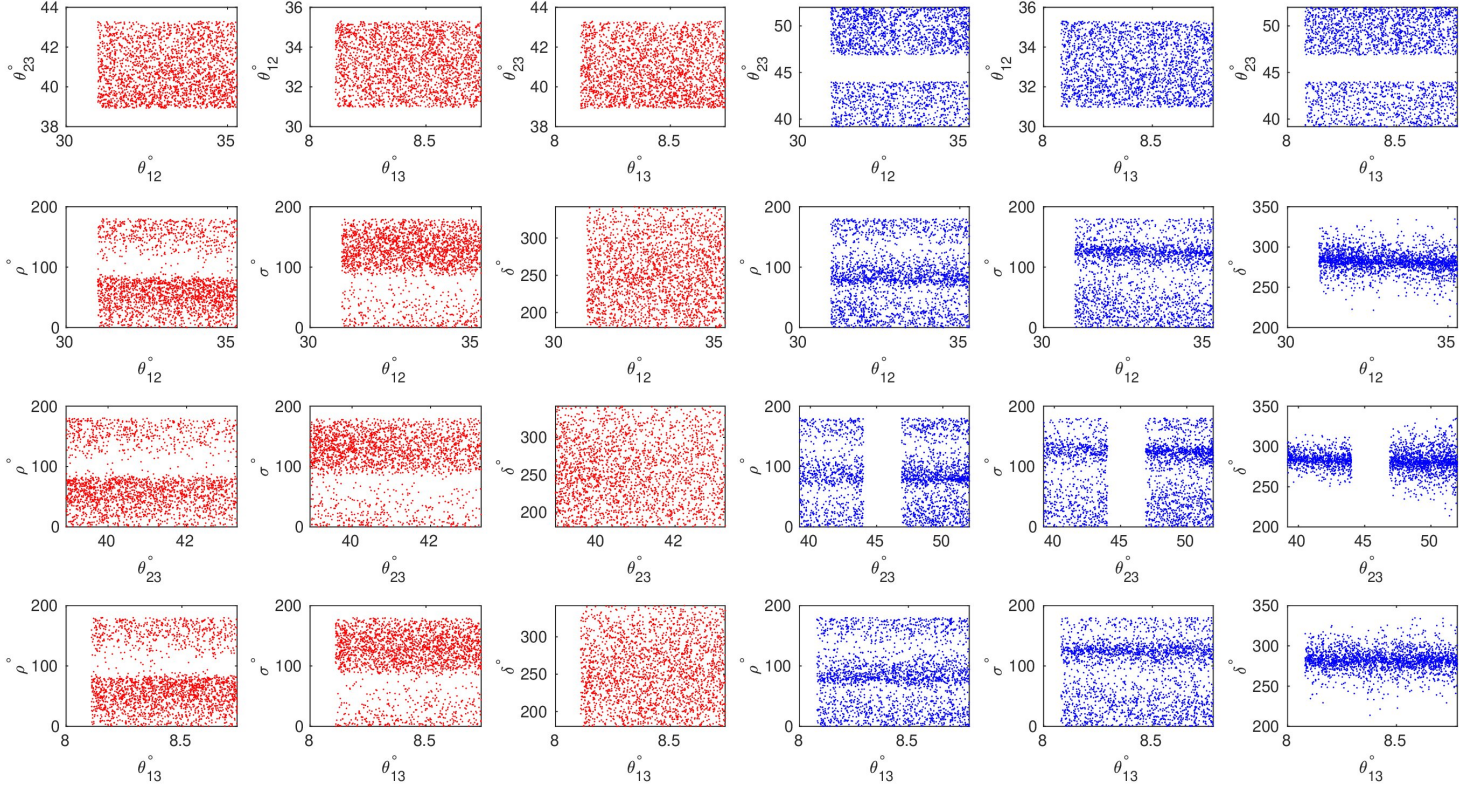


Figure 4: The correlation plots for  $B$  pattern: the red (blue) plots represent the normal (inverted) ordering. The first row represents the correlations between the mixing angles while the next three ones depict the correlations between each mixing angle with the CP-violating phases.



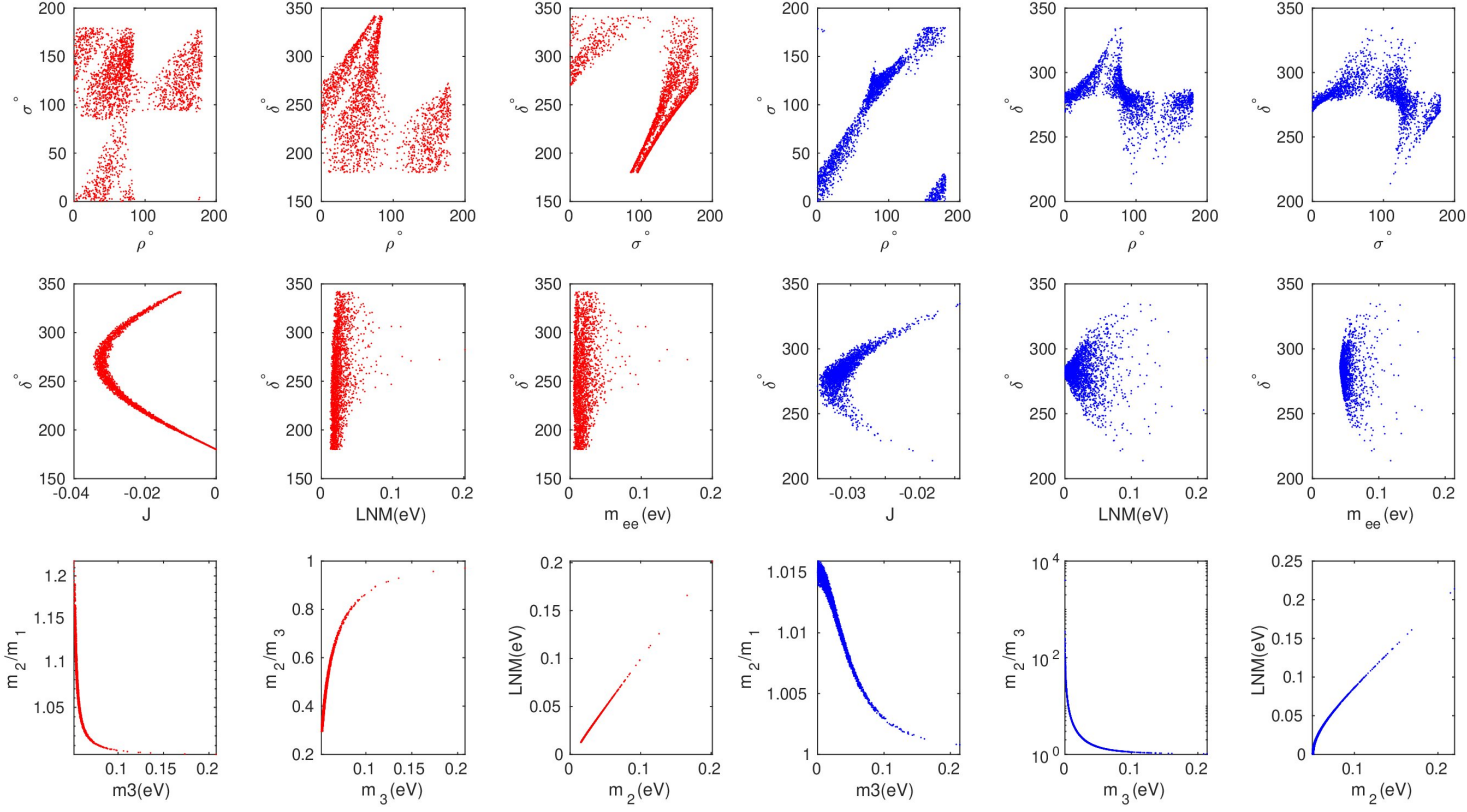


Figure 5: The correlation plots for  $B$  pattern: the red (blue) plots represent the normal (inverted) ordering. The first row represents the correlations between the CP-violating phases, the second one represents the correlations between  $\delta$  and each of  $J$ ,  $LNM$  (the lowest neutrino mass),  $m_{ee}$  parameters. The last row shows the degree of hierarchy.

### 5.3 Pattern C: $M_{\nu 23} = M_{\nu 33}$

The expressions for  $A_1$ ,  $A_2$  and  $A_3$  coefficients for this pattern are

$$\begin{aligned} A_1 &= (-c_{12}s_{23}s_{13} - s_{12}c_{23}e^{-i\delta})(-c_{12}c_{23}s_{13} + s_{12}s_{23}e^{-i\delta}) - (-c_{12}c_{23}s_{13} + s_{12}s_{23}e^{-i\delta})^2, \\ A_2 &= (-s_{12}s_{23}s_{13} + c_{12}c_{23}e^{-i\delta})^2(-s_{12}c_{23}s_{13} - c_{12}s_{23}e^{-i\delta}) - (-s_{12}c_{23}s_{13} - c_{12}s_{23}e^{-i\delta})^2, \\ A_3 &= s_{23}c_{13}^2c_{23} - c_{23}^2c_{13}^2. \end{aligned} \quad (50)$$

For normal ordering, the representative point is taken as:

$$\begin{aligned} (\theta_{12}, \theta_{23}, \theta_{13}) &= (33.4943^\circ, 40.1410^\circ, 8.4563^\circ), \\ (\delta, \rho, \sigma) &= (197.7906^\circ, 45.8379^\circ, 120.1734^\circ), \\ (m_1, m_2, m_3) &= (0.0082\text{eV}, 0.0118\text{eV}, 0.0519\text{eV}), \\ (m_{ee}, m_e) &= (0.0026\text{eV}, 0.0120\text{eV}), \end{aligned} \quad (51)$$

the corresponding neutrino mass matrix (in eV) is

$$M_\nu = \begin{pmatrix} -0.0008 + 0.0025i & 0.0089 + 0.0053i & 0.0028 - 0.0049i \\ 0.0089 + 0.0053i & 0.0168 - 0.0018i & 0.0279 + 0.0005i \\ 0.0028 - 0.0049i & 0.0279 + 0.0005i & 0.0279 + 0.0005i \end{pmatrix}. \quad (52)$$

From Table (2), we find that this texture can not accommodate the experimental data for inverted ordering at all  $\sigma$ -levels. For normal ordering, the mixing angles  $\theta_{12}$  and  $\theta_{13}$  extend over their allowed experimental ranges at all  $\sigma$ -levels. However, there exists a restricted region for the mixing angle  $\theta_{23}$  at all statistical levels. There are forbidden gaps  $[110^\circ, 144^\circ]$  and  $[7^\circ, 114^\circ]$  for  $\rho$  and  $\sigma$  phases at the 1- $\sigma$ -level. We find also a disallowed region  $[273^\circ, 289^\circ]$  for  $\delta$  at the 1- $\sigma$ -level. We note that  $m_1$  can reach a vanishing value at all  $\sigma$ -levels in normal type. Therefore, the singular pattern is predicted in normal type at all  $\sigma$ -levels. The allowed values of J at the 1-2- $\sigma$ -levels are negative, so the corresponding  $\delta$  lies in the third or fourth quarters.

For normal ordering plots shown in Figs.(6,7), we see a linear correlation between  $(\sigma, \delta)$  represented by two narrow ribbons. We see also a forbidden gap for  $\sigma$  and  $\theta_{23}$ . The correlations between  $(\delta, m_{ee})$  and between  $(\delta, \text{LNM})$  show that when  $m_{ee}$  and LNM increase, the allowed parameter space becomes more restricted. We find a mild mass hierarchy where  $(0.16 \leq \frac{m_2}{m_3} \leq 0.54)$  together with a severe mass hierarchy where  $\frac{m_2}{m_1}$  can reach  $10^3$  indicating the possibility of a vanishing  $m_1$ .



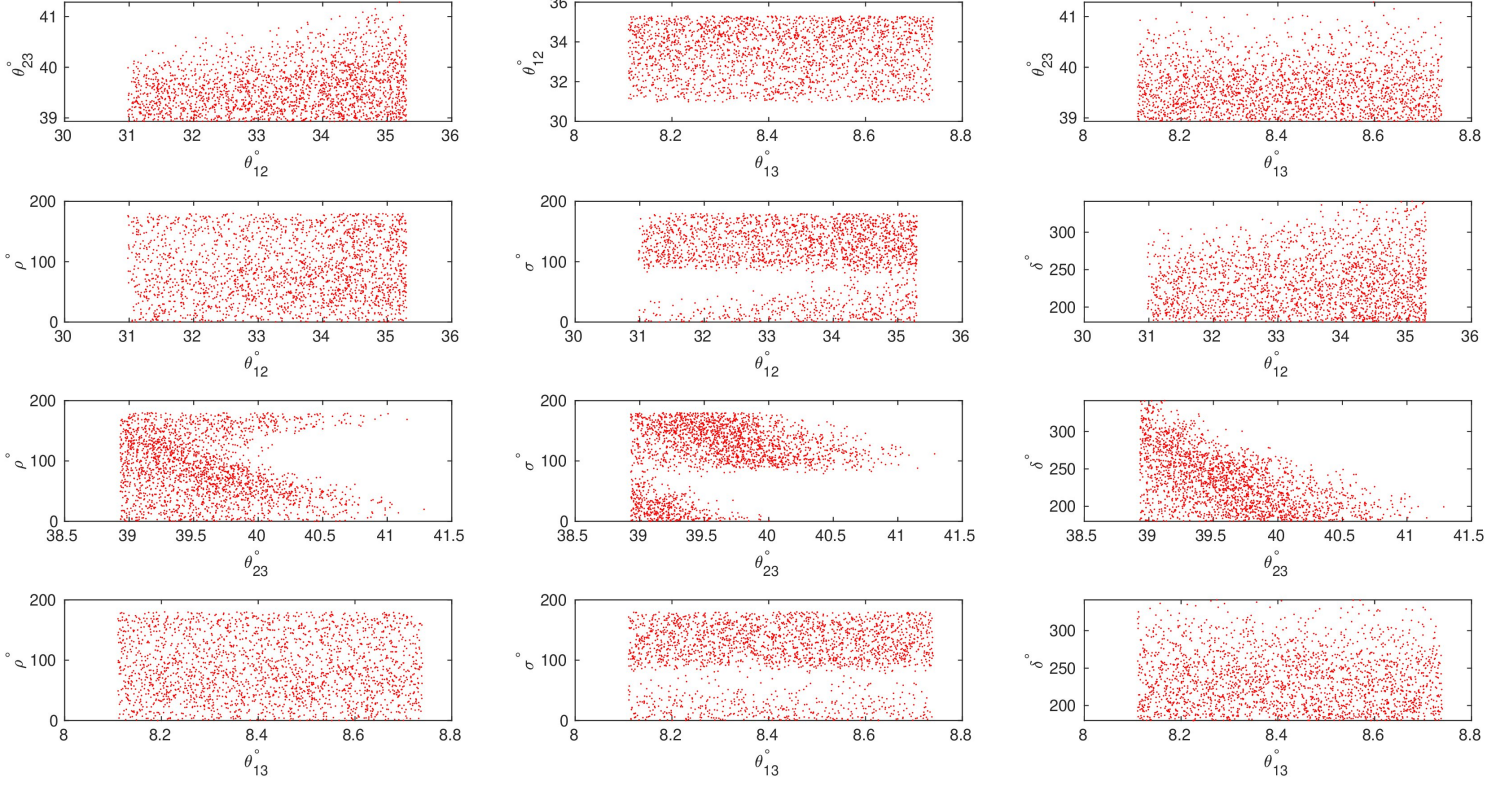


Figure 6: The correlation plots for  $C$  pattern. The first row represents the correlations between the mixing angles while the next three ones depict the correlations between each mixing angle with the CP-violating phases.

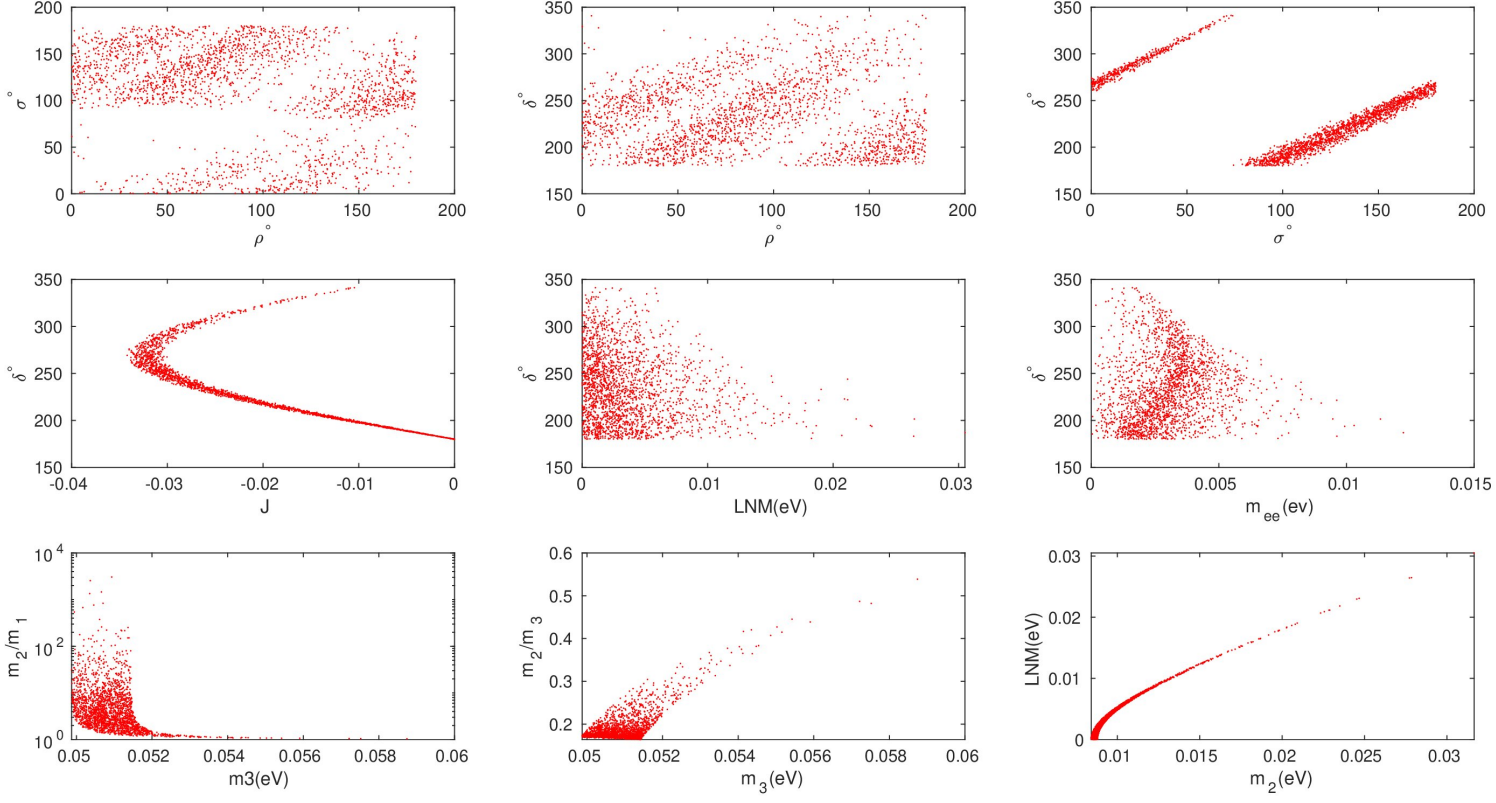


Figure 7: The correlation plots for  $C$  pattern. The first row represents the correlations between the CP-violating phases, the second one represents the correlations between  $\delta$  and each of  $J$ ,  $LNM$  (the lowest neutrino mass) and  $m_{ee}$  parameters. The last row shows the degree of hierarchy.

#### 5.4 Pattern D: $M_{\nu 13} = M_{\nu 22}$

The expressions for  $A_1$ ,  $A_2$  and  $A_3$  coefficients for this pattern are

$$\begin{aligned} A_1 &= c_{12}c_{13}(-c_{12}c_{23}s_{13} + s_{12}s_{23}e^{-i\delta}) - (-c_{12}s_{23}s_{13} - s_{12}c_{23}e^{-i\delta})^2, \\ A_2 &= s_{12}c_{13}(-s_{12}c_{23}s_{13} - c_{12}s_{23}e^{-i\delta}) - (-s_{12}s_{23}s_{13} + c_{12}c_{23}e^{-i\delta})^2, \\ A_3 &= s_{13}c_{23}c_{13} - s_{23}^2c_{13}^2. \end{aligned} \quad (53)$$

For normal ordering, the representative point is taken as:

$$\begin{aligned} (\theta_{12}, \theta_{23}, \theta_{13}) &= (33.0546^\circ, 40.1246^\circ, 8.3158^\circ), \\ (\delta, \rho, \sigma) &= (248.7062^\circ, 151.2423^\circ, 157.4505^\circ), \\ (m_1, m_2, m_3) &= (0.0311\text{eV}, 0.0323\text{eV}, 0.0589\text{eV}), \\ (m_{ee}, m_e) &= (0.0314\text{eV}, 0.0323\text{eV}), \end{aligned} \quad (54)$$

the corresponding neutrino mass matrix (in eV) is

$$M_\nu = \begin{pmatrix} 0.0194 - 0.0247i & 0.0019 + 0.0039i & 0.0060 + 0.0015i \\ 0.0019 + 0.0039i & 0.0060 + 0.0015i & 0.0442 - 0.0020i \\ 0.0060 + 0.0015i & 0.0442 - 0.0020i & 0.0205 + 0.0014i \end{pmatrix}. \quad (55)$$

For inverted ordering, the representative point is taken as:

$$\begin{aligned} (\theta_{12}, \theta_{23}, \theta_{13}) &= (33.1550^\circ, 42.7806^\circ, 8.3517^\circ), \\ (\delta, \rho, \sigma) &= (235.5059^\circ, 114.9130^\circ, 63.0067^\circ), \\ (m_1, m_2, m_3) &= (0.0517\text{eV}, 0.0524\text{eV}, 0.0153\text{eV}), \\ (m_{ee}, m_e) &= (0.0348\text{eV}, 0.0514\text{eV}), \end{aligned} \quad (56)$$

the corresponding neutrino mass matrix (in eV) is

$$M_\nu = \begin{pmatrix} -0.0316 - 0.0147i & -0.0182 - 0.0133i & 0.0263 + 0.0152i \\ -0.0182 - 0.0133i & 0.0263 + 0.0152i & -0.0065 - 0.0114i \\ 0.0263 + 0.0152i & -0.0065 - 0.0114i & 0.0161 + 0.0075i \end{pmatrix}. \quad (57)$$

We see from Table (2) that the allowed experimental ranges for the mixing angles  $(\theta_{12}, \theta_{23}, \theta_{13})$  can be covered for both normal and inverted orderings at all  $\sigma$ -levels. For normal ordering, a large forbidden gap  $[46^\circ, 92^\circ]$  ( $[45^\circ, 95^\circ]$ ) exists for  $\rho$  ( $\sigma$ ) at the 1- $\sigma$ -level. For inverted ordering, we notice a very tight forbidden gap  $[51.23^\circ, 53.62^\circ]$  for  $\rho$  at the 2- $\sigma$ -level in addition to disallowed regions for  $\delta$  at the 2-3- $\sigma$ -levels. Table (2) also reveals that  $m_1$  does not reach zero value at all  $\sigma$ -levels, whereas  $m_3$  can reach a vanishing value at all  $\sigma$ -levels. Thus, the singular pattern is predicted in inverted type at all  $\sigma$ -levels. The allowed values of J at the 1-2- $\sigma$ -levels for normal ordering and 1- $\sigma$ -level for inverted ordering are negative, so the corresponding  $\delta$  lies in the third or fourth quarters.

For normal ordering plots, we find a mild mass hierarchy where  $(0.40 \leq \frac{m_2}{m_3} \leq 0.97)$  together with a quasi degeneracy characterized by  $m_1 \approx m_2$ .

As to the inverted plots, we get an acute mass hierarchy where  $\frac{m_2}{m_3}$  can reach  $10^3$  besides a quasi degeneracy where  $(1 \leq \frac{m_2}{m_1} \leq 1.01)$ .

For both normal and inverted ordering, the correlations between  $(\delta, m_{ee})$  and between  $(\delta, \text{LNM})$  show that when  $m_{ee}$  and LNM increase, the allowed parameter space becomes more restricted.

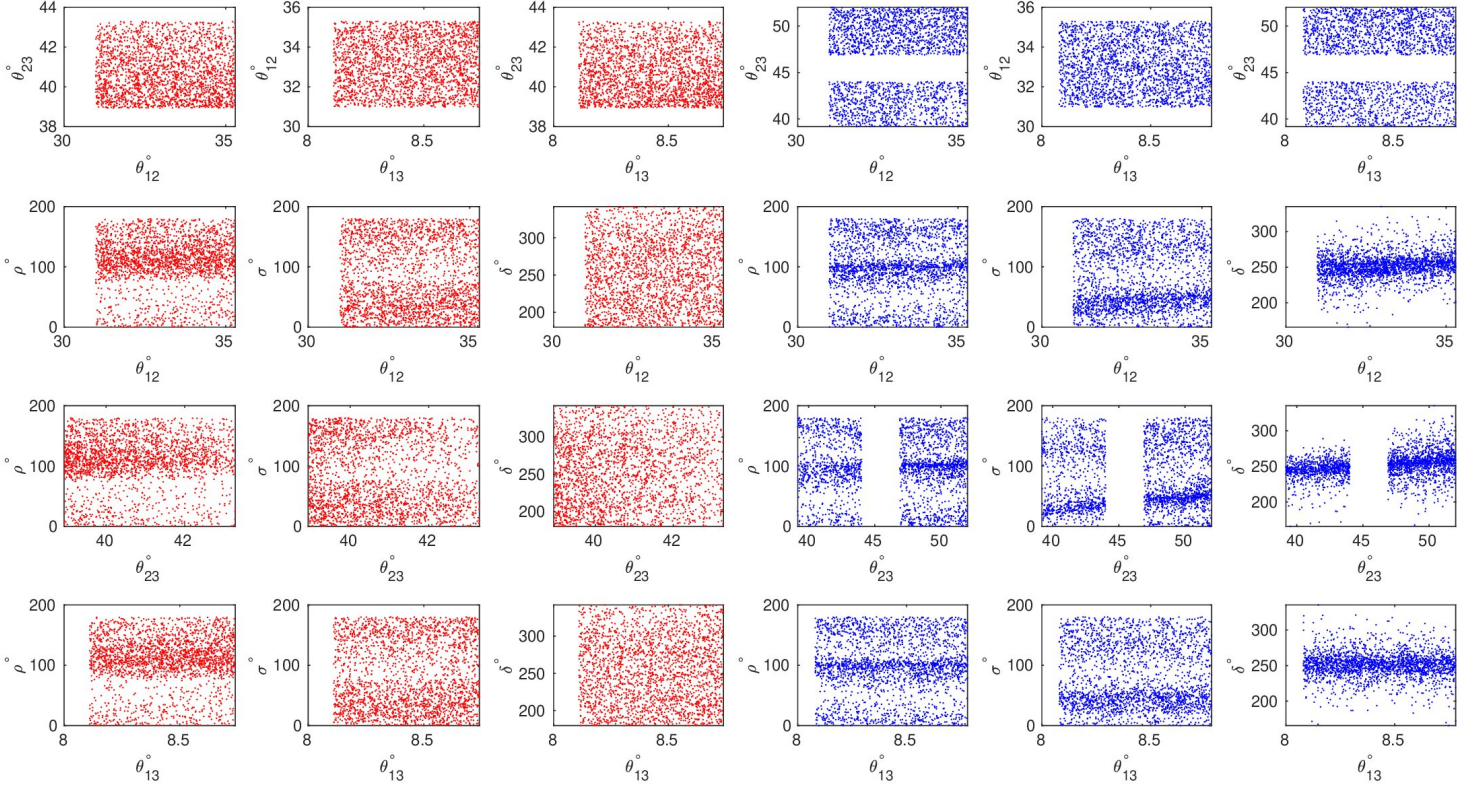


Figure 8: The correlation plots for  $D$  pattern, the red (blue) plots represent the normal (inverted) ordering. The first row represents the correlations between the mixing angles while the next three ones depict the correlations between each mixing angle with the CP-violating phases.

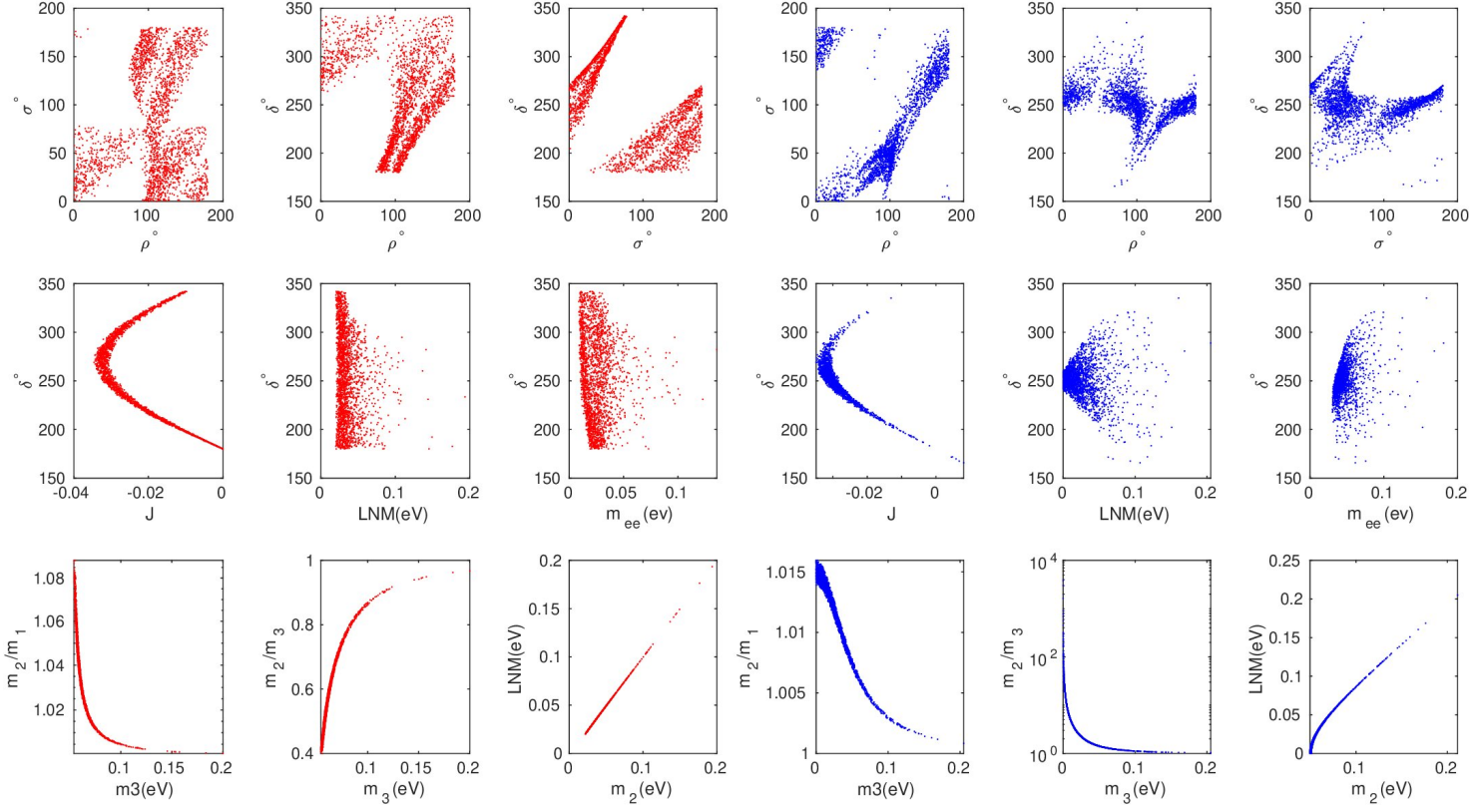


Figure 9: The correlation plots for  $D$  pattern, the red (blue) plots represent the normal (inverted) ordering. The first row represents the correlations between the CP-violating phases, the second one represent the correlations between  $\delta$  and each of  $J$ ,  $LNM$  (the lowest neutrino mass) and  $m_{ee}$  parameters. The last one shows the degree of hierarchy.

### 5.5 Pattern E: $M_{\nu 11} = M_{\nu 22}$

The expressions for  $A_1$ ,  $A_2$  and  $A_3$  coefficients for this pattern are

$$\begin{aligned} A_1 &= c_{12}^2 c_{13}^2 - (-c_{12} s_{23} s_{13} - s_{12} c_{23} e^{-i\delta})^2, \\ A_2 &= s_{12}^2 c_{13}^2 - (-s_{12} s_{23} s_{13} + c_{12} c_{23} e^{-i\delta})^2, \\ A_3 &= s_{13}^2 - s_{23}^2 c_{13}^2. \end{aligned} \quad (58)$$

For normal ordering, the representative point is taken as:

$$\begin{aligned} (\theta_{12}, \theta_{23}, \theta_{13}) &= (33.0094^\circ, 40.1340^\circ, 8.4327^\circ), \\ (\delta, \rho, \sigma) &= (337.2171^\circ, 21.2764^\circ, 11.6665^\circ), \\ (m_1, m_2, m_3) &= (0.0382\text{eV}, 0.0392\text{eV}, 0.0631\text{eV}), \\ (m_{ee}, m_e) &= (0.0384\text{eV}, 0.0392\text{eV}), \end{aligned} \quad (59)$$

the corresponding neutrino mass matrix (in eV) is

$$M_\nu = \begin{pmatrix} 0.0312 + 0.0223i & 0.0069 - 0.0044i & 0.0003 - 0.0006i \\ 0.0069 - 0.0044i & 0.0312 + 0.0223i & 0.0255 - 0.0180i \\ 0.0003 - 0.0006i & 0.0255 - 0.0180i & 0.0415 + 0.0153i \end{pmatrix}. \quad (60)$$

For inverted ordering, the representative point is taken as:

$$\begin{aligned} (\theta_{12}, \theta_{23}, \theta_{13}) &= (33.3064^\circ, 42.1821^\circ, 8.4522^\circ), \\ (\delta, \rho, \sigma) &= (220.4427^\circ, 178.5371^\circ, 61.7794^\circ), \\ (m_1, m_2, m_3) &= (0.0628\text{eV}, 0.0633\text{eV}, 0.0375\text{eV}), \\ (m_{ee}, m_e) &= (0.0359\text{eV}, 0.0625\text{eV}), \end{aligned} \quad (61)$$

the corresponding neutrino mass matrix (in eV) is

$$M_\nu = \begin{pmatrix} 0.0333 + 0.0134i & 0.0132 - 0.0370i & -0.0111 + 0.0308i \\ 0.0132 - 0.0370i & 0.0333 + 0.0134i & 0.0012 - 0.0047i \\ -0.0111 + 0.0308i & 0.0012 - 0.0047i & 0.0387 - 0.0019i \end{pmatrix}. \quad (62)$$

We see from Table (3), the mixing angles  $(\theta_{12}, \theta_{23}, \theta_{13})$  extend over their allowed experimental ranges for both normal and inverted ordering at all  $\sigma$ -levels. We notice a persistent wide forbidden gap for the phase  $\rho$  with each hierarchy type at all  $\sigma$ -levels. For normal ordering, at the 1(2)- $\sigma$ -levels, there is a gap  $[56^\circ, 94^\circ]$  ( $[83^\circ, 86^\circ]$ ) for the phase  $\sigma$ . For inverted ordering, we find that  $\sigma$  is bounded at all  $\sigma$ -levels with a forbidden gap around  $0^\circ$ . Table (3) also reveals that neither  $m_1$  in normal type nor  $m_3$  in inverted type can reach a vanishing value. Thus, the singular pattern is not predicted at any  $\sigma$ -level. The allowed values of J at the 1-2- $\sigma$ -levels for normal ordering and 1- $\sigma$ -level for inverted ordering are negative, so the corresponding  $\delta$  lies in the third or fourth quarters.

For normal ordering plots, a forbidden gap exists for  $\rho$  and  $\sigma$ . We see a mild mass hierarchy where  $(0.26 \leq \frac{m_2}{m_3} \leq 0.95)$  and a quasi degenerate mass spectrum characterized by  $(1 \leq \frac{m_2}{m_1} \leq 1.28)$ .

As to inverted ordering plots, we see a wide forbidden gap for the phase  $\rho$ . We also see a quasi degenerate mass spectrum characterized by  $(1 \leq \frac{m_2}{m_1} \leq 1.01)$  and a mild mass hierarchy where  $(1.02 \leq \frac{m_2}{m_3} \leq 3.25)$ .

For both normal and inverted ordering, the correlations between  $(\delta, m_{ee})$  and between  $(\delta, \text{LNM})$  show that when  $m_{ee}$  and LNM increase, the allowed parameter space becomes more restricted.



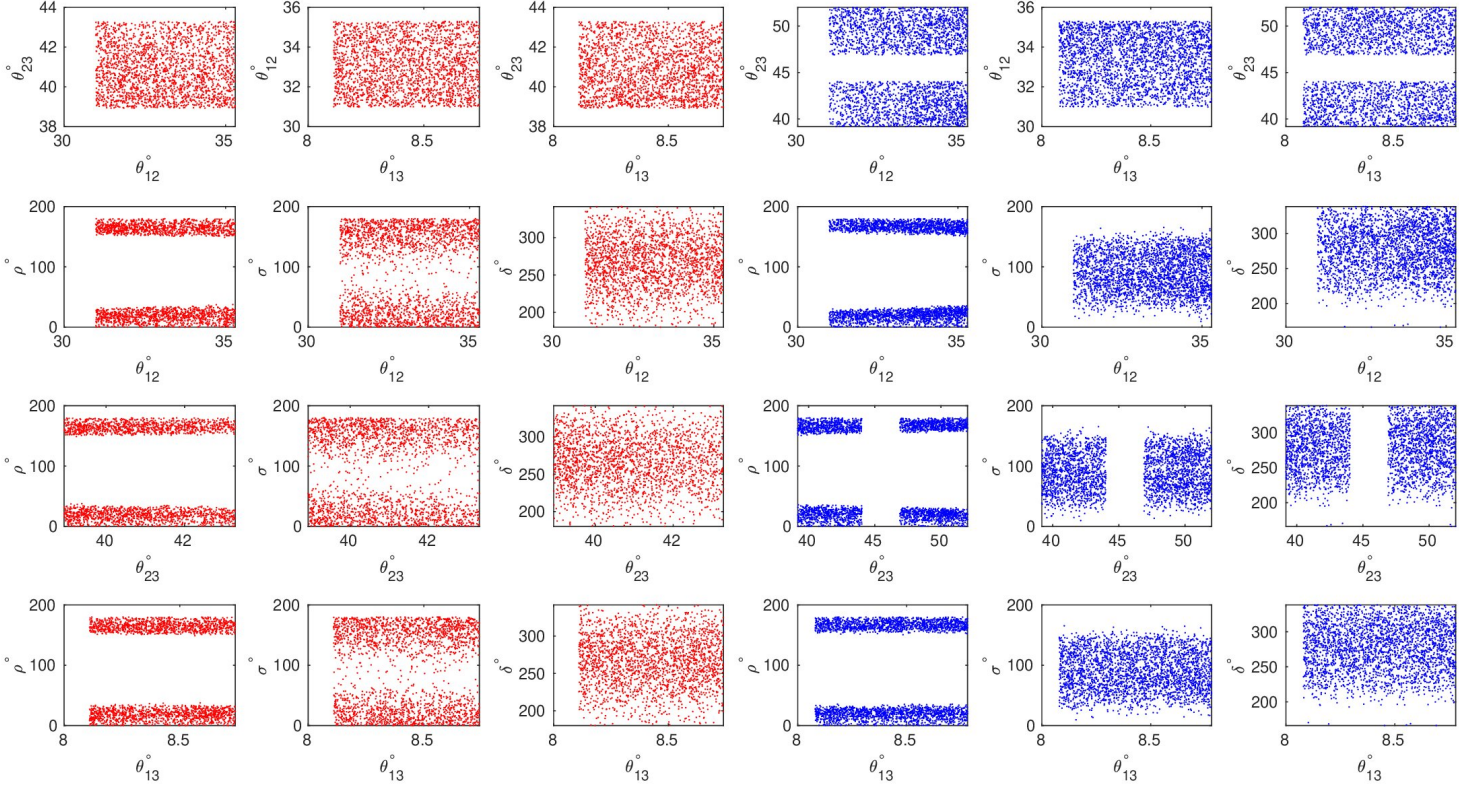


Figure 10: The correlation plots for  $E$  pattern, the red (blue) plots represent the normal (inverted) ordering. The first row represents the correlations between the mixing angles while the next three ones depict the correlations between each mixing angle with the CP-violating phases.

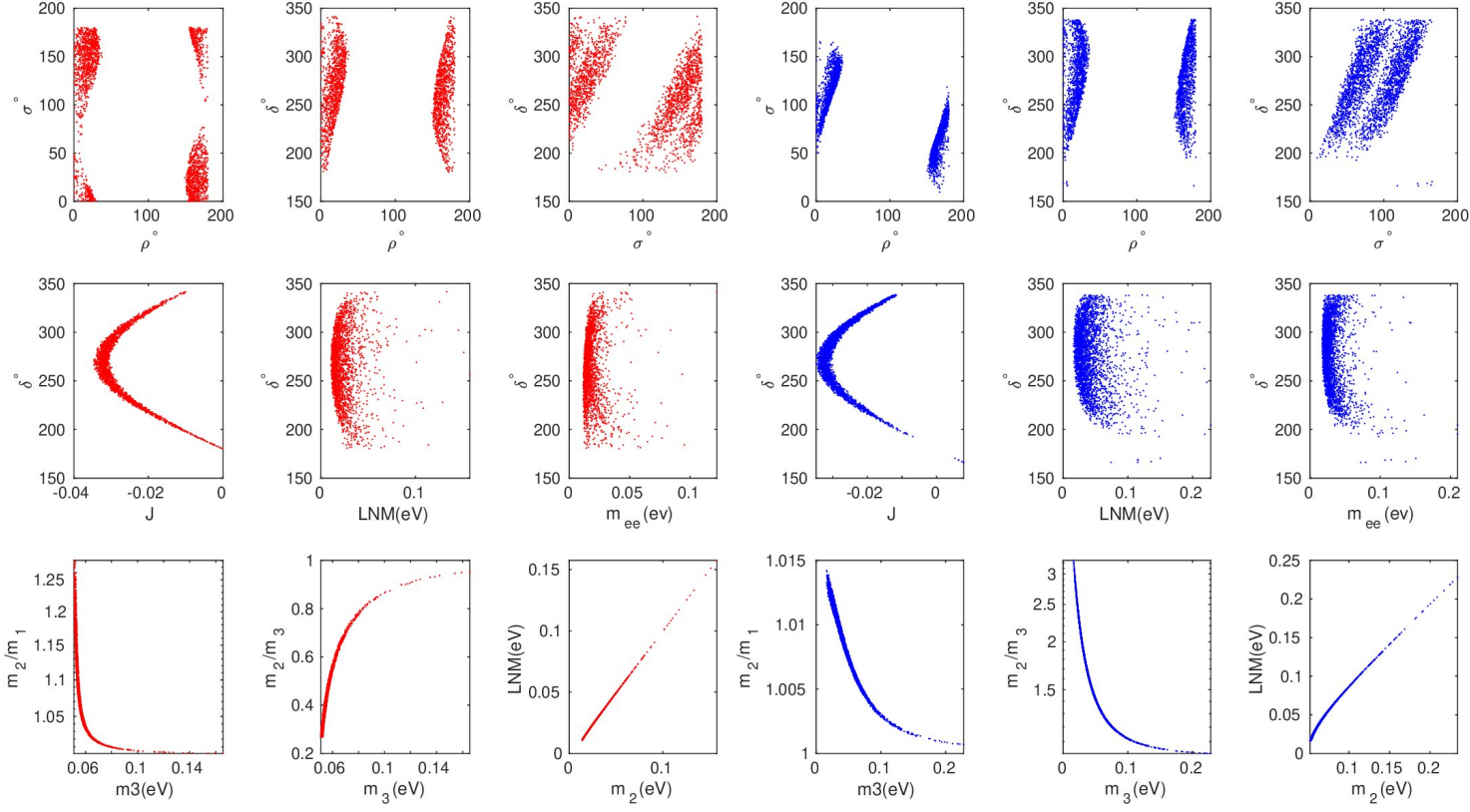


Figure 11: The correlation plots for  $E$  pattern, the red (blue) plots represents the normal (inverted) ordering. The first row represents the correlations between the CP-violating phases, the second one represent the correlations between  $\delta$  and each of  $J$ ,  $LNM$  (the lowest neutrino mass) and  $m_{ee}$  parameters. The last one shows the degree of hierarchy.



## 5.6 Pattern $F$ : $M_{\nu 12} = M_{\nu 23}$

The expressions for  $A_1$ ,  $A_2$  and  $A_3$  coefficients for this pattern are

$$\begin{aligned} A_1 &= c_{12}c_{13}(-c_{12}s_{23}s_{13} - s_{12}c_{23}e^{-i\delta}) - (-c_{12}s_{23}s_{13} - s_{12}c_{23}e^{-i\delta})(-c_{12}c_{23}s_{13} + s_{12}s_{23}e^{-i\delta}), \\ A_2 &= s_{12}c_{13}(-s_{12}s_{23}s_{13} + c_{12}c_{23}e^{-i\delta}) - (-s_{12}s_{23}s_{13} + c_{12}c_{23}e^{-i\delta})(-s_{12}c_{23}s_{13} - c_{12}s_{23}e^{-i\delta}), \\ A_3 &= s_{13}s_{23}c_{13} - s_{23}c_{13}^2c_{23}. \end{aligned} \quad (63)$$

For normal ordering, the representative point is taken as:

$$\begin{aligned} (\theta_{12}, \theta_{23}, \theta_{13}) &= (33.3697^\circ, 41.3769^\circ, 8.4277^\circ), \\ (\delta, \rho, \sigma) &= (247.6273^\circ, 51.4357^\circ, 92.2980^\circ), \\ (m_1, m_2, m_3) &= (0.0255\text{eV}, 0.0269\text{eV}, 0.0568\text{eV}), \\ (m_{ee}, m_e) &= (0.0195\text{eV}, 0.0270\text{eV}), \end{aligned} \quad (64)$$

the corresponding neutrino mass matrix (in eV) is

$$M_\nu = \begin{pmatrix} -0.0106 + 0.0164i & 0.0179 - 0.0047i & -0.0024 + 0.0010i \\ 0.0179 - 0.0047i & 0.0325 + 0.0065i & 0.0179 - 0.0047i \\ -0.0024 + 0.0010i & 0.0179 - 0.0047i & 0.0416 + 0.0040i \end{pmatrix}. \quad (65)$$

For inverted ordering, the representative point is taken as:

$$\begin{aligned} (\theta_{12}, \theta_{23}, \theta_{13}) &= (33.3485^\circ, 42.2305^\circ, 8.4914^\circ), \\ (\delta, \rho, \sigma) &= (231.5721^\circ, 12.3694^\circ, 131.7511^\circ), \\ (m_1, m_2, m_3) &= (0.0614\text{eV}, 0.0619\text{eV}, 0.0370\text{eV}), \\ (m_{ee}, m_e) &= (0.0368\text{eV}, 0.0611\text{eV}), \end{aligned} \quad (66)$$

the corresponding neutrino mass matrix (in eV) is

$$M_\nu = \begin{pmatrix} 0.0368 - 0.0007i & 0.0361 + 0.0018i & -0.0327 - 0.0015i \\ 0.0361 + 0.0018i & -0.0108 - 0.0023i & 0.0361 + 0.0018i \\ -0.0327 - 0.0015i & 0.0361 + 0.0018i & 0.0108 - 0.0013i \end{pmatrix}. \quad (67)$$

We see from Table (3) that the mixing angles  $(\theta_{12}, \theta_{23}, \theta_{13})$  extend over their allowed experimental ranges with each hierarchy type at all statistical levels. For normal ordering, We find that the ranges for  $\rho$  ( $\sigma$ ) are restricted to be nearly in the interval  $[10^\circ, 116^\circ]$  ( $[37^\circ, 147^\circ]$ ) at the 1- $\sigma$ -level and tending to be wider at the 2- $\sigma$ -level to be nearly in  $[2^\circ, 178^\circ]$  ( $[19^\circ, 178^\circ]$ ). We also find, for normal type, disallowed regions for the phase  $\rho$  besides a tight forbidden gap  $[39.50^\circ, 44.10^\circ]$  for the phase  $\sigma$  at the 3- $\sigma$ -level. One notes also that there are forbidden gaps for the Dirac phase  $\delta$  at the 3- $\sigma$ -level in normal type and at the 2-3- $\sigma$ -levels in inverted type. Table (3) also reveals that  $m_1$  does not reach zero value at any  $\sigma$ -level, whereas  $m_3$  can reach a vanishing value at all  $\sigma$ -levels. Thus, the singular pattern is predicted for inverted ordering at all  $\sigma$ -levels. The allowed values of  $J$  at the 1-2- $\sigma$ -levels for normal ordering and 1- $\sigma$ -level for inverted ordering are negative, so the corresponding  $\delta$  lies in the third or fourth quarters.

For normal ordering plots, we see a mild mass hierarchy where  $(0.40 \leq \frac{m_2}{m_3} \leq 0.97)$  and a quasi degeneracy characterized by  $m_1 \approx m_2$ .

As to inverted ordering plots, we find a quasi degeneracy characterized by  $m_1 \approx m_2$  as well as an acute mass hierarchy where  $\frac{m_2}{m_3}$  can reach  $10^4$  indicating the possibility of a vanishing  $m_3$ .

For both normal and inverted ordering, the correlations between  $(\delta, m_{ee})$  and between  $(\delta, \text{LNM})$  show that when  $m_{ee}$  and LNM increase, the allowed parameter space becomes more restricted.

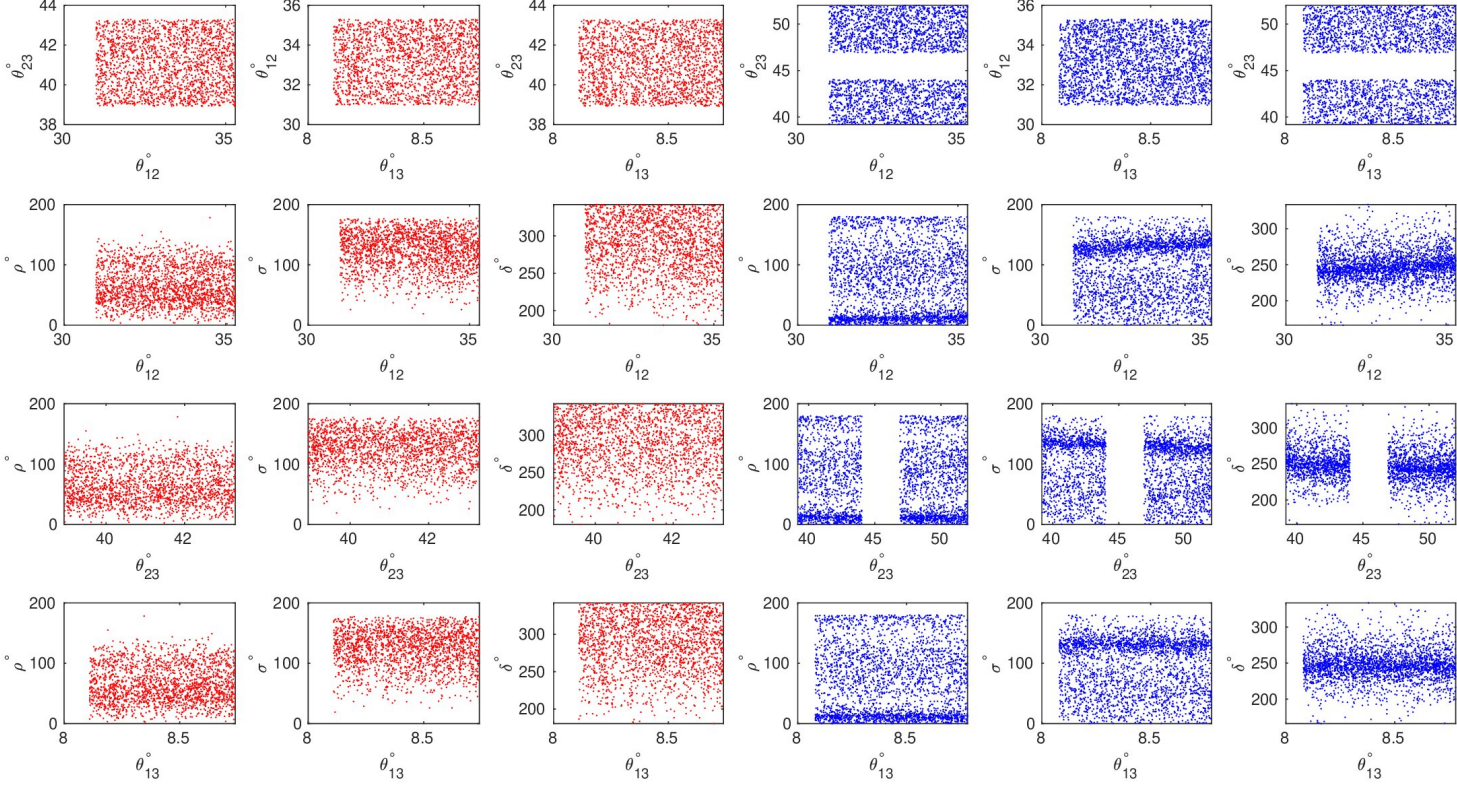


Figure 12: The correlation plots for  $F$  pattern, the red plots represents the normal ordering, whereas the blue ones represents the inverted ordering. The first row represents the correlations between the mixing angles while the next three ones depict the correlations between each mixing angle with the CP-violating phases.

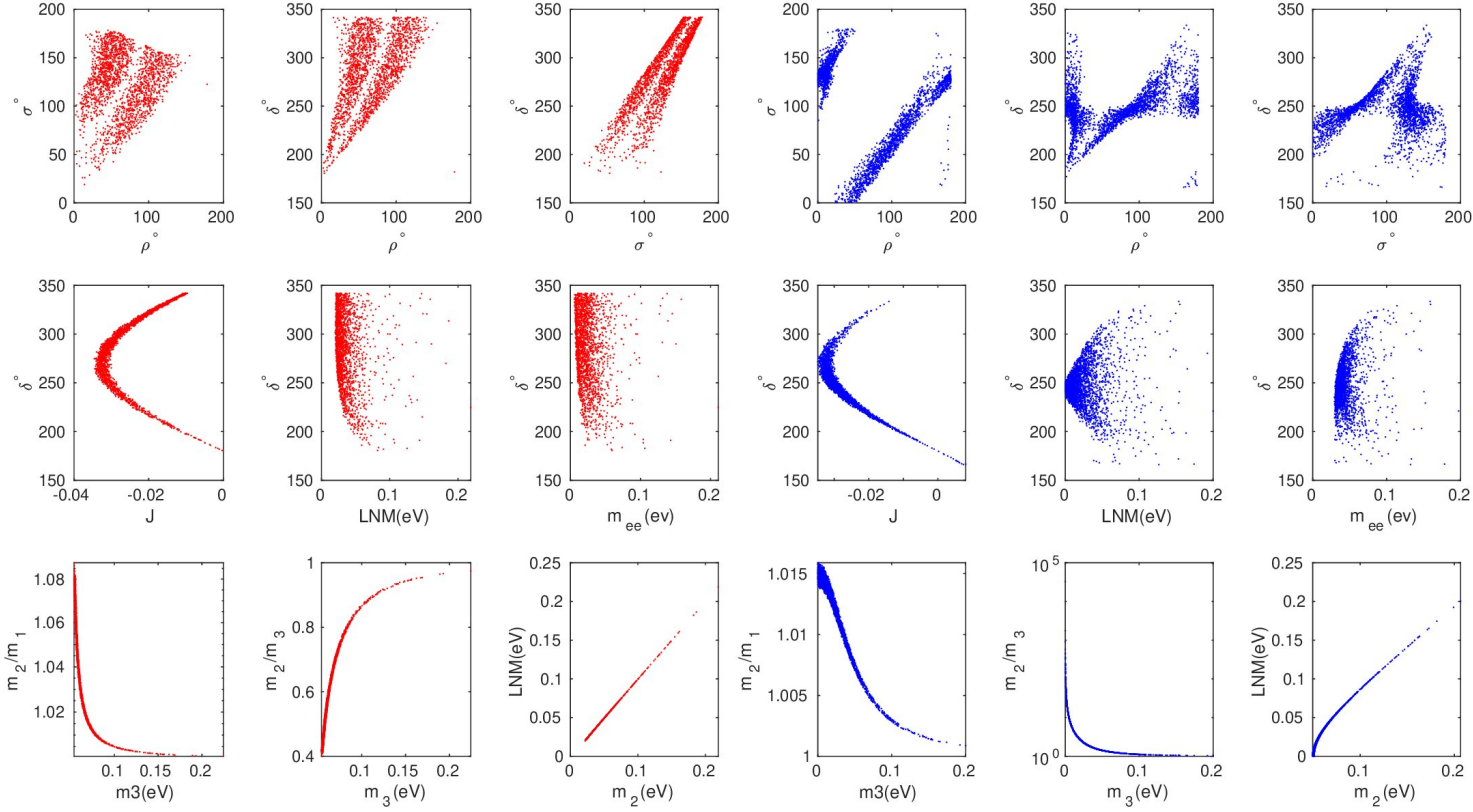


Figure 13: The correlation plots for  $F$  pattern, the red (blue) plots represent the normal (inverted) ordering. The first row represents the correlations between the CP-violating phases, the second one represents the correlations between  $\delta$  and each of  $J$ ,  $\text{LNM}$  (the lowest neutrino mass) and  $m_{ee}$  parameters. The last one shows the degree of hierarchy.

### 5.7 Pattern $G_1$ : $M_{\nu 11} = M_{\nu 23}$

The expressions for  $A_1$ ,  $A_2$  and  $A_3$  coefficients for this pattern are

$$\begin{aligned} A_1 &= c_{12}^2 c_{13}^2 - (-c_{12} s_{23} s_{13} - s_{12} c_{23} e^{-i\delta})(-c_{12} c_{23} s_{13} + s_{12} s_{23} e^{-i\delta}), \\ A_2 &= s_{12}^2 c_{13}^2 - (-s_{12} s_{23} s_{13} + c_{12} c_{23} e^{-i\delta})(-s_{12} c_{23} s_{13} - c_{12} s_{23} e^{-i\delta}), \\ A_3 &= s_{13}^2 - s_{23} c_{13}^2 c_{23}. \end{aligned} \quad (68)$$

For normal ordering, the representative point is taken as follows.

$$\begin{aligned} (\theta_{12}, \theta_{23}, \theta_{13}) &= (33.8880^\circ, 40.4840^\circ, 8.3779^\circ), \\ (\delta, \rho, \sigma) &= (328.6882^\circ, 162.0965^\circ, 179.3086^\circ), \\ (m_1, m_2, m_3) &= (0.0214\text{eV}, 0.0231\text{eV}, 0.0546\text{eV}), \\ (m_{ee}, m_e) &= (0.0217\text{eV}, 0.0231\text{eV}), \end{aligned} \quad (69)$$

The corresponding neutrino mass matrix (in eV) is

$$M_\nu = \begin{pmatrix} 0.0199 - 0.0086i & 0.0029 + 0.0054i & 0.0043 - 0.0030i \\ 0.0029 + 0.0054i & 0.0307 + 0.0089i & 0.0199 - 0.0086i \\ 0.0043 - 0.0030i & 0.0199 - 0.0086i & 0.0368 + 0.0079i \end{pmatrix}. \quad (70)$$

For inverted ordering, the representative point is taken as follows.

$$\begin{aligned} (\theta_{12}, \theta_{23}, \theta_{13}) &= (32.9986^\circ, 42.0093^\circ, 8.4570^\circ), \\ (\delta, \rho, \sigma) &= (173.1587^\circ, 159.5782^\circ, 58.7789^\circ), \\ (m_1, m_2, m_3) &= (0.0631\text{eV}, 0.0637\text{eV}, 0.0393\text{eV}), \\ (m_{ee}, m_e) &= (0.0279\text{eV}, 0.0629\text{eV}), \end{aligned} \quad (71)$$

The corresponding neutrino mass matrix (in eV) is

$$M_\nu = \begin{pmatrix} 0.0252 - 0.0120i & 0.0311 - 0.0283i & -0.0252 + 0.0279i \\ 0.0311 - 0.0283i & 0.0044 - 0.0196i & 0.0252 - 0.0120i \\ -0.0252 + 0.0279i & 0.0252 - 0.0120i & 0.0216 + 0.0052i \end{pmatrix}. \quad (72)$$

From Table (3), we see that the mixing angles  $(\theta_{12}, \theta_{23}, \theta_{13})$  extend over their allowed experimental ranges at all  $\sigma$ -levels for both normal and inverted ordering. There exists a large forbidden gap for  $\rho$  at all  $\sigma$ -levels with each hierarchy type. For normal ordering, there are narrow disallowed regions for  $\delta$  at 2- $\sigma$ -level and for the phase  $\sigma$  at 2-3- $\sigma$ -levels. For inverted ordering, the phase  $\sigma$  is restricted at all  $\sigma$ -levels to be nearly in the interval  $[16^\circ, 168^\circ]$ . We also note persistent forbidden gaps for  $\delta$  in inverted type. The allowed values of  $J$  at 1-2- $\sigma$ -levels for normal ordering and at 1- $\sigma$ -level for inverted ordering are negative, so the corresponding  $\delta$  lies in the third or fourth quarters. Neither  $m_1$  in normal type nor  $m_3$  in inverted type can reach a vanishing value. Thus, the singular pattern is not predicted at any  $\sigma$ -level.

For normal ordering plots, a large forbidden gap exists for  $\rho$ , whereas narrow gaps are noticed for  $\sigma$  and  $\delta$ . We find a moderate mass hierarchy where  $(0.34 \leq \frac{m_2}{m_3} \leq 0.97)$  together with a quasi degenerate mass spectrum characterized by  $(1 \leq \frac{m_2}{m_1} \leq 1.14)$ .

For inverted ordering plots, as in normal type, a large forbidden gap exists for  $\rho$ . We also see a tight forbidden gap in all correlations including  $\delta$ . We get a mild mass hierarchy characterized by  $(1.02 \leq \frac{m_2}{m_3} \leq 3.70)$  and a quasi degeneracy where  $(1 \leq \frac{m_2}{m_1} \leq 1.01)$ .

For both normal and inverted ordering, the correlations between  $(\delta, m_{ee})$  and between  $(\delta, \text{LNM})$  show that when  $m_{ee}$  and LNM increase, the allowed parameter space becomes more restricted.

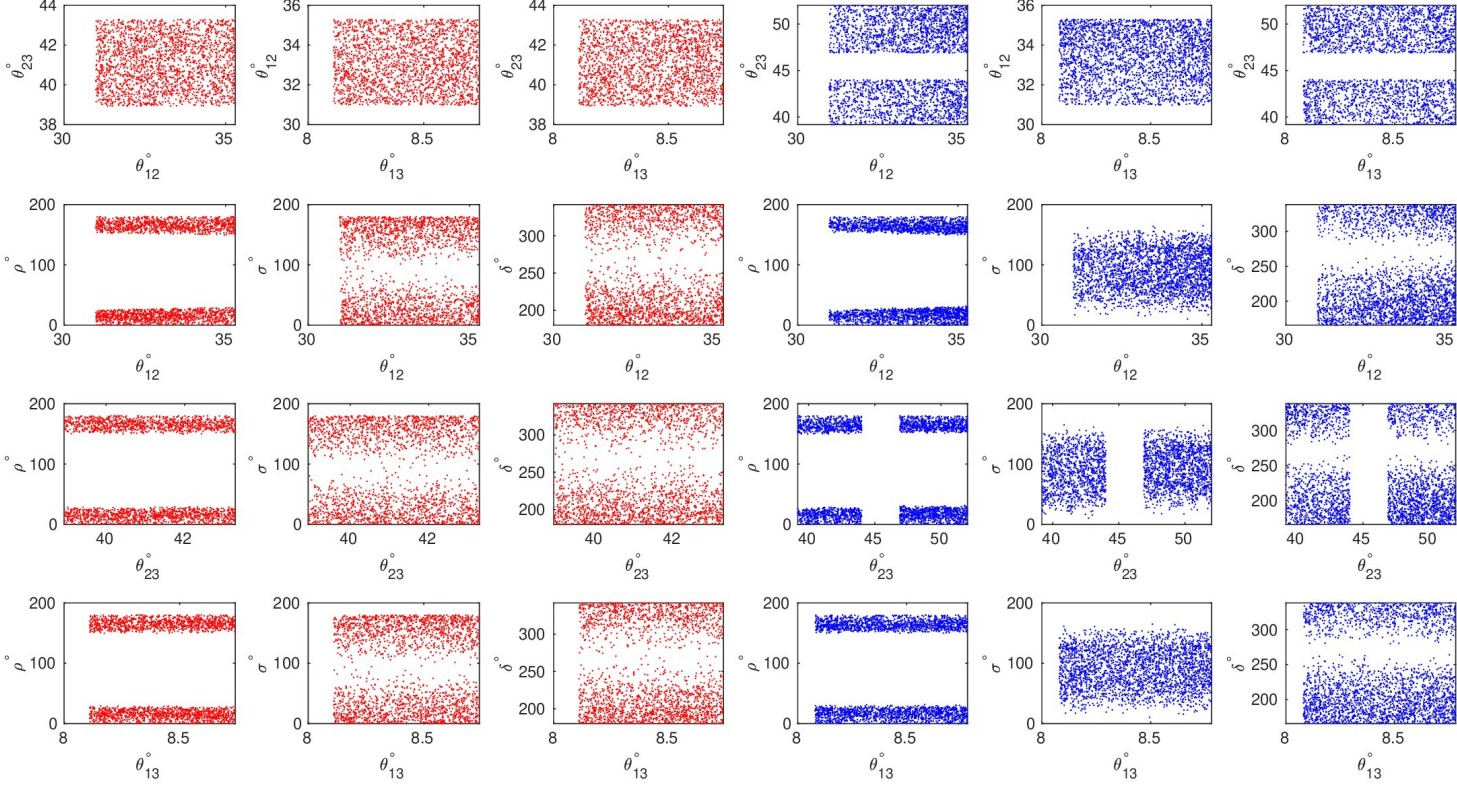


Figure 14: The correlation plots for  $G_1$  pattern, the red (blue) plots represents the normal (inverted) ordering. The first row represents the correlations between the mixing angles while the next three ones depict the correlations between each mixing angle with the CP-violating phases



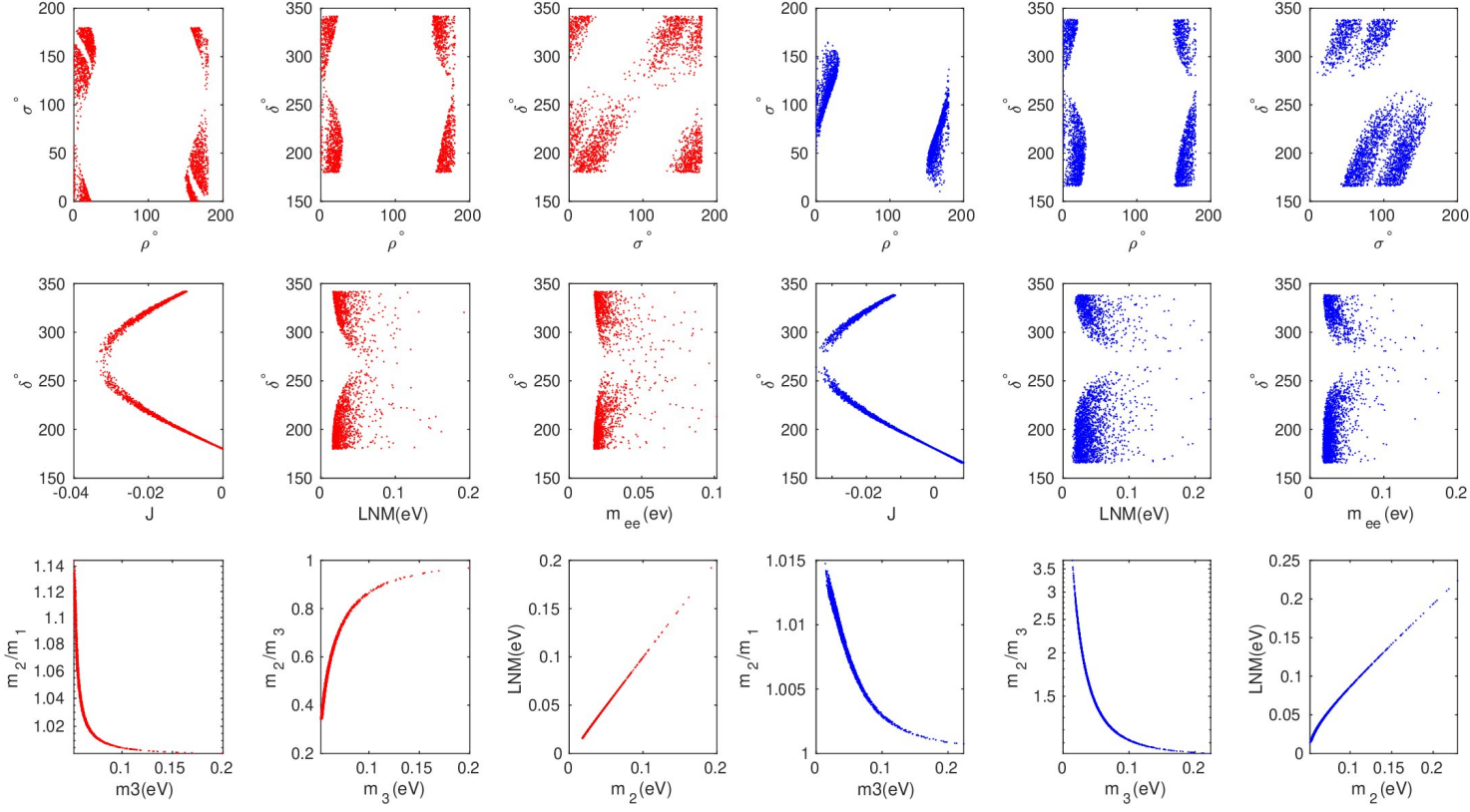


Figure 15: The correlation plots for  $G_1$  pattern, the red (blue) plots represent the normal (inverted) ordering. The first row represents the correlations between the CP-violating phases, the second one represents the correlations between  $\delta$  and each of  $J$ ,  $LNM$  (the lowest neutrino mass) and  $m_{ee}$  parameters. The last one shows the degree of hierarchy.

### 5.8 Pattern $G_2$ : $M_{\nu 22} = M_{\nu 33}$

The expressions for  $A_1$ ,  $A_2$  and  $A_3$  coefficients for this pattern are

$$\begin{aligned} A_1 &= (-c_{12}s_{23}s_{13} - s_{12}c_{23}e^{-i\delta})^2 - (-c_{12}c_{23}s_{13} + s_{12}s_{23}e^{-i\delta})^2, \\ A_2 &= (-s_{12}s_{23}s_{13} + c_{12}c_{23}e^{-i\delta})^2 - (-s_{12}c_{23}s_{13} - c_{12}s_{23}e^{-i\delta})^2, \\ A_3 &= s_{23}^2 c_{13}^2 - c_{23}^2 c_{13}^2. \end{aligned} \quad (73)$$

For normal ordering, the representative point is taken as follows.

$$\begin{aligned} (\theta_{12}, \theta_{23}, \theta_{13}) &= (33.6290^\circ, 42.9356^\circ, 8.3673^\circ), \\ (\delta, \rho, \sigma) &= (240.1034^\circ, 126.8967^\circ, 30.8559^\circ), \\ (m_1, m_2, m_3) &= (0.0117\text{eV}, 0.0146\text{eV}, 0.0522\text{eV}), \\ (m_{ee}, m_e) &= (0.0039\text{eV}, 0.0147\text{eV}), \end{aligned} \quad (74)$$

The corresponding neutrino mass matrix (in eV) is

$$M_\nu = \begin{pmatrix} 0.0010 - 0.0038i & -0.0035 - 0.0007i & 0.0136 + 0.0014i \\ -0.0035 - 0.0007i & 0.0269 - 0.0030i & 0.0242 + 0.0030i \\ 0.0136 + 0.0014i & 0.0242 + 0.0030i & 0.0269 - 0.0030i \end{pmatrix}. \quad (75)$$

For inverted ordering, the representative point is taken as follows.

$$\begin{aligned} (\theta_{12}, \theta_{23}, \theta_{13}) &= (33.2711^\circ, 41.6181^\circ, 8.4068^\circ), \\ (\delta, \rho, \sigma) &= (232.3966^\circ, 177.7075^\circ, 24.2744^\circ), \\ (m_1, m_2, m_3) &= (0.0830\text{eV}, 0.0834\text{eV}, 0.0669\text{eV}), \\ (m_{ee}, m_e) &= (0.0756\text{eV}, 0.0828\text{eV}), \end{aligned} \quad (76)$$

The corresponding neutrino mass matrix (in eV) is

$$M_\nu = \begin{pmatrix} 0.0743 + 0.0139i & -0.0136 - 0.0231i & 0.0106 + 0.0177i \\ -0.0136 - 0.0231i & 0.0456 - 0.0359i & 0.0216 + 0.0364i \\ 0.0106 + 0.0177i & 0.0216 + 0.0364i & 0.0456 - 0.0359i \end{pmatrix}. \quad (77)$$

We see from Table (3) that the mixing angles  $(\theta_{12}, \theta_{23}, \theta_{13})$  extend over their allowed experimental ranges with each hierarchy type at all  $\sigma$ -levels. The allowed experimental ranges for the Dirac phase  $\delta$  can be covered in normal type at all  $\sigma$ -levels, whereas narrow forbidden gaps exist in inverted type. We find that  $\rho$  ( $\sigma$ ) is restricted at the 1- $\sigma$ -level to be nearly in the interval  $[45^\circ, 166^\circ]$  ( $[7^\circ, 105^\circ]$ ) in the case of normal ordering. Table (3) also reveals that  $m_1$  can reach zero value at the 3- $\sigma$ -level while  $m_3$  can reach a vanishing value at all  $\sigma$ -levels. Thus, we predict a singular case with each hierarchy type, at the 3- $\sigma$ -level in normal type and at all  $\sigma$ -levels in inverted type. The allowed values of  $J$  at the 1-2- $\sigma$ -levels for normal ordering and at the 1- $\sigma$ -level for inverted ordering are negative, so the corresponding  $\delta$  lies in the third or fourth quarters.

For normal ordering plots, we see narrow forbidden bands for the phases  $\rho$  and  $\sigma$ . We also see a moderate mass hierarchy where  $(0.23 \leq \frac{m_2}{m_3} \leq 0.97)$  besides a quasi degeneracy characterized by  $(1 \leq \frac{m_2}{m_1} \leq 1.46)$ .

As to inverted ordering plots, we find a linear correlation between  $(\rho, \sigma)$ . We also find a quasi degeneracy characterized by  $m_1 \approx m_2$  as well as an acute hierarchy where  $\frac{m_2}{m_3}$  can reach  $10^4$  indicating the possibility of a vanishing  $m_3$ .

For both normal and inverted ordering, the correlations between  $(\delta, m_{ee})$  and between  $(\delta, \text{LNM})$  show that when  $m_{ee}$  and LNM increase, the allowed parameter space becomes more limited.

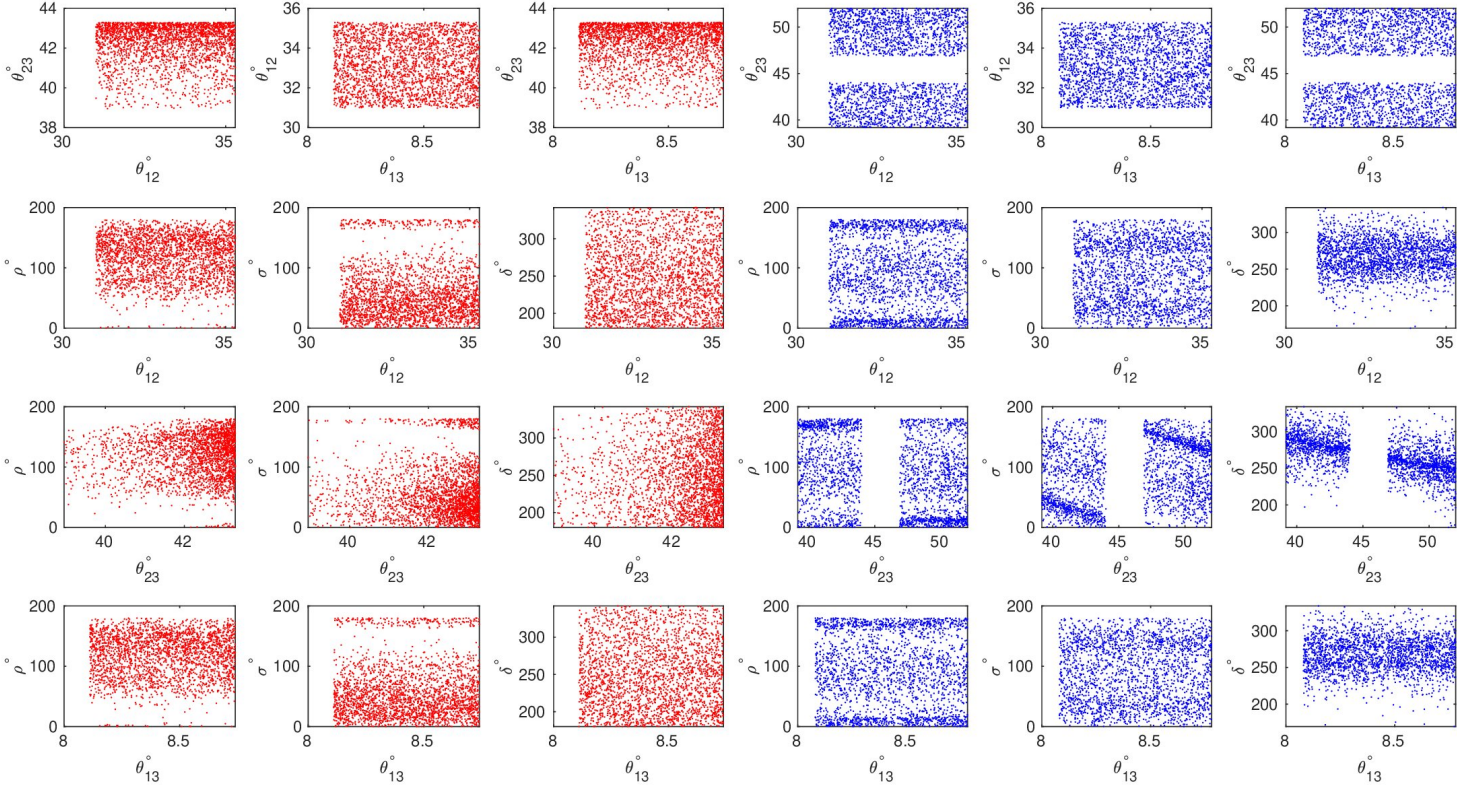


Figure 16: The correlation plots for  $G_2$  pattern, the red (blue) plots represent the normal (inverted) ordering. The first row represents the correlations between the mixing angles while the next three ones depict the correlations between each mixing angle with the CP-violating phases.



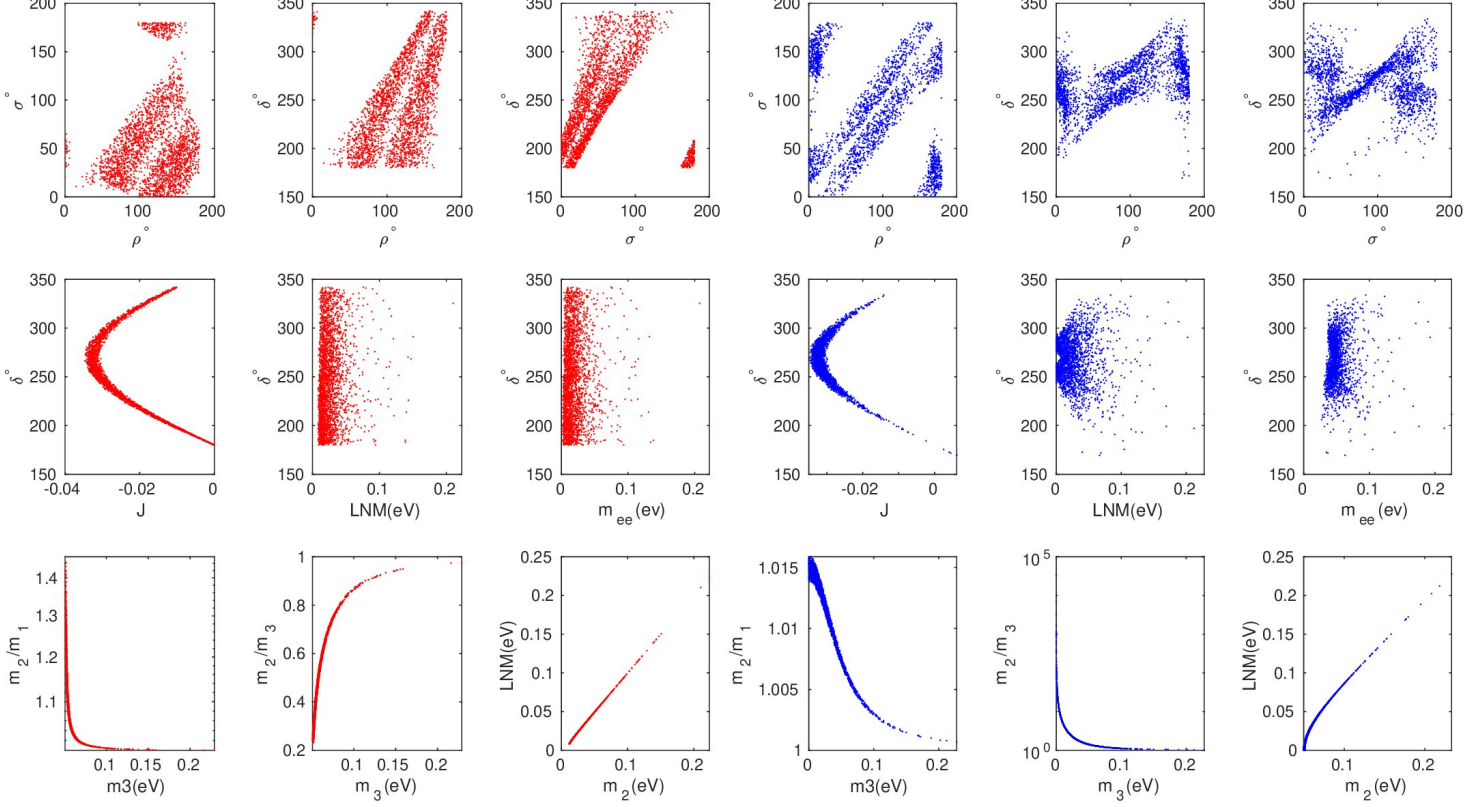


Figure 17: The correlation plots for  $G_2$  pattern, the red (blue) plots represent the normal (inverted) ordering. The first row represents the correlations between the CP-violating phases, the second one represent the correlations between  $\delta$  and each of  $J$ ,  $LNM$  (the lowest neutrino mass) and  $m_{ee}$  parameters. The last one shows the degree of hierarchy.

### 5.9 Pattern $G_3$ : $M_{\nu 12} = M_{\nu 13}$

The expressions for  $A_1$ ,  $A_2$  and  $A_3$  coefficients for this pattern are

$$\begin{aligned}
 A_1 &= c_{12}c_{13}(-c_{12}s_{23}s_{13} - s_{12}c_{23}e^{-i\delta}) - c_{12}c_{13}(-c_{12}c_{23}s_{13} + s_{12}s_{23}e^{-i\delta}), \\
 A_2 &= s_{12}c_{13}(-s_{12}s_{23}s_{13} + c_{12}c_{23}e^{-i\delta}) - s_{12}c_{13}(-s_{12}c_{23}s_{13} - c_{12}s_{23}e^{-i\delta}), \\
 A_3 &= s_{13}s_{23}c_{13} - s_{13}c_{23}c_{13}.
 \end{aligned} \tag{78}$$

The leading order approximation of  $s_{13}$  for the mass ratios are given by

$$\begin{aligned}
 \frac{m_1}{m_3} &\approx \frac{2(\sin 2\theta_{23} - 1) \sin(2\sigma - \delta)}{\cos 2\theta_{23} \sin 2\theta_{12} \sin(2\sigma - 2\rho)} \sin \theta_{13}, \\
 \frac{m_2}{m_3} &\approx -\frac{2 \cos 2\theta_{23} \sin(2\rho - \delta)}{\sin 2\theta_{12} (\sin 2\theta_{23} + 1) \sin(2\sigma - 2\rho)} \sin \theta_{13}.
 \end{aligned} \tag{79}$$

For normal ordering, the representative point is taken as follows.

$$\begin{aligned}
(\theta_{12}, \theta_{23}, \theta_{13}) &= (33.2699^\circ, 40.8019^\circ, 8.4560^\circ), \\
(\delta, \rho, \sigma) &= (247.2253^\circ, 99.1743^\circ, 100.7789^\circ), \\
(m_1, m_2, m_3) &= (0.0290\text{eV}, 0.0302\text{eV}, 0.0591\text{eV}), \\
(m_{ee}, m_e) &= (0.0275\text{eV}, 0.0303\text{eV}),
\end{aligned} \tag{80}$$

The corresponding neutrino mass matrix (in eV) is

$$M_\nu = \begin{pmatrix} -0.0258 - 0.0095i & 0.0090 + 0.0010i & 0.0090 + 0.0010i \\ 0.0090 + 0.0010i & 0.0312 + 0.0155i & 0.0224 - 0.0136i \\ 0.0090 + 0.0010i & 0.0224 - 0.0136i & 0.0381 + 0.0115i \end{pmatrix}. \tag{81}$$

For inverted ordering, the representative point is taken as follows.

$$\begin{aligned}
(\theta_{12}, \theta_{23}, \theta_{13}) &= (33.1636^\circ, 42.3774^\circ, 8.4760^\circ), \\
(\delta, \rho, \sigma) &= (194.7693^\circ, 143.2909^\circ, 143.2999^\circ), \\
(m_1, m_2, m_3) &= (0.0506\text{eV}, 0.0513\text{eV}, 0.0119\text{eV}), \\
(m_{ee}, m_e) &= (0.0498\text{eV}, 0.0503\text{eV}),
\end{aligned} \tag{82}$$

The corresponding neutrino mass matrix (in eV) is

$$M_\nu = \begin{pmatrix} 0.0144 - 0.0476i & -0.0003 + 0.0050i & -0.0003 + 0.0050i \\ -0.0003 + 0.0050i & -0.0008 - 0.0277i & 0.0116 + 0.0243i \\ -0.0003 + 0.0050i & 0.0116 + 0.0243i & 0.0013 - 0.0231i \end{pmatrix}. \tag{83}$$

We see from Table (3) that the allowed experimental ranges for the mixing angles  $\theta_{12}$  and  $\theta_{13}$  can be covered for both normal and inverted ordering at all  $\sigma$ -levels. However, we find a very tight forbidden gap for the mixing angle  $\theta_{23}$   $[44.52^\circ, 45.46^\circ]$  with each hierarchy type at the 3- $\sigma$ -level. For normal ordering, we find that the ranges for  $\rho$  ( $\sigma$ ) are restricted to be nearly in the interval  $[40^\circ, 178^\circ]$  ( $[41^\circ, 178^\circ]$ ) at the 1- $\sigma$ -level and tending to be wider at the 2- $\sigma$ -level to be nearly in  $[19^\circ, 179^\circ]$  ( $[25^\circ, 179^\circ]$ ). Table (3) also reveals that  $m_1$  does not approach zero value at any  $\sigma$ -level, whereas  $m_3$  can reach a vanishing value at all  $\sigma$ -levels. Therefore, the singular pattern is predicted in inverted type at all  $\sigma$ -levels. The allowed values of J at the 1-2- $\sigma$ -levels for normal ordering and 1- $\sigma$ -level for inverted ordering are negative, so the corresponding  $\delta$  lies in the third or fourth quarters.

For normal ordering plots, a strong linear correlation exists between  $(\rho, \sigma)$ . We see a mild mass hierarchy where  $(0.32 \leq \frac{m_2}{m_3} \leq 0.97)$  together with a quasi degeneracy characterized by  $m_1 \approx m_2$ .

For inverted ordering plots, we find a strong linear correlation between  $(\rho, \sigma)$  as in normal type and a severe hierarchy where  $\frac{m_2}{m_3}$  can reach  $10^3$  indicating the possibility of a vanishing  $m_3$ .

For both normal and inverted ordering, the correlations between  $(\delta, m_{ee})$  and between  $(\delta, \text{LNM})$  show that when  $m_{ee}$  and LNM increase, the allowed parameter space becomes more restricted.

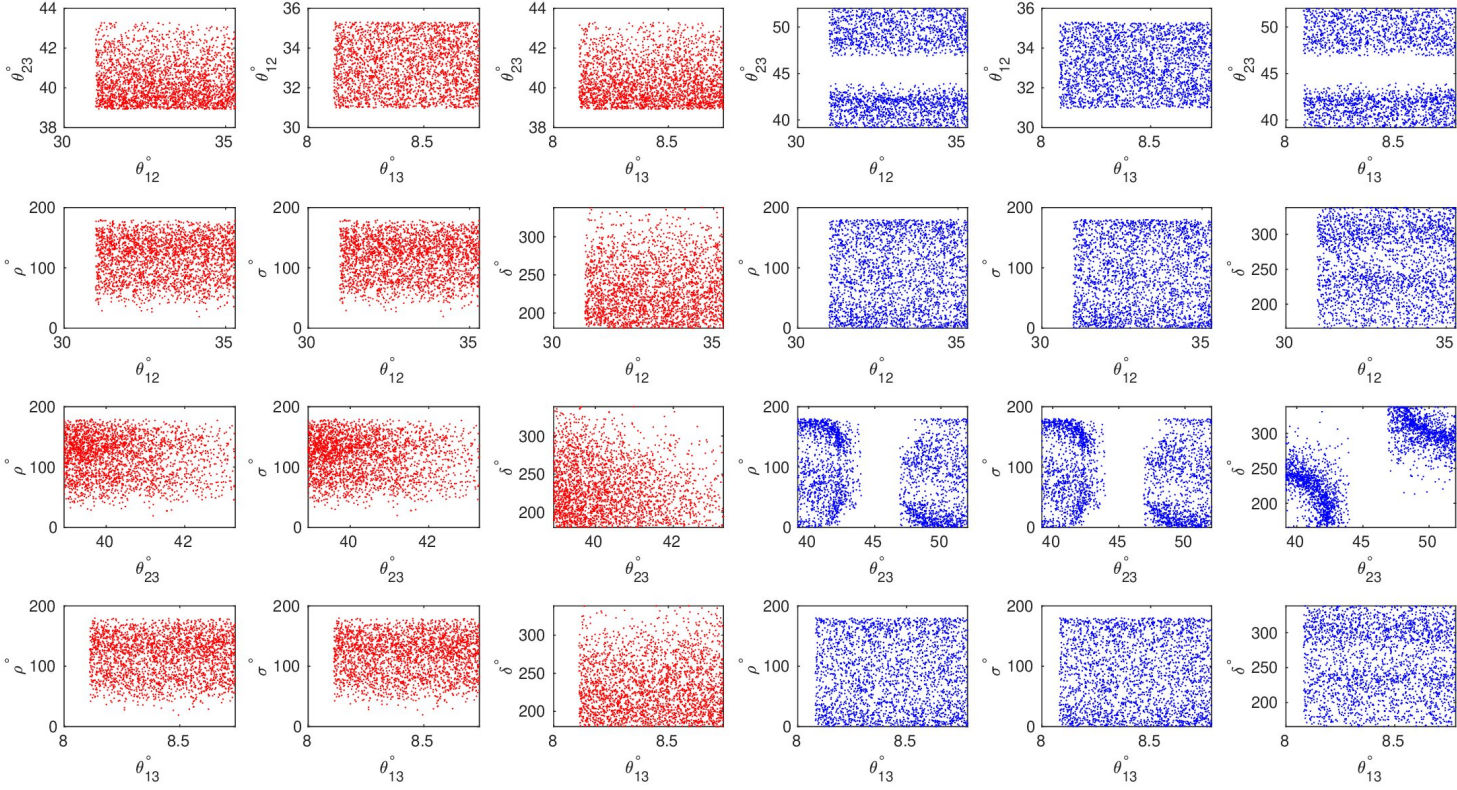


Figure 18: The correlation plots for  $G_3$  pattern, the red (blue) plots represent the normal (inverted) ordering. The first row represents the correlations between the mixing angles while the next three ones depict the correlations between each mixing angle with the CP-violating phases.

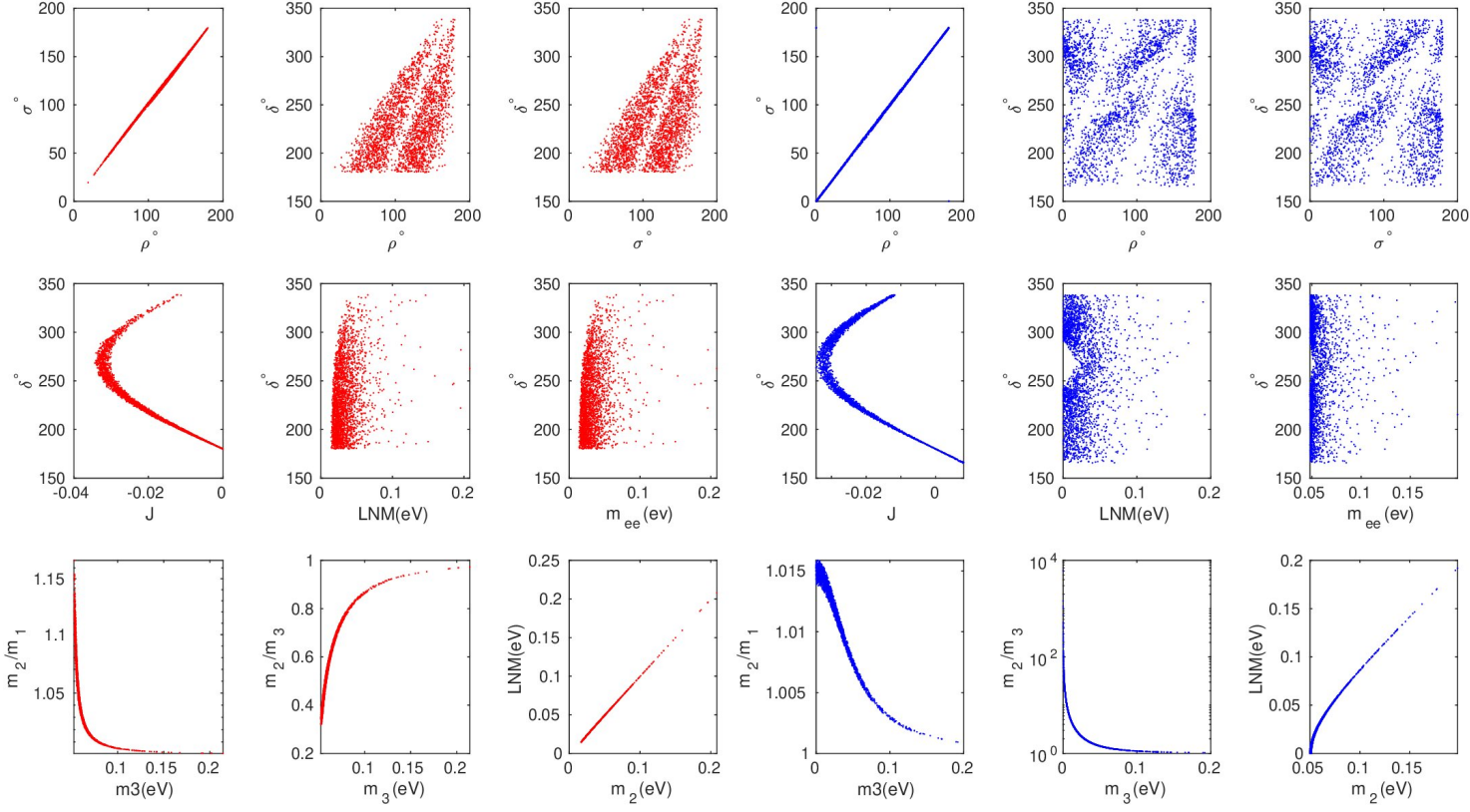


Figure 19: The correlation plots for  $G_3$  pattern, the red (blue) plots represent the normal (inverted) ordering. The first row represents the correlations between the CP-violating phases, the second one represent the correlations between  $\delta$  and each of  $J$ ,  $LNM$  (the lowest neutrino mass) and  $m_{ee}$  parameters. The last one shows the degree of hierarchy.

## 6 Symmetry realization

In this section, we introduce symmetry realizations for four, out of the stated nine phenomenologically allowed textures, in different seesaw scenarios. As a matter of fact, there are various realization methods which have been used to realize the Equality textures in  $M_\nu$ . Neutrino mass matrices with two equalities have been realized through a non-Abelian  $A_4$  flavor symmetry in [16], whereas the authors of [17] used  $S_3$  symmetry to realize one equality texture in  $M_\nu$ . In [18], the Abelian  $S_{\mu-\tau} \times Z_8$  symmetry with Froggatt-Nielsen mechanism including non-renormalizable 5-dim operators has been introduced to realize equalities in  $M_\nu$  with either  $m_1$  or  $m_3$  equal to zero. In this study, we adopt realization methods depending on Abelian discrete flavor symmetries by extending the standard model with some additional matter fields. We present symmetry realizations for the patterns  $E$ ,  $F$ ,  $G_2$  and  $G_3$ . We use  $Z_2 \times Z_6$ ,  $Z_2 \times Z'_2$  and  $Z_2 \times Z'_2 \times U(1)^3$  within type-I, type-II and mixed type (I+II) seesaw scenarios respectively. For the purpose of illustration, we take the pattern  $E$  where  $(M_\nu)_{11} = (M_\nu)_{22}$  as a concrete example whereas the realizations for the remaining three patterns are summarized in the tables.

### 6.1 Type-I seesaw

The standard model (SM) particle content is extended with three-right handed neutrinos  $\nu_{Ri}$  ( $i = 1, 2, 3$ ), four SM Higgs doublets  $\phi_i$  ( $i = 1, 2, 3, 4$ ) and a scalar singlet  $\chi$ . The general gauge-invariant Lagrangian is given by

$$\mathcal{L} = Y_{lij}^k \bar{D}_{Li} \phi_k l_{Rj} + Y_{vij}^k \bar{D}_{Li} \tilde{\phi}_k \nu_{Rj} + X_{ij} \chi \nu_{Ri} \nu_{Rj} + h.c \quad (84)$$

where  $D_{Li} = (\nu_{Li}, l_{Li})^T$  are three left-handed lepton doublets,  $l_{Rj}$  are three right-handed charged leptons and  $\tilde{\phi}_k = i\sigma_2 \phi_k^*$ . The effective Majorana mass matrix of light neutrino  $M_\nu$  is generated through a type-I seesaw formula  $M_\nu = M_D M_R^{-1} M_D^T$ . We impose  $Z_2 \times Z_6$  flavor symmetry on the Lagrangian in Eq.(84), and assume the leptons transform under  $Z_6$  as

$$\begin{aligned} D_{L1} &\rightarrow D_{L1}, & D_{L2} &\rightarrow D_{L2}, & D_{L3} &\rightarrow \omega D_{L3}, \\ \nu_{R1} &\rightarrow \nu_{R1}, & \nu_{R2} &\rightarrow \nu_{R2}, & \nu_{R3} &\rightarrow \omega \nu_{R3}, \\ l_{R1} &\rightarrow \omega^3 l_{R1}, & l_{R2} &\rightarrow \omega^3 l_{R2}, & l_{R3} &\rightarrow \omega^4 l_{R3}, \end{aligned} \quad (85)$$

while the scalar multiplets transform as

$$\phi_1 \rightarrow \phi_1, \phi_2 \rightarrow \omega \phi_2, \phi_3 \rightarrow \omega^5 \phi_3, \phi_4 \rightarrow \omega^3 \phi_4, \phi_5 \rightarrow \omega^3 \phi_5, \chi \rightarrow \omega^4 \chi, \quad (86)$$

where  $\omega = e^{\pi i/3}$ . The bilinear  $\nu_{Ri} \nu_{Rj}$  transform under  $Z_6$  as

$$\nu_{Ri} \nu_{Rj} \cong \begin{pmatrix} 1 & 1 & \omega \\ 1 & 1 & \omega \\ \omega & \omega & \omega^2 \end{pmatrix}. \quad (87)$$

The elements (1,1), (1,2), (2,1) and (2,2) are thus directly existent in the Lagrangian because they are  $Z_6$  invariant. A real scalar singlet ( $\chi$ ) generates a non-vanishing matrix element (3,3) when acquiring a vacuum expectation value (VEV) at the seesaw scale. Under the action of  $Z_6$ ,  $\bar{D}_{Li} \nu_{Rj}$  and  $\bar{D}_{Li} l_{Rj}$  transform as

$$\bar{D}_{Li} \nu_{Rj} \cong \begin{pmatrix} 1 & 1 & \omega \\ 1 & 1 & \omega \\ \omega^5 & \omega^5 & 1 \end{pmatrix}, \quad \bar{D}_{Li} l_{Rj} \cong \begin{pmatrix} \omega^3 & \omega^3 & \omega^4 \\ \omega^3 & \omega^3 & \omega^4 \\ \omega^2 & \omega^2 & \omega^3 \end{pmatrix}. \quad (88)$$

The SM Higgs doublet  $\phi_1$  generates (1,1), (1,2), (2,1), (2,2) and (3,3) matrix elements in the Dirac neutrino mass matrix  $M_D$  while  $\phi_2$  and  $\phi_3$  generate (1,3), (2,3) and (3,1), (3,2) non-vanishing elements. The scalar doublets  $\phi_4$  and  $\phi_5$  are responsible for generating (1,1), (1,2), (2,1), (2,2) and (3,3) matrix elements in the charged lepton mass matrix  $M_l$ .

We set up that under the action of  $Z_2$ , the leptons transform as

$$\begin{aligned} D_{L1} &\rightarrow D_{L2}, & D_{L2} &\rightarrow D_{L1}, & D_{L3} &\rightarrow D_{L3}, \\ \nu_{R1} &\rightarrow \nu_{R2}, & \nu_{R2} &\rightarrow \nu_{R1}, & \nu_{R3} &\rightarrow \nu_{R3}, \\ l_{R1} &\rightarrow l_{R1}, & l_{R2} &\rightarrow l_{R2}, & l_{R3} &\rightarrow l_{R3}, \end{aligned} \quad (89)$$

while the scalar multiplets transform as:

$$\phi_1 \rightarrow \phi_1, \phi_2 \rightarrow -\phi_2, \phi_3 \rightarrow \phi_3, \phi_4 \rightarrow \phi_5, \phi_5 \rightarrow \phi_4, \chi \rightarrow \chi. \quad (90)$$

As we see from Eqs.(89,90), the Yukawa couplings  $X_{ij}$ ,  $Y_{\nu ij}$  and  $Y_{l ij}$  are constrained by the  $Z_2$  symmetry

$$\begin{aligned} Y_{l11}^4 &= Y_{l21}^5, \quad Y_{l12}^4 = Y_{l22}^5, \quad Y_{l21}^4 = Y_{l11}^5, \quad Y_{l22}^4 = Y_{l12}^5, \quad Y_{l33}^4 = Y_{l33}^5, \\ Y_{\nu11}^1 &= Y_{\nu22}^1, \quad Y_{\nu12}^1 = Y_{\nu21}^1, \quad Y_{\nu13}^2 = -Y_{\nu23}^2, \quad Y_{\nu31}^3 = Y_{\nu32}^3, \\ X_{11} &= X_{22}, \quad X_{12} = X_{21}. \end{aligned} \quad (91)$$

The resulting right-handed Majorana mass matrix  $M_R$  and Dirac neutrino mass matrix  $M_D$  under  $Z_6 \times Z_2$ -symmetry take the form

$$M_R = \begin{pmatrix} x & y & 0 \\ y & x & 0 \\ 0 & 0 & z \end{pmatrix}, \quad M_D = \begin{pmatrix} A & B & C \\ B & A & -C \\ D & D & E \end{pmatrix}. \quad (92)$$

Hence, the effective Majorana mass matrix of light neutrino takes the form,

$$M_\nu = M_D M_R^{-1} M_D^T = \begin{pmatrix} a & b & c \\ b & a & d \\ c & d & e \end{pmatrix}. \quad (93)$$

which is of the requested form.

We need to check that one can, to a good approximation, be in the flavor basis, as we assumed during the phenomenological study, corresponding to a diagonal charged lepton mass matrix  $M_l$  which takes the form,

$$M_l = \begin{pmatrix} Y_{l11}^4 v_4 + Y_{l21}^4 v_5 & Y_{l12}^4 v_4 + Y_{l22}^4 v_5 & 0 \\ Y_{l21}^4 v_4 + Y_{l11}^4 v_5 & Y_{l22}^4 v_4 + Y_{l12}^4 v_5 & 0 \\ 0 & 0 & Y_{l33}^4 v_4 + Y_{l33}^4 v_5 \end{pmatrix}, \quad (94)$$

where  $v_4$  and  $v_5$  are VEVs of the scalar doublets  $\phi_4$  and  $\phi_5$ . We follow the procedure presented in [14] and assume the hierarchy ( $v_4 \ll v_5 \approx v$ ). Then we get

$$M_l \approx v \begin{pmatrix} Y_{l21}^4 & Y_{l22}^4 & 0 \\ Y_{l11}^4 & Y_{l12}^4 & 0 \\ 0 & 0 & Y_{l33}^4 \end{pmatrix} = v \begin{pmatrix} \mathbf{a}^T \\ \mathbf{b}^T \\ \mathbf{c}^T \end{pmatrix} \Rightarrow M_l M_l^\dagger = v^2 \begin{pmatrix} |\mathbf{a}|^2 & \mathbf{a} \cdot \mathbf{b} & 0 \\ \mathbf{b} \cdot \mathbf{a} & |\mathbf{b}|^2 & 0 \\ 0 & 0 & |\mathbf{c}|^2 \end{pmatrix}, \quad (95)$$

The matter content				
$D_L$	$\nu_R$	$l_R$	$\phi$	$\chi$
Symmetry under $Z_6$				
$T_D D_L$ $T_D = \text{diag}(1, \omega, 1)$	$T_\nu \nu_R$ $T_\nu = \text{diag}(1, \omega, 1)$	$T_l l_R$ $T_l = \text{diag}(\omega^3, \omega^4, \omega^3)$	$T_\phi \phi$ $T_\phi = \text{diag}(1, \omega, \omega^3, \omega^3)$	$T_\chi \chi$ $T_\chi = \text{diag}(1, \omega^4)$
Symmetry under $Z_2$				
$S_D D_L$ $S_D = \begin{pmatrix} 0 & 0 & 1 \\ 0 & 1 & 0 \\ 1 & 0 & 0 \end{pmatrix}$	$S_\nu \nu_R$ $S_\nu = \begin{pmatrix} 0 & 0 & 1 \\ 0 & 1 & 0 \\ 1 & 0 & 0 \end{pmatrix}$	$S_l l_R$ $S_l = \begin{pmatrix} 1 & 0 & 0 \\ 0 & 1 & 0 \\ 0 & 0 & 1 \end{pmatrix}$	$S_\phi \phi$ $S_\Phi = \begin{pmatrix} 1 & 0 & 0 & 0 \\ 0 & 1 & 0 & 0 \\ 0 & 0 & 0 & 1 \\ 0 & 0 & 1 & 0 \end{pmatrix}$	$S_\chi \chi$ $S_\chi = \begin{pmatrix} -1 & 0 \\ 0 & 1 \end{pmatrix}$
Mass matrices				
$M_R = \begin{pmatrix} x & 0 & z \\ 0 & y & 0 \\ z & 0 & w \end{pmatrix}$	$M_D = \begin{pmatrix} A & D & C \\ 0 & B & 0 \\ C & D & A \end{pmatrix}$	$M_\nu = \begin{pmatrix} a & b & c \\ b & d & b \\ c & b & e \end{pmatrix}$	$M_l \stackrel{v_3 \ll v_4}{\approx} v_4 \begin{pmatrix} Y_{l31}^3 & 0 & Y_{l33}^3 \\ 0 & Y_{l22}^3 & 0 \\ Y_{l11}^3 & 0 & Y_{l13}^3 \end{pmatrix}$	

Table 4: The  $Z_2 \times Z_6$  symmetry realization for the  $F : M_{\nu 12} = M_{\nu 23}$  pattern within type-I seesaw scenario. S and T are the symmetry transformation matrices for  $Z_2$  and  $Z_6$  respectively.

The matter content				
$D_L$	$\nu_R$	$l_R$	$\phi$	$\chi$
Symmetry under $Z_6$				
$T_D D_L$ $T_D = \text{diag}(\omega, 1, 1)$	$T_\nu \nu_R$ $T_\nu = \text{diag}(\omega, 1, 1)$	$T_l l_R$ $T_l = \text{diag}(\omega^4, \omega^3, \omega^3)$	$T_\phi \phi$ $T_\phi = \text{diag}(1, \omega^5, \omega, \omega^3, \omega^3)$	$T_\chi \chi$ $T_\chi = \omega^4$
Symmetry under $Z_2$				
$S_D D_L$ $S_D = \begin{pmatrix} 1 & 0 & 0 \\ 0 & 0 & 1 \\ 0 & 1 & 0 \end{pmatrix}$	$S_\nu \nu_R$ $S_\nu = \begin{pmatrix} 1 & 0 & 0 \\ 0 & 0 & 1 \\ 0 & 1 & 0 \end{pmatrix}$	$S_l l_R$ $S_l = \begin{pmatrix} 1 & 0 & 0 \\ 0 & 1 & 0 \\ 0 & 0 & 1 \end{pmatrix}$	$S_\phi \phi$ $S_\Phi = \begin{pmatrix} 1 & 0 & 0 & 0 & 0 \\ 0 & 1 & 0 & 0 & 0 \\ 0 & 0 & -1 & 0 & 0 \\ 0 & 0 & 0 & 0 & 1 \\ 0 & 0 & 0 & 1 & 0 \end{pmatrix}$	$S_\chi \chi$ $S_\chi = 1$
Mass matrices				
$M_R = \begin{pmatrix} x & 0 & 0 \\ 0 & y & z \\ 0 & z & y \end{pmatrix}$	$M_D = \begin{pmatrix} A & D & D \\ E & B & C \\ -E & C & B \end{pmatrix}$	$M_\nu = \begin{pmatrix} a & b & c \\ b & d & e \\ c & e & d \end{pmatrix}$	$M_l \stackrel{v_4 \ll v_5}{\approx} v_5 \begin{pmatrix} Y_{l11}^4 & 0 & 0 \\ 0 & Y_{l32}^4 & Y_{l33}^4 \\ 0 & Y_{l22}^4 & Y_{l23}^4 \end{pmatrix}$	

Table 5: The  $Z_2 \times Z_6$  symmetry realization for the  $G_2 : M_{\nu 22} = M_{\nu 33}$  pattern within type-I seesaw scenario. S and T are the symmetry transformation matrices for  $Z_2$  and  $Z_6$  respectively.

The matter content				
$D_L$	$\nu_R$	$l_R$	$\phi$	$\chi$
Symmetry under $Z_6$				
$T_D D_L$ $T_D = \text{diag}(\omega, 1, 1)$	$T_\nu \nu_R$ $T_\nu = \text{diag}(\omega, 1, 1)$	$T_l l_R$ $T_l = \text{diag}(\omega^4, \omega^3, \omega^3)$	$T_\phi \phi$ $T_\phi = \text{diag}(1, \omega, \omega^3, \omega^3)$	$T_\chi \chi$ $T_\chi = \text{diag}(1, \omega^4)$
Symmetry under $Z_2$				
$S_D D_L$ $S_D = \begin{pmatrix} 1 & 0 & 0 \\ 0 & 0 & 1 \\ 0 & 1 & 0 \end{pmatrix}$	$S_\nu \nu_R$ $S_\nu = \begin{pmatrix} 1 & 0 & 0 \\ 0 & 0 & 1 \\ 0 & 1 & 0 \end{pmatrix}$	$S_l l_R$ $S_l = \begin{pmatrix} 1 & 0 & 0 \\ 0 & 1 & 0 \\ 0 & 0 & 1 \end{pmatrix}$	$S_\phi \phi$ $S_\phi = \begin{pmatrix} 1 & 0 & 0 & 0 \\ 0 & 1 & 0 & 0 \\ 0 & 0 & 0 & 1 \\ 0 & 0 & 1 & 0 \end{pmatrix}$	$S_\chi \chi$ $S_\chi = \begin{pmatrix} -1 & 0 \\ 0 & 1 \end{pmatrix}$
Mass matrices				
$M_R = \begin{pmatrix} x & 0 & 0 \\ 0 & y & z \\ 0 & z & w \end{pmatrix}$	$M_D = \begin{pmatrix} A & 0 & 0 \\ D & B & C \\ D & C & B \end{pmatrix}$	$M_\nu = \begin{pmatrix} a & b & b \\ b & c & d \\ b & d & e \end{pmatrix}$	$M_l \stackrel{v_3 \ll v_4}{\approx} v_4 \begin{pmatrix} Y_{l11}^3 & 0 & 0 \\ 0 & Y_{l32}^3 & Y_{l33}^3 \\ 0 & Y_{l22}^3 & Y_{l23}^3 \end{pmatrix}$	

Table 6: The  $Z_2 \times Z_6$  symmetry realization for the  $G_3 : M_{\nu 12} = M_{\nu 13}$  pattern within type-I seesaw scenario. S and T are the symmetry transformation matrices for  $Z_2$  and  $Z_6$  respectively.

where the vectors **a**, **b** and **c** are defined as  $\mathbf{a} = (Y_{l21}^4, Y_{l22}^4, 0)$ ,  $\mathbf{b} = (Y_{l11}^4, Y_{l12}^4, 0)$  and  $\mathbf{c} = (0, 0, Y_{l33}^4)$ . By adjusting the magnitudes of the Yukawa couplings,  $M_l M_l^\dagger$  can be diagonalized by the infinitesimal rotation with an angle less than  $10^{-2}$ .

The symmetry assignments for the other cases,  $F$ ,  $G_2$  and  $G_3$ , are summarized in the tables 4, 5 and 6.

We could check that one can apply the method for the  $\mu$ - $\tau$ -transformation related patterns ( $E_2, F_2$ ). We could not, however, find suitable assignments for the method to be applicable for the remaining five cases (A,B,C,D,  $G_3$ ) and their  $\mu$ - $\tau$ -transformation related patterns ( $A_2, B_2, C_2, D_2$ ).

## 6.2 type-II seesaw

We present another realization method for the four patterns by using a simpler Abelian flavor symmetry within type-II seesaw scenario. We extend the standard model with  $SU(2)_L$  scalar triplets  $\Delta_k$ ,  $k=(1,2,\dots,N)$ ,

$$\Delta \equiv [\Delta_k^{++}, \Delta_k^+, \Delta_k^0]. \quad (96)$$

The gauge-invariant Yukawa interaction Lagrangian for scalar triplets  $\Delta_k$  takes the form,

$$-\mathcal{L}_\Delta = \sum_{k=1}^N \sum_{i,j=1}^3 \Gamma_{ij}^k [\Delta_k^0 \nu_{Li}^T \mathcal{C} \nu_{Lj} + \Delta_k^+ (\nu_{Li}^T \mathcal{C} l_{Lj} + l_{Lj}^T \mathcal{C} \nu_{Li}) + \Delta_k^{++} l_{Li}^T \mathcal{C} l_{Lj}], \quad (97)$$

where  $\Gamma_{ij}^k$  are the Yukawa couplings and  $\mathcal{C}$  is the charge conjugation matrix. The light neutrino mass matrix  $M_\nu$  takes the form,

$$M_{\nu ij} = \sum_{k=1}^N \Gamma_{ij}^k \langle \Delta_k^0 \rangle, \quad (98)$$

where  $\langle \Delta_k^0 \rangle$  are the VEVs of the  $\Delta_k^0$  fields. The smallness of  $\langle \Delta_k^0 \rangle$  is attributed to the largeness of the triplet scalars mass scale [26]. As in the type-I scenario, we take a pattern  $E$  as a concrete



example. The particle content of the standard model is extended with one Higgs doublet  $\phi$  and three scalar triplets  $\Delta_k (k = 1, 2, 3)$ . We impose  $Z_2 \times Z_2'$  symmetry on Eq.(97) in order to generate a desired form of  $M_\nu$ . The lepton fields transform under  $Z_2$  symmetry as

$$\begin{aligned} D_{L1} &\rightarrow D_{L1}, & D_{L2} &\rightarrow D_{L2}, & D_{L3} &\rightarrow -D_{L3}, \\ l_{R1} &\rightarrow -l_{R1}, & l_{R2} &\rightarrow -l_{R2}, & l_{R3} &\rightarrow l_{R3}, \end{aligned} \quad (99)$$

while the scalar multiplets transform as

$$\begin{aligned} \Delta_1 &\rightarrow \Delta_1, & \Delta_2 &\rightarrow -\Delta_2, & \Delta_3 &\rightarrow -\Delta_3, \\ \phi_1 &\rightarrow -\phi_1, & \phi_2 &\rightarrow -\phi_2. \end{aligned} \quad (100)$$

The bilinears  $\nu_{Li}\nu_{Lj}$  and  $\bar{D}_{Li}l_{Rj}$  transform under  $Z_2$  as

$$\nu_{Li}\nu_{Lj} \cong \begin{pmatrix} 1 & 1 & -1 \\ 1 & 1 & -1 \\ -1 & -1 & 1 \end{pmatrix}, \quad \bar{D}_{Li}l_{Rj} \cong \begin{pmatrix} -1 & -1 & 1 \\ -1 & -1 & 1 \\ 1 & 1 & -1 \end{pmatrix}. \quad (101)$$

The matrix elements (1,1), (1,2), (2,1), (2,2) and (3,3) are generated in  $M_\nu$  when the scalar triplet  $\Delta_1^\circ$  acquiring a small vacuum expectation value while  $\Delta_2^\circ$  and  $\Delta_3^\circ$  enforce the non-vanishing matrix elements (1,3), (2,3), (3,1) and (3,2). The nonzero elements (1,1), (1,2), (2,1), (2,2) and (3,3) exist in  $M_l$  through the scalar doublets  $\phi_1$  and  $\phi_2$ . Under the action of  $Z_2'$  symmetry, the lepton fields transform as

$$\begin{aligned} D_{L1} &\rightarrow D_{L2}, & D_{L2} &\rightarrow D_{L1}, & D_{L3} &\rightarrow D_{L3}, \\ l_{R1} &\rightarrow l_{R2}, & l_{R2} &\rightarrow l_{R1}, & l_{R3} &\rightarrow l_{R3}, \end{aligned} \quad (102)$$

whereas  $\Delta_k (k = 1, 2, 3)$  and  $\phi_i (i = 1, 2)$  transform as

$$\begin{aligned} \Delta_1 &\rightarrow \Delta_1, & \Delta_2 &\rightarrow \Delta_2, & \Delta_3 &\rightarrow -\Delta_3, \\ \phi_1 &\rightarrow \phi_2, & \phi_2 &\rightarrow \phi_1. \end{aligned} \quad (103)$$

Thus, the  $Z_2'$  invariance implies the constraints:

$$\begin{aligned} \Gamma_{11}^1 &= \Gamma_{22}^1, & \Gamma_{12}^1 &= \Gamma_{21}^1, & \Gamma_{13}^2 &= \Gamma_{23}^2, & \Gamma_{31}^2 &= \Gamma_{32}^2, & \Gamma_{13}^3 &= -\Gamma_{23}^3, & \Gamma_{31}^3 &= -\Gamma_{32}^3, \\ Y_{l11}^1 &= Y_{l21}^2, & Y_{l12}^1 &= Y_{l22}^2, & Y_{l21}^1 &= Y_{l11}^2, & Y_{l22}^1 &= Y_{l12}^2, & Y_{l33}^1 &= Y_{l33}^2. \end{aligned} \quad (104)$$

The resulting light neutrino mass matrix takes, under  $Z_2 \times Z_2'$ , the form:

$$M_\nu = \begin{pmatrix} \Gamma_{11}^1 \langle \Delta_1^0 \rangle & \Gamma_{12}^1 \langle \Delta_1^0 \rangle & \Gamma_{13}^2 \langle \Delta_2^0 \rangle + \Gamma_{13}^3 \langle \Delta_3^0 \rangle \\ \Gamma_{12}^1 \langle \Delta_1^0 \rangle & \Gamma_{11}^1 \langle \Delta_1^0 \rangle & \Gamma_{13}^2 \langle \Delta_2^0 \rangle - \Gamma_{13}^3 \langle \Delta_3^0 \rangle \\ \Gamma_{13}^2 \langle \Delta_2^0 \rangle + \Gamma_{13}^3 \langle \Delta_3^0 \rangle & \Gamma_{13}^2 \langle \Delta_2^0 \rangle - \Gamma_{13}^3 \langle \Delta_3^0 \rangle & \Gamma_{33}^1 \langle \Delta_1^0 \rangle \end{pmatrix} \quad (105)$$

which is of the requested form.

The charged lepton mass matrix takes a form,

$$M_l = \begin{pmatrix} Y_{l11}^1 v_1 + Y_{l21}^1 v_2 & Y_{l12}^1 v_1 + Y_{l22}^1 v_2 & 0 \\ Y_{l21}^1 v_1 + Y_{l11}^1 v_2 & Y_{l22}^1 v_1 + Y_{l12}^1 v_2 & 0 \\ 0 & 0 & Y_{l33}^1 v_1 + Y_{l33}^1 v_2 \end{pmatrix}. \quad (106)$$

As in the type-I scenario,  $M_l$  can be diagonalized through an infinitesimal rotation with an angle less than  $10^{-2}$  by considering the vacuum condition  $v_1 \ll v_2$ . The  $Z_2 \times Z_2'$  symmetry realization of the remaining three patterns  $F$ ,  $G_1$  and  $G_2$  are presented in the tables 7, 8 and 9.

The matter content			
$D_L$	$l_R$	$\phi$	$\Delta$
Symmetry under $Z_2$			
$T_D D_L$ $T_D = \text{diag}(1, -1, 1)$	$T_l l_R$ $T_l = \text{diag}(-1, 1, -1)$	$T_\phi \phi$ $T_\phi = \text{diag}(-1, -1)$	$T_\Delta \Delta$ $T_\Delta = \text{diag}(1, 1, -1)$
Symmetry under $Z'_2$			
$S_D D_L$ $S_D = \begin{pmatrix} 0 & 0 & 1 \\ 0 & 1 & 0 \\ 1 & 0 & 0 \end{pmatrix}$	$S_l l_R$ $S_l = \begin{pmatrix} 1 & 0 & 0 \\ 0 & 1 & 0 \\ 0 & 0 & 1 \end{pmatrix}$	$S_\phi \phi$ $S_\phi = \begin{pmatrix} 0 & 1 \\ 1 & 0 \end{pmatrix}$	$S_\Delta \Delta$ $S_\Delta = \begin{pmatrix} 1 & 0 & 0 \\ 0 & -1 & 0 \\ 0 & 0 & 1 \end{pmatrix}$
Mass matrices			
$M_\nu = \begin{pmatrix} \Gamma_{11}^1 \langle \Delta_1^0 \rangle + \Gamma_{11}^2 \langle \Delta_2^0 \rangle & \Gamma_{12}^3 \langle \Delta_3^0 \rangle & \Gamma_{13}^1 \langle \Delta_1^0 \rangle \\ \Gamma_{12}^3 \langle \Delta_3^0 \rangle & \Gamma_{22}^1 \langle \Delta_1^0 \rangle & \Gamma_{12}^3 \langle \Delta_3^0 \rangle \\ \Gamma_{13}^1 \langle \Delta_1^0 \rangle & \Gamma_{12}^3 \langle \Delta_3^0 \rangle & \Gamma_{11}^1 \langle \Delta_1^0 \rangle - \Gamma_{11}^2 \langle \Delta_2^0 \rangle \end{pmatrix}, \quad M_l^{v_1 \ll v_2} v_2 \begin{pmatrix} Y_{l31}^1 & 0 & Y_{l33}^1 \\ 0 & Y_{l22}^1 & 0 \\ Y_{l11}^1 & 0 & Y_{l13}^1 \end{pmatrix}$			

Table 7: The  $Z_2 \times Z'_2$  symmetry realization for the  $F : M_{\nu 12} = M_{\nu 23}$  pattern within type-II seesaw scenario. S and T are the symmetry transformation matrices for  $Z'_2$  and  $Z_2$  respectively.

The matter content			
$D_L$	$l_R$	$\phi$	$\Delta$
Symmetry under $Z_2$			
$T_D D_L$ $T_D = \text{diag}(-1, 1, 1)$	$T_l l_R$ $T_l = \text{diag}(1, -1, -1)$	$T_\phi \phi$ $T_\phi = \text{diag}(-1, -1)$	$T_\Delta \Delta$ $T_\Delta = \text{diag}(1, -1, -1)$
Symmetry under $Z'_2$			
$S_D D_L$ $S_D = \begin{pmatrix} 1 & 0 & 0 \\ 0 & 0 & 1 \\ 0 & 1 & 0 \end{pmatrix}$	$S_l l_R$ $S_l = \begin{pmatrix} 1 & 0 & 0 \\ 0 & 1 & 0 \\ 0 & 0 & 1 \end{pmatrix}$	$S_\phi \phi$ $S_\phi = \begin{pmatrix} 0 & 1 \\ 1 & 0 \end{pmatrix}$	$S_\Delta \Delta$ $S_\Delta = \begin{pmatrix} 1 & 0 & 0 \\ 0 & 1 & 0 \\ 0 & 0 & -1 \end{pmatrix}$
Mass matrices			
$M_\nu = \begin{pmatrix} \Gamma_{11}^1 \langle \Delta_1^0 \rangle & \Gamma_{12}^2 \langle \Delta_2^0 \rangle + \Gamma_{12}^3 \langle \Delta_3^0 \rangle & \Gamma_{12}^2 \langle \Delta_2^0 \rangle - \Gamma_{12}^3 \langle \Delta_3^0 \rangle \\ \Gamma_{12}^2 \langle \Delta_2^0 \rangle + \Gamma_{12}^3 \langle \Delta_3^0 \rangle & \Gamma_{22}^1 \langle \Delta_1^0 \rangle & \Gamma_{23}^1 \langle \Delta_1^0 \rangle \\ \Gamma_{12}^2 \langle \Delta_2^0 \rangle - \Gamma_{12}^3 \langle \Delta_3^0 \rangle & \Gamma_{23}^1 \langle \Delta_1^0 \rangle & \Gamma_{22}^1 \langle \Delta_1^0 \rangle \end{pmatrix}, \quad M_l^{v_1 \ll v_2} v_2 \begin{pmatrix} Y_{l11}^1 & 0 & 0 \\ 0 & Y_{l32}^1 & Y_{l33}^1 \\ 0 & Y_{l22}^1 & Y_{l23}^1 \end{pmatrix}$			

Table 8: The  $Z_2 \times Z'_2$  symmetry realization for the  $G_2 : M_{\nu 22} = M_{\nu 33}$  pattern within type-II seesaw scenario. S and T are the symmetry transformation matrices for  $Z'_2$  and  $Z_2$  respectively.

The matter content			
$D_L$	$l_R$	$\phi$	$\Delta$
Symmetry under $Z_2$			
$T_D D_L$ $T_D = \text{diag}(-1, 1, 1)$	$T_l l_R$ $T_l = \text{diag}(1, -1, -1)$	$T_\phi \phi$ $T_\phi = \text{diag}(-1, -1)$	$T_\Delta \Delta$ $T_\Delta = \text{diag}(1, 1, -1)$
Symmetry under $Z'_2$			
$S_D D_L$ $S_D = \begin{pmatrix} 1 & 0 & 0 \\ 0 & 0 & 1 \\ 0 & 1 & 0 \end{pmatrix}$	$S_l l_R$ $S_l = \begin{pmatrix} 1 & 0 & 0 \\ 0 & 1 & 0 \\ 0 & 0 & 1 \end{pmatrix}$	$S_\phi \phi$ $S_\phi = \begin{pmatrix} 0 & 1 \\ 1 & 0 \end{pmatrix}$	$S_\Delta \Delta$ $S_\Delta = \begin{pmatrix} 1 & 0 & 0 \\ 0 & -1 & 0 \\ 0 & 0 & 1 \end{pmatrix}$
Mass matrices			
$M_\nu = \begin{pmatrix} \Gamma_{11}^1 \langle \Delta_1^0 \rangle & \Gamma_{12}^3 \langle \Delta_3^0 \rangle & \Gamma_{12}^3 \langle \Delta_3^0 \rangle \\ \Gamma_{12}^3 \langle \Delta_3^0 \rangle & \Gamma_{22}^1 \langle \Delta_1^0 \rangle + \Gamma_{22}^2 \langle \Delta_2^0 \rangle & \Gamma_{23}^1 \langle \Delta_1^0 \rangle \\ \Gamma_{12}^3 \langle \Delta_3^0 \rangle & \Gamma_{23}^1 \langle \Delta_1^0 \rangle & \Gamma_{22}^1 \langle \Delta_1^0 \rangle - \Gamma_{22}^2 \langle \Delta_2^0 \rangle \end{pmatrix}, \quad M_l \stackrel{v_1 \ll v_2}{\approx} v_2 \begin{pmatrix} Y_{l11}^1 & 0 & 0 \\ 0 & Y_{l32}^1 & Y_{l33}^1 \\ 0 & Y_{l22}^1 & Y_{l23}^1 \end{pmatrix}$			

Table 9: The  $Z_2 \times Z'_2$  symmetry realization for the  $G_3 : M_{\nu 12} = M_{\nu 13}$  pattern within type-II seesaw scenario. S and T are the symmetry transformation matrices for  $Z'_2$  and  $Z_2$  respectively.

As in the type-I seesaw scenario, this method is not applicable for the other viable patterns  $(A, B, C, D, G_1)$ . We note that the particle content and flavor symmetry group in the type-II seesaw construction is simpler than the corresponding one in the type-I scheme.

### 6.3 Type (I+II) seesaw scenario

In this scenario, we follow the procedure of softly breaking a continuous symmetry adopted in [21] and [27] in order to enforce two equal entries in  $M_\nu$ . Moreover, going along the scheme presented in [28], applied for zero textures, we use a mixed type-I and type-II seesaw scenarios. The underlying symmetry is  $Z_2 \times Z'_2 \times U(1)^3$ , where  $U(1)^3$  is a global separate lepton number symmetry. We assume that  $U(1)^3$  symmetry is preserved by 4-D Lagrangian terms, whereas it is softly broken by 3-dim terms in order to avoid the existence of Goldstone bosons. We extend SM with two Higgs doublets  $(\phi_2, \phi_3)$ , one heavy scalar singlet  $\chi_{12}$  and two Higgs triplets  $(\Delta_1, \Delta_2)$ . Under the action of  $Z_2$ , the leptons transform as

$$\begin{aligned}
D_{L1} &\rightarrow D_{L1}, & D_{L2} &\rightarrow D_{L2}, & D_{L3} &\rightarrow -D_{L3}, \\
\nu_{R1} &\rightarrow -\nu_{R1}, & \nu_{R2} &\rightarrow -\nu_{R2}, & \nu_{R3} &\rightarrow \nu_{R3}, \\
l_{R1} &\rightarrow l_{R1}, & l_{R2} &\rightarrow l_{R2}, & l_{R3} &\rightarrow l_{R3},
\end{aligned} \tag{107}$$

while the scalar multiplets transform as

$$\begin{aligned}
\phi_1 &\rightarrow -\phi_1, & \phi_2 &\rightarrow \phi_2, & \phi_3 &\rightarrow \phi_3, & \chi_{12} &\rightarrow \chi_{12} \\
\Delta_1 &\rightarrow -\Delta_1, & \Delta_2 &\rightarrow -\Delta_2
\end{aligned} \tag{108}$$

We set  $\chi_{12}$  to have lepton numbers  $(L_e = -1, L_\mu = -1)$ , whereas  $\Delta_1$  and  $\Delta_2$  have  $(L_e = -1, L_\tau = -1)$  and  $(L_\mu = -1, L_\tau = -1)$  respectively. However, we set the scalar doublets  $\phi_1, \phi_2$  and

$\phi_3$  to be  $U(1)^3$  singlets. Therefore, we get under  $Z_2$ :

$$\begin{aligned} \nu_{Ri}^T \nu_{Rj} &\cong \begin{pmatrix} 1 & 1 & -1 \\ 1 & 1 & -1 \\ -1 & -1 & 1 \end{pmatrix}, \quad \bar{D}_{Li} \nu_{Rj} \cong \begin{pmatrix} -1 & -1 & 1 \\ -1 & -1 & 1 \\ 1 & 1 & -1 \end{pmatrix}, \quad \nu_{Li}^T \nu_{Lj} \cong \begin{pmatrix} 1 & 1 & -1 \\ 1 & 1 & -1 \\ -1 & -1 & 1 \end{pmatrix}, \\ \bar{D}_{Li} l_j &\cong \begin{pmatrix} 1 & 1 & 1 \\ 1 & 1 & 1 \\ -1 & -1 & -1 \end{pmatrix}. \end{aligned} \quad (109)$$

The  $Z_2 \times U(1)^3$  invariant Lagrangian is

$$\begin{aligned} -\mathcal{L} \supset & \nu_{R1}^T \mathcal{C}^{-1} \nu_{R1} + \nu_{R2}^T \mathcal{C}^{-1} \nu_{R2} + \nu_{R3}^T \mathcal{C}^{-1} \nu_{R3} + \nu_{R1}^T \mathcal{C}^{-1} \nu_{R2} + \nu_{R2}^T \mathcal{C}^{-1} \nu_{R1} \\ & + Y_{12}^\chi \nu_{R1}^T \mathcal{C}^{-1} \nu_{R2} \chi + Y_{21}^\chi \nu_{R2}^T \mathcal{C}^{-1} \nu_{R1} \chi + [Y_{11}^{\nu 1} \bar{D}_{L1} \nu_{R1} + Y_{22}^{\nu 1} \bar{D}_{L2} \nu_{R2} + Y_{33}^{\nu 1} \bar{D}_{L3} \nu_{R3}] \tilde{\phi}_1 \\ & + [Y_{11}^{l2} \bar{D}_{L1} l_1 + Y_{22}^{l2} \bar{D}_{L2} l_2] \phi_2 + [Y_{11}^{l3} \bar{D}_{L1} l_1 + Y_{22}^{l3} \bar{D}_{L2} l_2] \phi_3 + Y_{33}^{l1} \bar{D}_{L3} l_3 \phi_1 \\ & + [Y_{13}^{\Delta 1} \nu_{L1}^T \mathcal{C}^{-1} \nu_{L3} + Y_{31}^{\Delta 1} \nu_{L3}^T \mathcal{C}^{-1} \nu_{L1}] \Delta_1 + [Y_{23}^{\Delta 2} \nu_{L2}^T \mathcal{C}^{-1} \nu_{L3} + Y_{32}^{\Delta 2} \nu_{L3}^T \mathcal{C}^{-1} \nu_{L2}] \Delta_2 + h.c. \end{aligned} \quad (110)$$

Under the action  $Z_2'$  symmetry, we assume the lepton fields to transform as

$$\begin{aligned} D_{L1} &\rightarrow D_{L2}, & D_{L2} &\rightarrow D_{L1}, & D_{L3} &\rightarrow D_{L3}, \\ \nu_{R1} &\rightarrow \nu_{R2}, & \nu_{R2} &\rightarrow \nu_{R1}, & \nu_{R3} &\rightarrow \nu_{R3}, \\ l_{R1} &\rightarrow l_{R2}, & l_{R2} &\rightarrow l_{R1}, & l_{R3} &\rightarrow l_{R3}, \end{aligned} \quad (111)$$

while the scalar multiplets transform as

$$\begin{aligned} \phi_1 &\rightarrow \phi_1, & \phi_2 &\rightarrow \phi_2, & \phi_3 &\rightarrow -\phi_3, & \chi_{12} &\rightarrow \chi_{12} \\ \Delta_1 &\rightarrow \Delta_2, & \Delta_2 &\rightarrow \Delta_1 \end{aligned} \quad (112)$$

Thus, the  $Z_2'$  implies the constraints

$$Y_{12}^\chi = Y_{21}^\chi, \quad Y_{11}^{\nu 1} = Y_{22}^{\nu 1}, \quad Y_{11}^{l2} = Y_{22}^{l2}, \quad Y_{11}^{l3} = -Y_{22}^{l3}, \quad Y_{13}^{\Delta 1} = Y_{23}^{\Delta 2}, \quad Y_{31}^{\Delta 1} = Y_{32}^{\Delta 2}. \quad (113)$$

When  $\phi_1$  and  $\chi$  take vev, the Dirac neutrino mass matrix  $M_D$  and the right-handed neutrino mass matrix  $M_R$  are given by

$$M_D = \begin{pmatrix} A & 0 & 0 \\ 0 & A & 0 \\ 0 & 0 & B \end{pmatrix}, \quad M_R = \begin{pmatrix} x & y & 0 \\ y & x & 0 \\ 0 & 0 & z \end{pmatrix} \quad (114)$$

The neutrino mass matrix which comes from the type-I seesaw is given by

$$M_I = -M_D M_R^{-1} M_D^T = \begin{pmatrix} -\frac{A^2 x}{x^2 + y^2} & \frac{A^2 y}{x^2 + y^2} & 0 \\ \frac{A^2 y}{x^2 + y^2} & -\frac{A^2 x}{x^2 + y^2} & 0 \\ 0 & 0 & -\frac{B^2}{z} \end{pmatrix}, \quad (115)$$

where  $A = Y_{11}^{\nu 1} v_1^\phi$ ,  $B = Y_{33}^{\nu 1} v_1^\phi$ ,  $y = Y_{12}^{\chi} v^\chi$ . We see that  $M_{\nu 11} = M_{\nu 22}$  in  $M_I$ . In order to enforce non-zero degenerate elements (1,3) and (2,3) in  $M_\nu$ , we have to go to type-II seesaw. When  $\Delta_1$  and  $\Delta_2$  take VEV, the type-II neutrino mass matrix is given by

$$M_{II} = \begin{pmatrix} 0 & 0 & X \\ 0 & 0 & Y \\ X & Y & 0 \end{pmatrix} \quad (116)$$

where  $X = Y_{13}^{H1} v_1^\Delta$  and  $Y = Y_{13}^{H1} v_2^\Delta$ . The effective neutrino mass matrix  $M_\nu$  after the mixed type (I+II) seesaw mechanism becomes

$$M_\nu = M_I + M_{II} = \begin{pmatrix} a & b & c \\ b & a & d \\ c & d & e \end{pmatrix}. \quad (117)$$

As to the charged lepton mass matrix, it is by construction diagonal, meaning we are in the flavor basis:

$$M_l = \begin{pmatrix} Y_{11}^{l2} v_2^\phi + Y_{11}^{l3} v_3^\phi & 0 & 0 \\ 0 & Y_{11}^{l2} v_2^\phi - Y_{11}^{l3} v_3^\phi & 0 \\ 0 & 0 & Y_{33}^{l1} v_1^\phi \end{pmatrix}. \quad (118)$$

where  $v_k^\phi$  is the VEV of  $\phi_k$ , and one can arrange so that the diagonal elements come in hierarchical ratios corresponding to the charged lepton masses hierarchy.

The symmetry realization for the other cases  $F$ ,  $G_2$  and  $G_3$  are summarized in the tables 10, 11 and 12.

matter content $F_1$ pattern													
$D_{L1}$	$D_{L2}$	$D_{L3}$	$l_1$	$l_2$	$l_3$	$\nu_{R1}$	$\nu_{R2}$	$\nu_{R3}$	$\Delta_1$	$\Delta_2$	$\phi_1$	$\phi_2$	$\phi_3$
Becoming under $Z_2$ symmetry													
$-D_{L1}$	$-D_{L2}$	$-D_{L3}$	$-l_1$	$l_2$	$-l_3$	$\nu_{R1}$	$\nu_{R2}$	$\nu_{R3}$	$\Delta_1$	$\Delta_2$	$-\phi_1$	$\phi_2$	$\phi_3$
Becoming under $Z_2'$ symmetry													
$D_{L3}$	$D_{L2}$	$D_{L1}$	$l_3$	$l_2$	$l_1$	$\nu_{R3}$	$\nu_{R2}$	$\nu_{R1}$	$\Delta_2$	$\Delta_1$	$\phi_1$	$\phi_2$	$-\phi_3$
the field charge $\mathbf{q}$ under $U(1)^3$ symmetry													
$(1, 0, 0)$	$(0, 1, 0)$	$(0, 0, 1)$	$(1, 0, 0)$	$(0, 1, 0)$	$(0, 0, 1)$	$(1, 0, 0)$	$(0, 1, 0)$	$(0, 0, 1)$	$(-2, 0, 0)$	$(0, 0, -2)$	$\mathbf{0}$	$\mathbf{0}$	$\mathbf{0}$

Table 10: The  $Z_2 \times Z_2' \times U(1)^3$  symmetry realization for  $F : M_{\nu \ 12} = M_{\nu \ 23}$  pattern within type I+II seesaw scenario .

matter content $G_2$ pattern														
$D_{L1}$	$D_{L2}$	$D_{L3}$	$l_1$	$l_2$	$l_3$	$\nu_{R1}$	$\nu_{R2}$	$\nu_{R3}$	$\Delta_1$	$\Delta_2$	$\chi_{23}$	$\phi_1$	$\phi_2$	$\phi_3$
Becoming under $Z_2$ symmetry														
$-D_{L1}$	$D_{L2}$	$D_{L3}$	$l_1$	$l_2$	$l_3$	$\nu_{R1}$	$-\nu_{R2}$	$-\nu_{R3}$	$-\Delta_1$	$-\Delta_2$	$\chi_{23}$	$-\phi_1$	$\phi_2$	$\phi_3$
Becoming under $Z_2'$ symmetry														
$D_{L1}$	$D_{L3}$	$D_{L2}$	$l_1$	$l_3$	$l_2$	$\nu_{R1}$	$\nu_{R3}$	$\nu_{R2}$	$\Delta_2$	$\Delta_1$	$\chi_{23}$	$\phi_1$	$\phi_2$	$-\phi_3$
the field charge $\mathbf{q}$ under $U(1)^3$ symmetry														
$(1, 0, 0)$	$(0, 1, 0)$	$(0, 0, 1)$	$(1, 0, 0)$	$(0, 1, 0)$	$(0, 0, 1)$	$(1, 0, 0)$	$(0, 1, 0)$	$(0, 0, 1)$	$(-1, -1, 0)$	$(-1, 0, -1)$	$(0, -1, -1)$	$\mathbf{0}$	$\mathbf{0}$	$\mathbf{0}$

Table 11: The  $Z_2 \times Z_2' \times U(1)^3$  symmetry realization for  $G_2 : M_{\nu \ 22} = M_{\nu \ 33}$  pattern within type I+II seesaw scenario .

matter content $G_3$ pattern													
$D_{L1}$	$D_{L2}$	$D_{L3}$	$l_1$	$l_2$	$l_3$	$\nu_{R1}$	$\nu_{R2}$	$\nu_{R3}$	$\Delta_1$	$\Delta_2$	$\phi_1$	$\phi_2$	$\phi_3$
Becoming under $Z_2$ symmetry													
$-D_{L1}$	$-D_{L2}$	$-D_{L3}$	$l_1$	$-l_2$	$-l_3$	$\nu_{R1}$	$\nu_{R2}$	$\nu_{R3}$	$\Delta_1$	$\Delta_2$	$-\phi_1$	$\phi_2$	$\phi_3$
Becoming under $Z_2'$ symmetry													
$D_{L1}$	$D_{L3}$	$D_{L2}$	$l_1$	$l_3$	$l_2$	$\nu_{R1}$	$\nu_{R3}$	$\nu_{R2}$	$\Delta_2$	$\Delta_1$	$\phi_1$	$\phi_2$	$-\phi_3$
the field charge $\mathbf{q}$ under $U(1)^3$ symmetry													
$(1, 0, 0)$	$(0, 1, 0)$	$(0, 0, 1)$	$(1, 0, 0)$	$(0, 1, 0)$	$(0, 0, 1)$	$(1, 0, 0)$	$(0, 1, 0)$	$(0, 0, 1)$	$(0, -2, 0)$	$(0, 0, -2)$	$\mathbf{0}$	$\mathbf{0}$	$\mathbf{0}$

Table 12: The  $Z_2 \times Z_2' \times U(1)^3$  symmetry realization for  $G_3 : M_{\nu \ 12} = M_{\nu \ 13}$  pattern within type I+II seesaw scenario .

## 7 Summary and conclusion

In this work, we have studied a specific texture characterized by one equality between two independent elements in the neutrino mass matrix. After we have checked that the  $\mu$ - $\tau$ -permutation related textures give similar phenomenology, we find that out of the 15 possible one-Equality textures, all can accommodate the experimental data in normal type ( $m_1 < m_2 < m_3$ ), while all except one pattern in  $C$  category are viable in inverted type ( $m_3 < m_1 < m_2$ ). We give the analytical formulae for the A's coefficients Eq.(38) corresponding to each independent texture. However, we find that the analytical expressions for the mass ratios and other neutrino physical parameters are too cumbersome to be presented even in their approximate form. The singular (non-invertible) neutrino mass matrices with one-equality texture are expected for five patterns in normal type and ten patterns in inverted type. The allowed ranges of the neutrino physical parameters at all  $\sigma$ -levels for each hierarchy type, and for 9 patterns not related by  $\mu$ - $\tau$ -symmetry, are listed in the Tables (2,3). In Fig.2-19, we introduce 21 correlation plots for each independent texture with either hierarchy type.

Finally, we present symmetry realizations for four viable patterns, from nine pattern not related by  $\mu$ - $\tau$ -symmetry, in different seesaw scenarios. In the framework of the type-I scenario, we use a  $Z_2 \times Z_6$  discrete flavor symmetry to enforce one equality in the neutrino mass matrix, while  $Z_2 \times Z'_2$  symmetry is used in the type-II scheme. The realization methods proposed in the different seesaw scenarios are applicable for only six texture structures out of fifteen. We find the particle content and flavor symmetry group in the type-II seesaw construction is simpler than the corresponding one in the type-I scheme.

In the realization methods, we have not yet touched the question of the scalar potential and finding its general form under the imposed symmetry. Nor did we deal with the radiative corrections effect on the phenomenology and whether or not it can spoil the form of the texture while running from the “ultraviolet” scale where the seesaw scale imposes the texture form to the low scale where phenomenology was analyzed. Some studies [19] argue that, unlike zero textures, Equality textures do not keep their form under RG running, and so this question is worthy of a separate study. Likewise, introducing many scalars may lead to rich phenomenology at colliders, and asking for just one SM-like Higgs at low scale requires a situation where fine tuning of the many parameters in the scalar potential, so that to ensure new scalars are out of reach at current experiments, is heavily called upon. For completeness, we treat in appendix the question of how to find the most general form of the scalar potential, within type II seesaw scenario, in one specific texture, noting that a corresponding rich colliders’ phenomenology needs a complete analysis of such a setup, which goes beyond the current study.

## Acknowledgements

E.I. Lashin and N.C. acknowledge support from ICTP-Associate program. N.C. acknowledges support of the Alexander von Humboldt Foundation and is grateful for the kind hospitality of the Bethe Center for Theoretical Physics at Bonn University.

## A Scalar potential for $E_1$ texture within $Z_2 \times Z'_2$ symmetry

In this appendix, we write down the  $Z_2 \times Z'_2$  invariant terms for the type-II scalar potential. For the sake of illustration, we take  $E_1$  texture as a concrete example. We extend the SM



with three  $SU(2)_L$  Higgs triplets  $(\Delta_1, \Delta_2, \Delta_3)$  besides one Higgs doublet. The  $Z_2$  and  $Z'_2$  symmetry transformation for the Higgs multiplets are given by Eqs. (100 and 103). The most renormalizable gauge invariant type-II scalar potential takes the following form [29, 30]:

$$\begin{aligned} V(\phi, \Delta) &= V_\phi + V_\Delta + V_{\phi\Delta}, \\ V_\phi &= a_{ij} \phi_i^\dagger \phi_j + c_{ijkl} \phi_i^\dagger \phi_j \phi_k^\dagger \phi_l, \\ V_\Delta &= b_{ij} \text{Tr}(\Delta_i^\dagger \Delta_j) + d_{ijkl} \text{Tr}(\Delta_i^\dagger \Delta_j) \text{Tr}(\Delta_k^\dagger \Delta_l) + f_{ijkl} \text{Tr}(\Delta_i^\dagger \Delta_j^\dagger) \text{Tr}(\Delta_k \Delta_l), \\ V_{\phi\Delta} &= \left( \frac{e_{ijkl} - h_{ijkl}}{2} \right) \phi_i^\dagger \phi_j \text{Tr}(\Delta_k^\dagger \Delta_l) + h_{ijkl} \phi_i^\dagger \Delta_j^\dagger \Delta_k \phi_l + (t_{ijk} \phi_i^\dagger \Delta_j \tilde{\phi}_k + h.c.). \end{aligned} \quad (119)$$

The lower indices of  $\phi$ 's run from 1 to 2, whereas the lower indices of  $\Delta$ 's run from 1 to 3. The scalar triplet  $\Delta$  is written as

$$\Delta = \vec{\Phi} \cdot \vec{\tau} = \begin{pmatrix} H^+ & \sqrt{2}H^{++} \\ \sqrt{2}H^0 & -H^+ \end{pmatrix}, \text{ where } \Phi_i = \begin{pmatrix} \frac{1}{\sqrt{2}}(H^0 + H^{++}) \\ -\frac{i}{\sqrt{2}}(H^0 - H^{++}) \\ H^+ \end{pmatrix}, \quad (120)$$

and  $\tau_i$  ( $i = 1, 2, 3$ ) are the Pauli matrices. However, the scalar doublet  $\phi$  is given by

$$\phi = \begin{pmatrix} \phi^+ \\ \phi^0 \end{pmatrix}. \quad (121)$$

The VEVs of the scalar multiplets are

$$\langle \phi_i \rangle_0 = \frac{1}{\sqrt{2}} \begin{pmatrix} 0 \\ |v_i| e^{i\alpha_i} \end{pmatrix}, \quad \langle \Delta_i \rangle_0 = \begin{pmatrix} 0 & 0 \\ |\omega_i| e^{i\beta_i} & 0 \end{pmatrix}. \quad (122)$$

The  $Z_2 \times Z'_2$  invariant  $V_\phi$  terms are given by

$$\begin{aligned} V_\phi &= a_{11}(\phi_1^\dagger \phi_1 + \phi_2^\dagger \phi_2) + a_{12}(\phi_1^\dagger \phi_2 + \phi_2^\dagger \phi_1) + c_{1111}[(\phi_1^\dagger \phi_1)^2 + (\phi_2^\dagger \phi_2)^2] + c_{1122} \phi_1^\dagger \phi_1 \phi_2^\dagger \phi_2 + c_{1221} \phi_1^\dagger \phi_2 \phi_2^\dagger \phi_1 \\ &+ c_{1212}[(\phi_1^\dagger \phi_2)^2 + (\phi_2^\dagger \phi_1)^2] + c_{1112}[\phi_1^\dagger \phi_1 \phi_1^\dagger \phi_2 + \phi_2^\dagger \phi_1 \phi_2^\dagger \phi_2 + \phi_2^\dagger \phi_1 \phi_1^\dagger \phi_1 + \phi_1^\dagger \phi_2 \phi_2^\dagger \phi_2]. \end{aligned} \quad (123)$$

We see that  $a$ 's and  $c$ 's parameters are real. Thus, we get

$$\begin{aligned} \langle 0 | V_\phi | 0 \rangle &= \frac{a_{11}}{2}(|v_1|^2 + |v_2|^2) + a_{12} \text{Re}(v_1^* v_2) + \frac{c_{1111}}{4}(|v_1|^4 + |v_2|^4) + \frac{c_{1122}}{4}|v_1 v_2|^2 + \frac{c_{1221}}{4}|v_1 v_2|^2 \\ &+ \frac{c_{1212}}{2} \text{Re}(v_1^{*2} v_2^2) + \frac{c_{1112}}{2}(|v_1|^2 + |v_2|^2) \text{Re}(v_1^* v_2). \end{aligned} \quad (124)$$

The  $Z_2 \times Z'_2$  invariant  $V_\Delta$  is

$$\begin{aligned} V_\Delta &= b_{11} \text{Tr}(\Delta_1^\dagger \Delta_1) + b_{22} \text{Tr}(\Delta_2^\dagger \Delta_2) + b_{33} \text{Tr}(\Delta_3^\dagger \Delta_3) + d_{1111} [\text{Tr}(\Delta_1^\dagger \Delta_1)]^2 + d_{1122} \text{Tr}(\Delta_1^\dagger \Delta_1) \text{Tr}(\Delta_2^\dagger \Delta_2) \\ &+ d_{2222} [\text{Tr}(\Delta_2^\dagger \Delta_2)]^2 + d_{3333} [\text{Tr}(\Delta_3^\dagger \Delta_3)]^2 + d_{1133} \text{Tr}(\Delta_1^\dagger \Delta_1) \text{Tr}(\Delta_3^\dagger \Delta_3) + d_{2233} \text{Tr}(\Delta_2^\dagger \Delta_2) \text{Tr}(\Delta_3^\dagger \Delta_3) \\ &+ d_{1221} \text{Tr}(\Delta_1^\dagger \Delta_2) \text{Tr}(\Delta_2^\dagger \Delta_1) + d_{1331} \text{Tr}(\Delta_1^\dagger \Delta_3) \text{Tr}(\Delta_3^\dagger \Delta_1) + d_{2332} \text{Tr}(\Delta_2^\dagger \Delta_3) \text{Tr}(\Delta_3^\dagger \Delta_2) \\ &+ d_{1212} [(\text{Tr}(\Delta_1^\dagger \Delta_2))^2 + h.c.] + d_{2323} [(\text{Tr}(\Delta_2^\dagger \Delta_3))^2 + h.c.] + d_{1313} [(\text{Tr}(\Delta_1^\dagger \Delta_3))^2 + h.c.] \\ &+ f_{1111} \text{Tr}(\Delta_1^\dagger \Delta_1^\dagger) \text{Tr}(\Delta_1 \Delta_1) + f_{2222} \text{Tr}(\Delta_2^\dagger \Delta_2^\dagger) \text{Tr}(\Delta_2 \Delta_2) + f_{3333} \text{Tr}(\Delta_3^\dagger \Delta_3^\dagger) \text{Tr}(\Delta_3 \Delta_3) \\ &+ f_{1212} \text{Tr}(\Delta_1^\dagger \Delta_2^\dagger) \text{Tr}(\Delta_1 \Delta_2) + f_{1313} \text{Tr}(\Delta_1^\dagger \Delta_3^\dagger) \text{Tr}(\Delta_1 \Delta_3) + f_{2323} \text{Tr}(\Delta_2^\dagger \Delta_3^\dagger) \text{Tr}(\Delta_2 \Delta_3) \\ &+ f_{1122} [\text{Tr}(\Delta_1^\dagger \Delta_1^\dagger) \text{Tr}(\Delta_2 \Delta_2) + h.c.] + f_{1133} [\text{Tr}(\Delta_1^\dagger \Delta_1^\dagger) \text{Tr}(\Delta_3 \Delta_3) + h.c.] \\ &+ f_{2233} [\text{Tr}(\Delta_2^\dagger \Delta_2^\dagger) \text{Tr}(\Delta_3 \Delta_3) + h.c.] \end{aligned} \quad (125)$$

where  $f$  and  $d$  parameters are all real. Then, we obtain

$$\begin{aligned} \langle 0 | V_\Delta | 0 \rangle = & b_{11} |\omega_1|^2 + b_{22} |\omega_2|^2 + b_{33} |\omega_3|^2 + d_{1111} |\omega_1|^4 + d_{2222} |\omega_2|^4 + d_{3333} |\omega_3|^4 + (d_{1122} + d_{1221}) |\omega_1^2 \omega_2^2| \\ & + (d_{1133} + d_{1331}) |\omega_1^2 \omega_3^2| + (d_{2233} + d_{2332}) |\omega_2^2 \omega_3^2| + 2d_{1212} \text{Re}(\omega_1^{*2} \omega_2^2) + 2d_{2323} \text{Re}(\omega_2^{*2} \omega_3^2) \\ & + 2d_{1313} \text{Re}(\omega_1^{*2} \omega_3^2). \end{aligned} \quad (126)$$

The  $Z_2 \times Z'_2$  invariant interaction potential  $V_{\phi\Delta}$  is given by

$$\begin{aligned} V_{\phi\Delta} = & \left( \frac{e-h}{2} \right)_{1111} \left[ \phi_1^\dagger \phi_1 \text{Tr}(\Delta_1^\dagger \Delta_1) + \phi_2^\dagger \phi_2 \text{Tr}(\Delta_1^\dagger \Delta_1) \right] + \left( \frac{e-h}{2} \right)_{2222} \left[ \phi_2^\dagger \phi_2 \text{Tr}(\Delta_2^\dagger \Delta_2) + \phi_1^\dagger \phi_1 \text{Tr}(\Delta_2^\dagger \Delta_2) \right] \\ & + \left( \frac{e-h}{2} \right)_{1133} \left[ \phi_1^\dagger \phi_1 \text{Tr}(\Delta_3^\dagger \Delta_3) + \phi_2^\dagger \phi_2 \text{Tr}(\Delta_3^\dagger \Delta_3) \right] + \left( \frac{e-h}{2} \right)_{1222} \left[ \phi_1^\dagger \phi_2 \text{Tr}(\Delta_2^\dagger \Delta_2) + \phi_2^\dagger \phi_1 \text{Tr}(\Delta_2^\dagger \Delta_2) \right] \\ & + \left( \frac{e-h}{2} \right)_{1233} \left[ \phi_1^\dagger \phi_2 \text{Tr}(\Delta_3^\dagger \Delta_3) + \phi_2^\dagger \phi_1 \text{Tr}(\Delta_3^\dagger \Delta_3) \right] + \left( \frac{e-h}{2} \right)_{1211} \left[ \phi_1^\dagger \phi_2 \text{Tr}(\Delta_1^\dagger \Delta_1) + \phi_2^\dagger \phi_1 \text{Tr}(\Delta_1^\dagger \Delta_1) \right] \\ & + h_{1111} \left[ \phi_1^\dagger \Delta_1^\dagger \Delta_1 \phi_1 + \phi_2^\dagger \Delta_1^\dagger \Delta_1 \phi_2 \right] + h_{2222} \left[ \phi_2^\dagger \Delta_2^\dagger \Delta_2 \phi_2 + \phi_1^\dagger \Delta_2^\dagger \Delta_2 \phi_1 \right] + h_{1331} \left[ \phi_1^\dagger \Delta_3^\dagger \Delta_3 \phi_1 + \phi_2^\dagger \Delta_3^\dagger \Delta_3 \phi_2 \right] \\ & + h_{1222} \left[ \phi_1^\dagger \Delta_2^\dagger \Delta_2 \phi_2 + \phi_2^\dagger \Delta_2^\dagger \Delta_2 \phi_1 \right] + h_{1332} \left[ \phi_1^\dagger \Delta_3^\dagger \Delta_3 \phi_2 + \phi_2^\dagger \Delta_3^\dagger \Delta_3 \phi_1 \right] + h_{1112} \left[ \phi_1^\dagger \Delta_1^\dagger \Delta_1 \phi_2 + \phi_2^\dagger \Delta_1^\dagger \Delta_1 \phi_1 \right] \\ & + \left[ \left( \frac{e-h}{2} \right)_{2223} \left( \phi_2^\dagger \phi_2 \text{Tr}(\Delta_2^\dagger \Delta_3) - \phi_1^\dagger \phi_1 \text{Tr}(\Delta_2^\dagger \Delta_3) \right) + \left( \frac{e-h}{2} \right)_{1223} \left( \phi_1^\dagger \phi_2 \text{Tr}(\Delta_2^\dagger \Delta_3) - \phi_2^\dagger \phi_1 \text{Tr}(\Delta_2^\dagger \Delta_3) \right) \right] \\ & + h_{2232} \left( \phi_2^\dagger \Delta_2^\dagger \Delta_3 \phi_2 - \phi_1^\dagger \Delta_2^\dagger \Delta_3 \phi_1 \right) + h_{1232} \left( \phi_1^\dagger \Delta_2^\dagger \Delta_3 \phi_2 - \phi_2^\dagger \Delta_2^\dagger \Delta_3 \phi_1 \right) + t_{111} (\phi_1^\dagger \Delta_1 \tilde{\phi}_1 + \phi_2^\dagger \Delta_1 \tilde{\phi}_2) \\ & + t_{112} (\phi_1^\dagger \Delta_1 \tilde{\phi}_2 + \phi_2^\dagger \Delta_1 \tilde{\phi}_1) + h.c. \end{aligned} \quad (127)$$

We used  $\left( \frac{e_{ijkl} - h_{ijkl}}{2} \right) = \left( \frac{e-h}{2} \right)_{ijkl}$ . We see that all the  $e$ - and  $h$ - parameters are real except  $e_{2223}$ ,  $e_{1223}$ ,  $h_{2223}$ ,  $h_{1223}$ ,  $h_{2232}$ ,  $h_{1232}$ ,  $t_{111}$  and  $t_{112}$  are complex. Thus, we get

$$\begin{aligned} \langle 0 | V_{\phi\Delta} | 0 \rangle = & \left[ \left( \frac{e-h}{4} \right)_{1111} |\omega_1|^2 + \left( \frac{e-h}{4} \right)_{2222} |\omega_2|^2 + \left( \frac{e-h}{4} \right)_{1133} |\omega_3|^2 \right] (|v_1|^2 + |v_2|^2) \\ & + \left[ \left( \frac{e-h}{2} \right)_{1211} |\omega_1|^2 + \left( \frac{e-h}{2} \right)_{1222} |\omega_2|^2 + \left( \frac{e-h}{2} \right)_{1233} |\omega_3|^2 \right] \text{Re}(v_1^* v_2) \\ & + \text{Re} \left[ (e-h)_{2223} \omega_2^* \omega_3 \right] \frac{|v_2|^2 - |v_1|^2}{2} + \frac{1}{2} \text{Re} \left[ (e-h)_{1223} \omega_2^* \omega_3 \text{Im}(v_1^* v_2) \right] \\ & + |t_{111} v_1^2 \omega_1| \cos(2\alpha_1 - \beta_1 - \gamma_1) + |t_{111} v_2^2 \omega_1| \cos(2\alpha_2 - \beta_1 - \gamma_1) \\ & + 2|t_{112} \omega_1 v_1 v_2| \cos(\alpha_1 + \alpha_2 - \beta_1 - \gamma_2) \end{aligned} \quad (128)$$

where  $t_{111} = |t_{111}| e^{i\gamma_1}$ ,  $t_{112} = |t_{112}| e^{i\gamma_2}$ .

In all, using the above expressions, one can now construct the  $3 \times 3$  mass matrix for the doubly charged scalars ( $H_k^{++}, k \in \{1, 2, 3\}$ ), and the  $5 \times 5$  mass matrix for the singly charged scalars ( $H_k^+, \phi_j^+, j \in \{1, 2\}$ ), whereas for the neutral scalars ( $H_k^0, \phi_j^0$ ) with real and imaginary parts, we have a  $10 \times 10$  mass matrix. For the latter, and due to  $SU(2)$  gauge invariance we should have at least three vanishing eigen masses corresponding to the three Goldstone bosons.

There are many ways to simplify the calculations, such as assuming all the VEVs are real so that no CP violation originating from them, or extending the gauge symmetry by an extra  $U(1)$ , with respect to which the neutrinos are neutral so that  $M_\nu$  structure remains invariant, in order to kill the cubic interaction terms. Furthermore, one can also assume ad hoc certain vanishing parameters so that no coupling between scalars and pseudo scalars. Such a full study

of the scalar potential is interesting and necessary for colliders' phenomenology, however it is beyond the scope of this paper.

## References

- [1] Y.Fukuda et al.(Super Kamiokande Collaboration). Evidence for oscillation of atmospheric neutrinos. *Phys. Rev. Lett.*, 81:1562–1567, Aug 1998.
- [2] Q.R. Ahmad et al.(SNO Collaboration). Direct evidence for neutrino flavor transformation from neutral-current interactions in the sudbury neutrino observatory. *Phys. Rev. Lett.*, 89:011301, Jun 2002.
- [3] K. Eguchi et al. (Kam-LAND Collaboration). First results from kamland: Evidence for reactor antineutrino disappearance. *Phys. Rev. Lett.*, 90:021802, Jan 2003.
- [4] F.P. An et al. (DAYA-BAY Collaboration). Observation of electron-antineutrino disappearance at daya bay. *Phys. Rev. Lett.*, 108:171803, Apr 2012.
- [5] M.H. Ahn et al. (K2K Collaboration). Indications of neutrino oscillation in a 250 km long-baseline experiment. *Phys. Rev. Lett.*, 90:041801, Jan 2003.
- [6] Harald Fritzsch, Zhi-zhong Xing, and Shun Zhou. Two-zero textures of the majorana neutrino mass matrix and current experimental tests. *Journal of High Energy Physics*, 2011(9), Sep 2011.
- [7] Paul H. Frampton, Sheldon L. Glashow, and Danny Marfatia. Zeroes of the neutrino mass matrix. *Physics Letters B*, 536(1-2):7982, May 2002.
- [8] Zhi-zhong Xing. Texture zeros and majorana phases of the neutrino mass matrix. *Physics Letters B*, 530(1-4):159166, Mar 2002.
- [9] E. I. Lashin and N. Chamoun. One-zero textures of majorana neutrino mass matrix and current experimental tests. *Physical Review D*, 85(11), Jun 2012.
- [10] E. I. Lashin and N. Chamoun. Zero minors of the neutrino mass matrix. *Physical Review D*, 78(7), Oct 2008.
- [11] E. I. Lashin and N. Chamoun. One vanishing minor in the neutrino mass matrix. *Physical Review D*, 80(9), Nov 2009.
- [12] S. Dev, Shivani Gupta, Radha Raman Gautam, and Lal Singh. Near maximal atmospheric mixing in neutrino mass matrices with two vanishing minors. *Physics Letters B*, 706(2-3):168176, Dec 2011.
- [13] H. A. Alhendi, E. I. Lashin, and A. A. Mudlej. Textures with two traceless submatrices of the neutrino mass matrix. *Physical Review D*, 77(1), Jan 2008.
- [14] E.I. Lashin, N. Chamoun, C. Hamzaoui, and S. Nasri. Neutrino mass textures and partial-symmetry. *Physical Review D*, 89(9), May 2014.
- [15] Francesco Capozzi, Eleonora Di Valentino, Eligio Lisi, Antonio Marrone, Alessandro Melchiorri, and Antonio Palazzo. Global constraints on absolute neutrino masses and their ordering. *Phys. Rev. D*, 95:096014, May 2017.
- [16] S. Dev, Radha Raman Gautam, and Lal Singh. Neutrino mass matrices with two equalities between the elements or cofactors. *Physical Review D*, 87(7), Apr 2013.

- [17] Ji-Yuan Liu and Shun Zhou. Hybrid textures of majorana neutrino mass matrix and current experimental tests. *Physical Review D*, 87(9), May 2013.
- [18] Jinzhong Han, Ruihong Wang, Weijian Wang, and Xing-Ning Wei. Neutrino mass matrices with one texture equality and one vanishing neutrino mass. *Physical Review D*, 96(7), Oct 2017.
- [19] A. Ismael, M. Alkhateeb, N. Chamoun, and E.I. Lashin. Texture of single vanishing subtrace in neutrino mass matrix. *to appear in Phys. Rev. D*, 2021.
- [20] M. Tanabashi et al. (Particle Data Group). Neutrino masses, mixing, and oscillations. *Phys. Rev. D*, 98:030001, 2018.
- [21] W. Grimus and L. Lavoura. - interchange symmetry and lepton mixing. *Fortschritte der Physik*, 61(4-5):535545, Oct 2012.
- [22] Deirdre Black, Amir H. Fariborz, Salah Nasri, and Joseph Schechter. Complementary ansatz for the neutrino mass matrix. *Phys. Rev. D*, 62:073015, Sep 2000.
- [23] C. Jarlskog. Commutator of the quark mass matrices in the standard electroweak model and a measure of maximal CP nonconservation. *Phys. Rev. Lett.*, 55:1039–1042, Sep 1985.
- [24] Heinrich Ps and Werner Rodejohann. Neutrinoless double beta decay. *New Journal of Physics*, 17(11):115010, nov 2015.
- [25] E. Andreotti et al.  $^{130}\text{Te}$  Neutrinoless Double-Beta Decay with CUORICINO. *Astropart. Phys.*, 34:822–831, 2011.
- [26] Ta-Pei Cheng and Ling-Fong Li. Neutrino masses, mixings, and oscillations in  $\text{su}(2)_\text{u}(1)$  models of electroweak interactions. *Phys. Rev. D*, 22, 12 1980.
- [27] Walter Grimus, Satoru Kaneko, Lus Lavoura, Hideyuki Sawanaka, and Morimitsu Tanimoto. antisymmetry and neutrino mass matrices. *Journal of High Energy Physics*, 2006(01):110110, Jan 2006.
- [28] S. Dev, Shivani Gupta, and Radha Raman Gautam. Zero textures of the neutrino mass matrix from cyclic family symmetry. *Physics Letters B*, 701(5):605608, Jul 2011.
- [29] W. Grimus, R. Pfeiffer, and T. Schwetz. A 4-neutrino model with a higgs triplet. *The European Physical Journal C*, 13(1):125132, Mar 2000.
- [30] Avinanda Chaudhuri, Walter Grimus, and Biswarup Mukhopadhyaya. Doubly charged scalar decays in a type ii seesaw scenario with two higgs triplets. *Journal of High Energy Physics*, 2014(2), Feb 2014.